UNCLASSIFIED

SECURITY CLASSIFICATION OF THIS PAGE *(When Data Entered)*

REPORT DOCUMENTATION PAGE		READ INSTRUCTIONS BEFORE COMPLETING FORM
1 REPORT NUMBER NAVENVPREDRSCHFAC Technical Paper No. 2-76	2. GOVT ACCESSION NO.	3. RECIPIENT'S CATALOG NUMBER
4. TITLE *(and Subtitle)* Tropical Cyclone Initiation By The Tropical Upper Tropospheric Trough		5. TYPE OF REPORT & PERIOD COVERED
		6. PERFORMING ORG. REPORT NUMBER UHMET 75-02
7. AUTHOR(s) James C. Sadler		8. CONTRACT OR GRANT NUMBER(s) N66314-73-C-1770
9. PERFORMING ORGANIZATION NAME AND ADDRESS Department of Meteorology University of Hawaii Honolulu, HI 96822		10. PROGRAM ELEMENT, PROJECT, TASK AREA & WORK UNIT NUMBERS NAVENVPREDRSCHFAC WU 055:3-2
11. CONTROLLING OFFICE NAME AND ADDRESS Naval Air Systems Command Department of the Navy Washington, D.C. 20361		12. REPORT DATE February 1976
		13. NUMBER OF PAGES 104
14. MONITORING AGENCY NAME & ADDRESS *(if different from Controlling Office)* Naval Environmental Prediction Research Facility Monterey, CA 93940		15. SECURITY CLASS. *(of this report)* UNCLASSIFIED
		15a. DECLASSIFICATION/DOWNGRADING SCHEDULE

16. DISTRIBUTION STATEMENT *(of this Report)*

Approved for public release; distribution unlimited.

17. DISTRIBUTION STATEMENT *(of the abstract entered in Block 20, if different from Report)*

18. SUPPLEMENTARY NOTES

Manuscript received March 1975.

19. KEY WORDS *(Continue on reverse side if necessary and identify by block number)*

Tropical Cyclone
Tropical Meteorology
Tropical Upper Tropospheric Trough (TUTT)
Cold Core Low

20. ABSTRACT *(Continue on reverse side if necessary and identify by block number)*

Improved satellite observations and an increased quantity of aircraft wind observations are meshed for case studies to modify the earlier synoptic model of tropical cyclone initiation by the Tropical Upper Tropospheric Trough (TUTT). The major modification is in the vertical linkage between the upper and lower cyclonic systems. In the

DD FORM 1 JAN 73 1473 EDITION OF 1 NOV 65 IS OBSOLETE
S N 0102-014-6601

UNCLASSIFIED

SECURITY CLASSIFICATION OF THIS PAGE *(When Data Entered)*

20. Abstract (continued)

previous model (Sadler, 1967) it was proposed that the surface system resulted from a sloping downward penetration of the strong TUTT cell and, due to the slope, the surface disturbance was properly positioned under the upper divergence for intensification. These current studies show that the TUTT cell does not penetrate into the near surface layer but that the surface disturbance is induced by the upper divergence to the east of the TUTT cell and the two systems are initially separated by some 300 to 500 km. The better observations also permit a more detailed description of the upper circulation patterns to show how the convection associated with the intensifying surface system "kills" the parent TUTT cell.

AN (1) AD-A025 456
FG (2) 04020Ø
CI (3) (U)
CA (5) HAWAII UNIV HONOLULU DEPT OF METEOROLOGY
T1 (6) Tropical Cyclone Initiation by the Tropical Upper Tropospheric Trough.
TC (8) (U)
DN (9) Technical paper,
AU (10) Sadler,James C.
RD (11) Feb 1976
PG (12) 107p
RS (14) UHMET-75-02
CT (15) N66314-73-C-1770
RN (18) NRPRF-TechnicalPaper-2-76
RC (20) Unclassified report
DE (23) *Tropical cyclones, *Marine meteorology, *Troposphere, Atmosphere models, Tropical regions, Meteorological satellites, Atmospheric circulation, Atlantic Ocean, Pacific Ocean
DC (24) (U)
ID (25) *Tropical meteorology
IC (26) (U)
AB (27) Improved satellite observations and an increased quantity of aircraft wind observations are meshed for case studies to modify the earlier synoptic model of tropical cyclone initiation by the Tropical Upper Tropospheric Trough (TUTT). The major modification is in the vertical linkage between the upper and lower cyclonic systems. In the previous model (Sadler, 1967) it was proposed that the surface system resulted from a sloping downward penetration of the strong TUTT cell and, due to the slope, the surface disturbance was properly positioned under the upper divergence for intensification. These current studies show that the TUTT cell does not penetrate into the near surface layer but that the surface disturbance is induced by the upper divergence to the east of the TUTT cell and the two systems are initially separated by some 300 to 500 km. The better observations also permit a more detailed description of the upper circulation patterns to show how the convection associated with the intensifying surface system 'kills' the parent TUTT cell. (Author)
AC (28) (U)
DL (33) Ø1
CC (35) 406655

Approved for public release;
Distribution unlimited

NAVENVPREDRSCHFAC
Technical Paper No. 2–76

UHMET 75–02

TROPICAL CYCLONE INITIATION BY THE TROPICAL UPPER TROPOSPHERIC TROUGH

by

JAMES C. SADLER

FEBRUARY 1976

NAVAL ENVIRONMENTAL PREDICTION RESEARCH FACILITY
MONTEREY, CALIFORNIA 93940

CONTENTS

ABSTRACT

Improved satellite observations and an increased quantity of aircraft wind observations are meshed for case studies to modify the earlier synoptic model of tropical cyclone initiation by the Tropical Upper Tropospheric Trough (TUTT). The major modification is in the vertical linkage between the upper and lower cyclonic systems. In the previous model (Sadler, 1967) it was proposed that the surface system resulted from a sloping downward penetration of the strong TUTT cell and, due to the slope, the surface disturbance was properly positioned under the upper divergence for intensification. These current studies show that the TUTT cell does not penetrate into the near surface layer but that the surface disturbance is induced by the upper divergence to the east of the TUTT cell and the two systems are initially separated by some 300 to 500 km. The better observations also permit a more detailed description of the upper circulation patterns to show how the convection associated with the intensifying surface system "kills" the parent TUTT cell.

1. INTRODUCTION

The Tropical Upper Tropospheric Trough (TUTT) is a dominant climatological system, and a daily synoptic feature, of the summer season over the tropical North Atlantic, North Pacific and South Pacific Oceans.

In earlier studies (Conover and Sadler, 1960; Sadler, 1962; and Sadler, 1967) the TUTT was shown to be the major initiator of weather disturbances in the trade-wind zone and the source of tropical cyclones outside the low-level near-equatorial monsoon trough. Those studies were based on rocket nose-cone photography, early TIROS satellite data, and a few aircraft wind observations at the beginning of the commercial jet aircraft era. Subsequently, the quantity and quality of jet aircraft wind observations have increased significantly and the polar-orbiting satellites now furnish day and night observations of cloudiness at greatly improved resolutions. Our investigations of the upper trough have continued with these improved data to test and modify the synoptic models proposed earlier (Sadler, 1967). This paper presents the modified model of the initiation of a tropical cyclone by the TUTT, and illustrates the model with selected case studies.

2. SYNOPTIC MODEL

The major modification of the previous model is in the vertical linkage of the upper and lower systems. Earlier it was proposed that the surface system resulted from a sloping downward penetration of the upper cyclonic cell and, due to the slope, the lower disturbance was properly located under the divergent flow aloft. Subsequent studies show that the upper cell does not penetrate into the lower troposphere but that the surface disturbance is induced by the upper divergence, and thus the TUTT cyclonic cell and the initial surface cyclonic disturbance are separated by some 300 to 500 km. Another modification is a more detailed description of the upper circulation patterns afforded by the better satellite data and the increased number of aircraft wind observations.

Figure 1 is a schematic depiction of the model in three stages. In stage 1 the upper cell is quite large and intense with typical dimensions in the central Pacific of 1000 to 2000 km and wind speeds in all quadrants of 40 kt and greater. The cell is shown as penetrating vertically to the 500 mb level. [NOTE: The weak link in the model is in the midlevels since there are essentially no observations between the surface and 30,000 ft except for the few widely spaced rawinsonde stations.] The flow to the east and southeast of the cell is divergent in direction and, in general, accelerates downstream due to the strong southwest current of the TUTT to the east. Underneath this divergent region a trough is induced in the lower levels and in stage 1 it is shown extending upward through 700 mb. The initial organized convective cloud system is observed to form in the region of the upper divergence and in the low level trough. The precise position of the clouds in respect to the low level trough cannot in general be determined since the pre-vortex

surface system is weak and the position and orientation of a minimum pressure line cannot be determined from the available observations. For the same reasons, it is not possible to specify precisely whether the cloud system forms prior to the surface trough, but suffice to state that extensive convective cloud systems, initiated from aloft, are often observed in regions where a surface pressure trough is difficult to find.

In stage 2 the satellite observes a significant increase in the area of organized convection under the upper divergent region east of the upper cell. The increased convection considerably alters the upper tropospheric flow as follows: (1) The convective heating builds a sharp ridge to the east and northeast of the TUTT cell which (2) "pushes" the TUTT northward beginning a split or segmentation of the TUTT and (3) decreases the size and circulation intensity of the TUTT cell. The lower circulation is indicated in the early depression stage with a closed vortex below 500 mb. The major convective cloud mass is to the east of the low level vortex. Other cloudiness may or may not be distributed around the surface system. Because the upper cell is decaying, it is depicted as not penetrating downward to the 500-mb level. Stage 3 depicts the strong depression or early tropical storm stage. The upper tropospheric flow becomes more complex as the increased convection intensifies the ridge or builds an anticyclone whose outflow interacts with and further distorts the TUTT. The parent TUTT cell is essentially destroyed and becomes just a weak cell in the southern branch of the split TUTT. In the western end of the northern branch it is quite common to observe a small cyclone formed between the northeast current south of the subtropical ridge and the south to southwest current west of the ridge or anticyclone. In the model it is only depicted for stage 3, but may also occur in stage 2. This secondary small cell often has an associated small cloud system as depicted in stage 3. The tropical storm is shown as

a cyclonic vortex up through 500 mb with the capping anti-cyclone in the upper troposphere. The storm center is depicted as located in the southwest sector of the anticyclone and central dense overcast (CDO). The storm center asymmetry with respect to the center of the satellite-observed CDO probably stems from the locations of the outflow channels available to the anticyclone. In this case the outflow is not impeded to the east where it merges with the larger scale westerlies south of the TUTT; therefore, the cirrus shield is skewed toward the east. Storms which are initiated by the cells in the upper trough, north of about 15°N, do not have an available upper-level outflow channel to a large scale easterly flow. This may be one of the reasons they seldom reach hurricane or typhoon intensity.

3. SELECTION OF CASE STUDIES, DATA SOURCES, AND ANALYSES

3.1 CASE STUDY PERIODS

Two periods have been selected to illustrate the model. The first period, during the development of T.S. Therese in late July and early August 1970, was selected because the TUTT cyclonic cell passed over Midway Island and the rawinsonde data provide additional clues concerning the vertical coupling of the upper and lower systems.

The second period was selected to take advantage of the Defense Meteorological Satellite Program (DMSP) high resolution satellite data. It covers the first 10 days of August 1973 during the initiation and development of T.S. Hope and T.D. No. 11 in the central Pacific, Typhoon Iris near Guam, and Typhoon Georgia just north of the Philippine Islands.

The model is best illustrated by systems in the central Pacific such as T.S. Hope, T.S. Therese and T.D. No. 11. In this region between Midway, Marcus, and Wake Islands there is little ambiguity in the observed order of events because: (1) the upper cyclones are initially quite intense and therefore persistent; (2) the surface cyclones are observed to definitely form in the easterlies far removed from any near-equatorial trough; and (3) the cloud system associated with the development is easily recognized for it is in an area of otherwise minimum cloudiness. Typhoon Iris will illustrate the origin uncertainty of some of the tropical cyclones in the western Pacific, particularly those forming between 15N and 20N.

3.2 KINEMATIC ANALYSES

The wind fields for the surface and upper troposphere were analyzed once daily. The 250-mb level was selected as the primary level for the upper troposphere due to the greater number of aircraft wind observations (PIREPS) near this altitude. However, the PIREPS data base is a composite of the observations from 30,000 to 40,000 ft and the 200-mb and 300-mb wind and temperature are additionally plotted at the rawinsonde stations (see plotting model, Figure 4). The upper troposphere data base was also augmented by off-time aircraft observations within $\pm$9 hours of map time. The off-time data were plotted in different colors and reproduced in the figures as lighter grey. The wind directions obtained from the satellite observations of cirrus clouds are shown by short arrows. The maximum wind speeds tend to occur in narrow bands or "jet streaks." These higher speed currents often have an associated narrow band of "independent" cirrus visible in the satellite data (Sadler, 1974). The positions of these bands are shown by lines of short arrows.

3.3 SATELLITE DATA

The observations for T.S. Therese in 1970 are from the gridded visual channel pictures of individual orbits from ITOS-1. The picture times in the central Pacific were between 0100 and 0400 GMT. The observations for the second period in early August 1973 are from the DMSP satellite 5528 and were obtained from the 1st Weather Wing stations on Guam and Hawaii. Only the visual-channel data were available from Guam. The times of observation were near 0000 GMT in the central Pacific and 0300 GMT in the western Pacific. The cloud systems observed by satellite are sketched on the surface and 250-mb analyses to aid in noting relationships between cloudiness and circulation.

4. FIRST PERIOD -- 26 JULY-2 AUGUST 1970

4.1 TROPICAL STORM THERESE

The 0000 GMT positions and track of T.S. Therese from the Joint Typhoon Warning Center (JTWC, 1970) are shown in Figure 2d. The surface disturbance on 30 July became a depression on 31 July and a tropical storm late on 1 August. We have extended the history back to a possible surface trough on the 28th and 29th of July. The track of the parent TUTT cell, noted as UC-1, is shown from our initial day of analysis on 26 July to 1 August. Note that the two tracks cross as the surface system intensifies and the UC-1 weakens and decays. The history of UC-1 previous to 26 July is unknown since continuity of these systems cannot normally be determined from the historical operational analyses.

The ITOS-1 observations of the area surrounding the UC-1 and developing Therese are shown in Figure 3 for the period 26 July-2 August.

a. 26 July

UC-1 was located near 31N, 167W (Figure 4). The center position was placed near the lighter winds. The peripheral winds were quite strong, being at least 70 kt to the south and 50 kt to the west and east of the system at 35,000 ft.

There was no organized significant convective cloud system within 1000 km to the east or south of UC-1 (Figure 3). This is important to establish the fact that there was no independent surface disturbance moving in from the east.

b. 27 July

UC-1 moved west-southwestward toward Midway (Figure 5) and an area of organized convective cloudiness formed southeast of the center (Figure 3). The winds derived from the cirrus cloudiness, particularly the thin east-west line near 28N between 168W and 164W and the short, thin cirrus line just west of 170W between 28N and 29N oriented south-southeast to north-northwest, aided the analysis and indicated the diverging flow over the convection. The westerly current south and east of the TUTT at 150W had an observed speed of 80 kt at 35,000 ft.

c. 28 July

UC-1 continued on a west-southwestward path and was located some 200-300 km east-northeast of Midway (Figure 6). There was only one off-time aircraft observation near the system, but the increased organized deep convection with "fanning" cirrus (Figure 3) aided the analysis and placement of the center and indicated the divergent wind flow and increase of ridging over the convection. As a consequence of this ridging, although UC-1 had moved southward, the TUTT moved northward just to the east of UC-1. At the surface (Figure 7) there was insufficient data to determine the existence or position of a trough. A ship in the cloud system reported showers and middle clouds.

d. 29 July

UC-1 continued west-southwestward and the center passed over or very near Midway prior to 1200 GMT (Figure 8). The satellite photograph (Figure 3) revealed a considerable increase in the convective cloud system to the east and southeast of the cell. The wind directions indicated by the blowoff cirrus and the thin line of cirrus crossing 30N near 175W, together with the few PIREPS to the south, showed

increased ridging over the convection which moved the TUTT further northward east of the cell and increased the "split" in the TUTT. The northern branch east of UC-1 was near 33N and the southern branch west of UC-1 was near 27N. The westerly current south of the TUTT to the east of the convection and ridge was quite strong and increased in speed downstream from 50-55 kt at 170W to 60-70 kt at 150W.

As on the 28th, the surface data (Figure 9) were insufficient to identify or position a surface trough. A ship near 24N, 174W, on the western edge of the cloud system, observed a southeast wind of 15 kt. This observation would support a weak trough near 175W.

Since it is rare to have the center of an upper cell pass so near a rawinsonde station, time-altitude sectional analyses of various parameters were made for the 5-day period from 27 through 31 July. Figure 10 is the sectional plot of temperature, humidity, height, and winds. The average base of the tropopause was near 42,000 ft. In the 5-day average of temperatures for 27-31 July, a stable layer of -63°C extended from 42,000 ft to 60,000 ft (not shown), above which the temperature increased to -57°C at 70,000 ft. The wind analysis of Figure 10 indicates that the upper cell was centered between 35,000 ft and 40,000 ft and extended downward as a closed cell through 30,000 ft and as a cyclonic wind perturbation to near 20,000 ft. Assuming the normal TUTT slope to the south with decreasing height, the cell was probably closed down through 25,000 ft.

The height anomalies, from the 5-day average of 27-31 July, were a maximum of minus 60 meters at the UC-1 center between 35,000 ft and 40,000 ft (Figure 11). The negative anomalies associated with UC-1 began near 1200 GMT on the 28th and extended through 0000 GMT on the 30th. There were negative height anomalies throughout the troposphere, except

for a very thin surface layer beneath the cell. The horizontal gradients of the height anomalies associated with UC-1 were well organized down to about 500 mb. Below this level the anomalies were weak and horizontally stratified. It appears as if the lower levels felt the effect of the imposed cell aloft, but not in a direct, vertically coupled sense.

The zero height anomaly isopleths outlining the size of the system were essentially vertical and spaced some 36 to 48 hours apart. UC-1 was moving at a speed of 4 degrees per day (Figure 2); therefore, its horizontal dimensions, as it passed Midway, were on the order of 600 km to 800 km. This is in agreement with the analysis of Figure 8, and a comparison of this analysis with those of the previous days (Figures 4, 5, and 6) would indicate that the upper circulation had decreased in size.

Figure 12 is an analysis of the temperature anomalies from the 5-day average of 27-31 July. Zero anomaly was observed at the level of the UC-1 center. Negative anomalies were observed throughout the layer below UC-1 with the largest anomaly of -3°C below the cell between 25,000 ft and 30,000 ft. Below 20,000 ft the weaker anomalies were in a layered pattern similar to that of the height anomalies in Figure 11. A strong positive anomaly was observed above the level of UC-1 with the maximum value of 5°C at 0000 GMT on the 29th at 42,000 ft near the base of the tropopause, which had lowered to near 40,000 ft.

Figures 13 and 14 are analyses of the 24-hour changes in height and temperature, respectively. As UC-1 approached Midway, the heights fell throughout the troposphere and lower stratosphere. The maximum change of -80 meters was at the level of UC-1 and leading in time by some 24 hours. The negative change pattern was well organized down to 500 mb. Below 500 mb the weak negative changes were horizontally stratified similar to the height anomalies discussed for

Figure 11. The zero isopleth of change through the cell center was essentially vertical down through 25,000 ft. Below this level there were weak layered changes, alternating positive and negative.

As UC-1 approached Midway, cooling was observed throughout the troposphere below the level of the cell center. The pattern was well organized down to 500 mb and was a maximum of 3° per day in the layer between 25,000 ft and 35,000 ft (Figure 14) and coincided in time with the maximum negative height changes. Below 500 mb weak cooling was observed and again in a layered structure. Above the level of UC-1 and over the area of strongest cooling in the midtroposphere was a region of strong 6°-per-day heating centered between 42,000 ft and 45,000 ft, in the tropopause stable layer.

The moisture analysis of Figure 15 reveals that the column was very dry underneath UC-1, particularly in the western sector at 0000 GMT 29 July, just prior to the center passage over Midway. The relative humidity was less than 10% at and above 700 mb and the 50% isoline was depressed to 850 mb. The observations of nearly clear skies and a very dry air column require a sinking motion beneath UC-1. The very low relative humidity and dew point at the surface and the absence of an inversion (Figure 10) would suggest that the sinking air reached the surface. The observed cooling of the sinking air implies a direct circulation which is in agreement with the previous findings of Ricks (1969) and Frank (1970) for cold lows in the Caribbean. Cooling of the sinking air requires that radiational heat loss overcome subsidence heating. This loss was probably due to two factors: (1) greater radiation due to the radiating surface -- the ocean or the top of the low, thin moist layer -- having a high radiating temperature; and (2) less absorption of the radiation by the very dry column above the radiating surface. Sinking of air within the tropopause stable layer

produces much greater adiabatic warming than within a comparable layer of the midtroposphere where the dry adiabats are near parallel to the observed temperature sounding. The height of the tropopause lowered some 2000 ft over UC-1. Comparable sinking of the air in the tropopause stable layer is more than sufficient to account for the observed warming above UC-1.

e. 30 July

UC-1 continued its slow westward movement (Figure 16). The observations were insufficient to determine the center of the cell or to determine the existence of a second cell to the north in the western end of the northern segment of the split TUTT. There were isolated cumulonimbus associated with the northern TUTT segment (Figure 3).

A small anticyclone associated with the increasing convective cloud system (Figure 3) passed over Midway just prior to 1200 GMT (Figure 16) and was centered between 35,000 ft and 40,000 ft (Figure 10). A strong trough was observed at the surface near 179W with the possibility of an initial small cyclonic center in the trough near 27N (Figure 17). The northern end of the trough was located just west of Midway and a 24-hour pressure fall of some 2 mb was observed at 1200 GMT with fresh southeasterly winds and showers (Figure 10). The sectional wind analysis of Figure 10 indicates that the trough sloped eastward with height and extended to 20,000 ft at Midway, was positioned beneath the upper anticyclone, and lagged the upper cell by some 18-24 hours with no direct vertical linkage between the upper cell and the lower disturbance.

Since the surface system was in the early development stage and Midway was on the northern edge, little detail is available from the Midway sectional analyses. The height and temperature anomalies were very weak negative up to 20,000 ft

(Figures 11 and 12). The 24-hour height change was essentially zero at the surface trough and weak positive from 850 mb to 400 mb (Figure 13), and the 24-hour temperature change was weak positive above a thin surface positive change of 2°-3°C (Figure 14). After the center of the upper cell passed but prior to the passage of the low level trough, the moisture increased in the midtroposphere up to 20,000 ft and altostratus clouds and showers were observed at 0000 GMT, 30 July (Figures 15 and 10). After trough passage, the moisture increased below 10,000 ft and above 20,000 ft and decreased in the midlevels.

f. 31 July

UC-1 continued to move westward and decrease in intensity (Figure 18). A secondary cell had formed in the western end of the northern branch of the split TUTT. The surface system (Therese) had intensified to a definite closed cyclonic circulation (Figure 19). The major convective cloud system (Figure 3) was located between UC-1 and the upper ridge and in the eastern sector of the surface cyclone. A small cloud system was associated with the secondary TUTT cell to the north of UC-1.

g. 1 August

Therese continued to intensify as indicated by the better organized cloud system (Figure 3) and a ship observation, just north of the center, of 35 kt winds, 1012.5 mb pressure, and heavy rain showers (Figure 20). UC-1 was essentially dead as an identifiable system (Figure 21) as the upper ridge continued to build over the convective cloud mass.

It is usually about this time in the development cycle that the tracks of the upper system and the lower system cross. The upper system, as a decayed entity, is "pushed" southwest by the intensifying ridge and the lower system

acquires a northerly component. One reason for the northerly component is illustrated in Figure 22. In the early stages, the lower system is shallow and moves with the lower tropospheric flow. As it intensifies and extends vertically, the upper portion is embedded in the larger-scale southerly flow of the upper troposphere. The resultant is a northwesterly direction.

h. 2 August

Therese intensified to tropical storm intensity early on the 2nd and continued northwestward through the subtropical ridge. The satellite view of the early tropical storm stage is shown in Figure 3 and her subsequent track, from JTWC (1970), is shown in Figure 2d.

5. SECOND PERIOD -- 1-12 AUGUST 1973

The summer circulation of 1973 was very anomalous. In the central and western Pacific these anomalies were quite striking in both the lower and upper troposphere. In the upper troposphere, westerly winds prevailed in the equatorial region east of 120E. In the lower troposphere, the monsoon westerlies were infrequent east of the Philippines and persistent moderate easterlies covered the tropical western Pacific. The western North Pacific tropical cyclone season was one of the most anomalous on record (JTWC, 1973). No tropical storms formed during the first 6 months and no storms of typhoon or tropical storm intensity occurred south of 15N in or east of the Philippine Sea until October. Most of the summer typhoons and tropical storms of the western Pacific, excluding the South China Sea, were initiated from aloft.

Tracks of three of the four which formed in early August are shown in Figure 2a, b, c. The tracks are from JTWC (1973) with noted adjustments from this study. The tracks of the parent TUTT cells are shown by lines of short arrows.

The satellite and PIREP data bases are superior to those of 1970; therefore, the upper tropospheric analyses are in more detail. The analyses and the satellite mosaic for most of the Pacific are presented in the figures for any detailed study the reader desires. Our discussions will cover only the general features for the development phase of each tropical cyclone. The history of the persistent upper cells is unknown prior to our initial day of analysis on 1 August for reasons previously stated.

5.1 TROPICAL STORM HOPE

The tracks of T.S. Hope and the parent upper cell UC-5 are shown in Figure 2a. UC-5 moved generally westward at a rather slow speed of 8-9 kt. The circulation was quite large but asymmetrically organized on the 1st (Figure 23) with troughs extending to the south, northeast and west. The peripheral circulation speeds were at least 40 kt in all quadrants. There were no surface systems of consequence to the east of UC-5 (Figure 33), only a hint of a very weak trough along 170W underneath the diverging winds aloft (Figure 23). No cloud system was observed near 170W (Figure 44). Isolated, scattered, towering cumulus and cumulonimbus were observed near UC-5 and in the three trough branches.

UC-5 was more circular and slightly larger on the 2nd (Figure 24). Scattered cumulonimbus remained near the center and thin lines of cirrus formed to the northwest of the center in the northeasterly current (Figure 45). A surface trough was no more apparent on the 2nd (Figure 34) than on the 1st. The clouds far to the east of UC-5 were from dying Tropical Storm Doreen as her top was being sheared off and advected to the north by the southerly winds aloft.

UC-5 was very large and symmetrical on the 3rd (Figure 25). The observed peripheral winds had increased to 50 kt or greater in the northwest and southerly sectors. The center was clear (Figure 46). Scattered cumulonimbus existed some 3 degrees west of the center and a very small convective area was observed east and northeast of the center. A satellite IR view is shown in Figure 47. A broad, weak, surface trough near 180° could be supported by the few observations (Figure 35).

Little change occurred in the UC-5 circulation between the 3rd and 4th except the beginning of ridging and divergence of the wind stream to the east of the cell (Figure 26). The northeasterly current, some 600 km northwest of the center, increased to at least 60 kt and had an associated well-defined cirrus band (Figure 48). A few scattered cumulonimbus were again observed near the center of UC-5 and narrow bands of cloudiness encircled the cell from the northwest through south to southeast. The convective area northeast of the center had increased. These cloud features are also prominent on the IR photograph (Figure 47). A weak surface trough was retained on continuity (Figure 36).

The convective area east of the center had increased considerably by the 5th (Figure 49). A few cumulonimbus were isolated near the cell center. The cirrus band northwest of UC-5 in the northeasterlies was not as sharply defined as on the 4th and the numerous PIREPS indicated a decrease to 50 kt in the speed of the current (Figure 27). The increased convection to the east of UC-5 coincided with the divergent wind region and a broad 40 kt current existed downstream to 165W, or some 2000 km. There were few observations at the surface (Figure 37); however, they would support a weak, broad trough east of UC-5.

The convection east of UC-5 continued to increase on the 6th (Figure 50) as did the ridging over the convection (Figure 28). UC-5 continued its decrease in size from the 3rd (Figures 25-28). The circulation to the north of the cell had changed considerably as the subtropical ridge was being segmented by the approaching deep trough in the westerlies, and some of the southerly flow east of UC-5 was through the ridge to the midlatitude westerlies. There were no observations at the surface near UC-5 and the trough was maintained on continuity (Figure 38).

The split in the subtropical ridge continued on the 7th (Figure 29) and the ridge sharpened east of UC-5. UC-5 continued to decrease in size. There was increased outflow and exchange to the midlatitude westerlies. A gap occurred in the satellite coverage, which was unfortunate at this critical time since the data indicated a surface low had formed (see Figures 51 and 39).

The satellite on the 8th revealed a very large cloud mass with increased organization but no obvious CDO (Figure 52). The large scale outflow, indicated by the cirrus, was on the west and north side into the midlatitude westerlies as confirmed by the observed upper flow pattern (Figure 30) around a cell in the subtropical ridge and in advance of the next deep trough in the westerlies just east of Japan. There was no path for outflow to a broad-scale easterly current, and outflow to the westerlies south of the TUTT was restricted by a southward protrusion of the ridge in advance of the next TUTT cell UC-7. UC-5 had decayed to a small, weak system in the TUTT. Data was insufficient to position the surface cyclone with any certainty (Figure 40).

Hope was classified as a tropical storm by JTWC late on the 9th (Figure 2a). She had a very small CDO (Figure 53) and a small capping anticyclone revealed by the cirrus, particularly the narrow cirrus band extending southeastward from north of the system to the TUTT at 22N. The cirrus pattern north of Hope also indicated that the subtropical cell was separate from the small anticyclone over Hope. This could be accommodated by the PIREPS (Figure 31); however, the principal outflow remained to the midlatitude westerlies. Marcus Island was in the surface westerly flow of Hope and located some 400 km southwest of the center (Figure 41).

Hope existed as a tropical storm through the 11th and then decayed. Subsequent satellite views are shown in Figures 54, 55, 56; her rather rapid demise is well illustrated by the photographs on the 12th and 13th (Figure 56).

5.2 TROPICAL DEPRESSION NO. 11

The tracks of T.D. 11 and its parent cell, UC-7, are shown in Figure 2b. The speed of UC-7 averaged about 12 kt, or somewhat greater than the speed of UC-5.

UC-7 was formed by the interaction of a midlatitude trough with the tropics. A shortwave trough located near 180° and 50N on the 1st (Figure 23) moved rapidly eastward (Figure 24) into the longwave position and northeast terminus of the mean TUTT (Sadler, 1972). It intensified and penetrated southward, and UC-7 was born near 38N, 158W (Figure 25) on the 3rd. The UC-7 circulation was well positioned by the associated cirrus on the 4th (Figure 47) and 5th (Figures 47 and 49). It had moved southwestward and crossed the surface ridge (Figures 36 and 37). A previous upper cell southeast of UC-7 (Figure 25) "opened up" and became a strong appendage trough to the southeast (Figures 26-29). The surface trough on the 6th and 7th (Figures 38 and 39) was probably associated with the appendage trough rather than with UC-7.

UC-7 was quite large and well organized on the 7th (Figure 29) and the convective area to the east had increased from a very small mass on the 6th (Figures 47 and 50) to an extensive one on the 7th (Figures 47 and 51). The convection continued to increase and was quite impressive on the 8th (Figure 52). An associated surface trough was positioned near 179E (Figure 40). UC-7 had begun to decrease in size and intensity (Figure 30).

Convection remained intense east and northeast of UC-7 on the 9th (Figure 53) and the upper ridge increased over the convection (Figure 31). The TUTT was "pushed" north by the ridging and became further segmented as the decaying UC-7 moved west-southwest. Two small isolated patches of convective clouds were observed in the segmented TUTT north of the ridging (Figure 53). There were insufficient data to properly identify or position the surface system (Figure 41); however,

by the 10th (Figure 42) we elected to show it as a small closed cyclone, based mainly on the two observations of lower pressure at 25N than at Wake Island near 19N. The surface system was on the western edge of a large, well-organized convective cloud system (Figure 54). The upper ridge increased in size over the convection and "pushed" the segmented TUTT further north (Figure 32). A small cell formed in the western end of the northern segment of the TUTT as shown by the satellite photograph (Figure 54).

The surface cyclone was verified on the 11th by the west wind observation at 24N; however, there were no observations near the center (Figure 43). Cloudiness surrounded the center, but there was no associated CDO (Figure 55).

On the 12th there were increased bands of convection east of the center (Figure 56) and by the 13th (Figure 56), the satellite-observed increase in cloud organization and a small CDO of almost 2° in diameter would support a weak tropical storm intensity of 35-40 kt (Dvorak, 1973). TD-11 moved northwestward (Figure 2b) and began a slow weakening on the 15th before changing course through north to east.

5.3 TYPHOON IRIS

The early stages of Typhoon Iris illustrate the difficulty of applying the generalized model to the development cycle in the western Pacific below 20N. In this region the cells in the TUTT are generally weaker; therefore, time and space continuity is more difficult to maintain than farther east. The general background cloudiness is greater and more variable, making it difficult to assign an observed cloud mass to a specific circulation. The position of the mean east-west surface monsoon trough is north of 10N, making it difficult to determine whether the surface system is initiated by the upper circulation or forms in the pre-existing surface trough with upper outflow aided by the TUTT as described by Sadler (1974).

The history of Iris is shown in Figure 2c. The JTWC track has been adjusted backward in time from the 8th to indicate a surface disturbance from the 6th. Also shown is a probable track of the upper cyclone UC-3. The cell could be identified from the 1st (Figure 23) as it moved westward (Figure 24) to a position just north of Guam on the 3rd (Figure 25). However, since the upper circulation over the western Pacific became more complex after the 1st (Figures 23-26) as UC-6 moved south and then west to link with a cell over the South China Sea, and as UC-4 continued west-northwest, and as an anticyclone formed over the convection generated to the east and northeast of UC-3, the history of UC-3 became indefinite after the 3rd. We chose to identify the weak cell northeast of Guam on the 4th, 5th, and 6th (Figures 26-28) as the looping UC-3 as indicated in Figure 2c.

Cloudiness in the western Pacific north of 10N was extensive on 1-6 August (Figures 44-50). It was also highly variable in time and space with large convective areas appearing and disappearing in association with the large variability in the upper circulation mentioned earlier. The observed cloudiness south of 10N was also highly variable, consisting of large convective masses with little or no continuity from day to day. The larger cloud systems have been "tagged" on the photographs for easier assessment of their history. Those south of 10N are numbered and those north of 10N are lettered. The ones with any reasonable 24-hour continuity keep their identifiers.

In contrast to the highly variable cloudiness and upper tropospheric circulation, the low level circulation was rather simple during early August (Figures 33-43). There was no monsoon trough and the flow was essentially easterly. Weak surface troughs in the easterlies were generated by the massive convective areas, but since these cloud masses had no time or space continuity, neither had the troughs.

The Iris surface depression formed in the easterlies on the 6th (Figure 38) and passed Guam between the 6th and 7th (Figure 39). Twenty-four-hour negative surface-pressure changes began at Guam late on the 5th and continued 1 to 2 mb negative through the 7th (not shown), indicating the system was deepening as it passed Guam.

The position of the weak UC-3 was northeast of Guam on the 6th; however, its center could not be accurately positioned from the wind observations (Figure 28) or the cloudiness (Figure 50). The cirrus bands indicated strong winds just to the east and southeast of UC-3 and their orientation showed a diffluent pattern. Speeds of 55 kt were observed in the southwesterly flow some 1000 km downstream from the cell. There were a few convective clouds around the Iris surface disturbance.

UC-3 moved southwest, the surface disturbance moved westward, the tracks crossed, and on the 7th the surface disturbance (Figure 39) was northwest of the UC-3 and the outflow for Iris was toward the northwest as shown by the satellite-observed cirrus pattern (Figure 51). The cloudiness around the surface circulation remained scattered as on the 6th.

By the 8th an anticyclone (Figure 30) had formed over the convection as indicated by the large convective cloud mass with streaming cirrus edges (Figure 52). The cloudiness had increased around the surface system (Figures 40 and 52), but there was no CDO. The outflow pattern was better organized and expanding. Unlike the three previous systems, Iris had an available outflow channel to the large scale easterlies across the southern Philippines and into the Indian Ocean.

The outflow pattern continued to expand on the 9th (Figure 31) and 10th (Figure 32), with good outflow channels to large scale easterlies across the southern Philippines and the large scale westerlies south of the TUTT. Iris reached storm intensity on the 10th and became a typhoon on the 12th. There was no associated CDO on the 9th (Figure 53) and the Iris circulation was outside the main cirrus shield on the 10th (Figure 54). The observed cloudiness became more symmetrical about the center on the 11th (Figure 55), 12th and 13th (Figure 56), but Iris never had a satellite-observed CDO throughout her lifetime.

Iris was moving northward from the 9th and, by the 10th, into the region of upper tropospheric westerlies south of the main TUTT positioned along 27N (Figure 32). She began a tight loop on the 11th and was essentially stalled for two days before continuing her northwest journey. It is very unlikely that the stall was due to a "Fujiwhara" interaction (Brand, 1968) with the distant (> 1000 nm) and weak Tropical Storm Hope. It was probably due to the entanglement with, and slow journey through, the TUTT. Since large forecast errors are associated with typhoons which loop or stall (the 24-hour forecast errors for Iris during the stall were in excess of 200 miles), a fruitful area of research would be the relationship between the observed typhoons which loop or stall and the position and intensity of the TUTT. The cases should be restricted to the most recent 10 years. Only during this period are the PIREPS and satellite data sufficient to permit a reasonable upper tropospheric analysis.

6. SUMMARY

Tropical cyclones initiated by cells in the TUTT are a summer feature of the central and western North Pacific. They are most prevalent in the region bounded by Wake Island, Midway Island, and Marcus Island during the period from July through September when the TUTT is most intense and at its most northern position (Sadler, 1972).

During the adjacent months of June and October the TUTT is weaker and some 5 degrees south of the midsummer position. The region of surface cyclone initiation by TUTT cells shifts southward to between 15N and 20N and is most likely west of Midway Island.

The surface system is initiated by the upper divergence to the east of the upper cell, and the associated convection builds an upper tropospheric ridge or anticyclone which segments the TUTT and weakens or destroys the parent upper cell. By examining case studies and meshing the satellite observations and conventional data, a synoptic model is developed and illustrated. The model differs from a previous one proposed by the author (Sadler, 1967) in the manner of vertical coupling between the upper cell and the surface system. The improved satellite data and increased quantity of PIREPS show that the surface system is not the result of a sloping penetration of the upper cell into the surface layer as previously proposed, but is initiated by the upper divergence which is characteristically some 500 km east of the upper cell. This feature was verified by rawinsonde observations during the early stages of T.S. Hope when the parent upper cell fortunately passed over Midway Island at a time near its maximum size and intensity and prior to the formation of the surface vortex.

The current study verifies a very important feature of the previous model: The surface system is initiated by the upper circulation and is not an independent system which had previously existed in the easterlies and, through relative motion, moved under the upper cell into a position favorable for intensification.

7. ADDITIONAL COMMENTS

7.1 THE ORIGIN AND HISTORY OF TUTT CELLS

The Tropical Upper Tropospheric Trough (TUTT) is a feature of the very large-scale general circulation (Sadler, 1972). The principal mechanism for the generation of an intense cyclonic cell in the trough is by the interaction with midlatitudes (Murakami and Sadler, 1974), as a shortwave trough in the westerlies moves into the longwave position, intensifies, penetrates southward, and forms a cutoff low. UC-7 is an excellent example. A most favorable position for such interaction is the eastern Pacific where the mean longwave in the westerlies merges with the mean northeast terminus of the TUTT (Sadler, 1972) and there is no intervening subtropical ridge separating the two. The subsequent track of the cells is generally southwesterly, then westerly, along the TUTT. The longwave position near Japan is another interaction region. However, there the deepening troughs in the westerlies must segment a persistent subtropical ridge to form cutoff lows south of the ridge. The cells are initially weaker than those of the eastern Pacific and continuity is difficult to maintain. There is an example in the first period (Figures 4, 5, 6, and 8), but the cell is unnumbered. The western Pacific cells also move southward and westward; two good examples are UC-6 and UC-8 of the second period.

UC-6 also illustrates another very interesting feature of TUTT cells: they grow and intensify significantly as they move inland over China. UC-6 was near 29N, 142E on 1 August (Figure 23). It moved southward to 27N and then westward as a weak cell (Figures 24-28) until moving over land on 7 August (Figure 29) where it increased, by 9 August (Figure 31), to a diameter of more than 1000 km with wind speeds of 45-55 kt

at 35,000 ft. On 10 August, our last day of analysis, it was located over the Himalayas near 27N, 100E, and was decreasing in size and intensity. Its average speed of movement during the 9 days was approximately 12 kt.

These observations lead to the conclusion that the energetics of cold lows should be studied over China. The principal advantages are (1) a good network of radiosonde stations and (2) the cells are not destroyed by an organized convective cloud system associated with an induced surface disturbance. There are thunderstorms during the afternoon due to extreme convective instability caused by the combination of surface heating and upper tropospheric cooling associated with the cold low; however, the thunderstorms are isolated and short-lived. Nights are clear and radiation ground fog is prevalent during early morning hours. It is a typical showers regime (see Ramage, 1971, p. 109).

7.2 THE TUTT AS THE PRIMARY SOURCE OF WEATHER DISTURBANCES IN THE TRADE-WIND ZONE

In the previous study (Sadler, 1967), the author proposed that most of the disturbed weather of the trade-wind zone is initiated by the circulations associated with the upper tropospheric trough. This paper supports those findings, but the details are left to the reader. To aid those who may wish to note the relationship between the satellite-observed cloudiness and the circulations of the upper and lower troposphere, the upper trough position is shown on the satellite photographs and the satellite-observed major cloud systems are sketched on the surface and upper air analyses.

The following general features are readily apparent from just a cursory inspection:

a. Most major cloud masses north of 10N, not associated with tropical cyclones, lie just to the east and south of the upper trough in a region of upper tropospheric westerlies and lower tropospheric easterlies.

b. Upper tropospheric cyclonic flow is associated with minimum cloudiness; however, isolated cumulonimbus often occur in the upper trough region due to the increased convective instability caused by the cooling of the upper troposphere.

c. The cloud systems not associated with tropical cyclones, particularly those south of 10N in the mean maximum cloud zone (MCZ), seldom have a lifetime of 24 hours.

7.3 EXTRAPOLATION OF RESULTS TO OTHER AREAS

These results are applicable to other areas dominated by the tropical upper tropospheric trough. In the Southern Hemisphere, a summer TUTT lies over the trade-wind region of the east central Pacific (Sadler, 1972) extending from French Polynesia toward Easter Island. Induced tropical cyclones have been observed in this area (Miyakoda, et al., 1974).

A TUTT is a dominant feature of the summer over the north Atlantic Ocean, Gulf of Mexico, and Caribbean Sea. A much larger percentage -- perhaps approaching 75% -- of the depressions and named storms in this area probably have their origin from upper level inducement because of the absence of a low level monsoon trough in the western Atlantic. The cyclones of low level origin over the western Atlantic migrate from the monsoon trough over Africa or the extreme eastern Atlantic and very few survive the journey, or they may form in the western Caribbean or southern Gulf of Mexico during

the occasional penetration of the monsoon westerlies of the eastern North Pacific across Central America. Detailed synoptic studies by Fernandez-Partagas (1969) and Fernandez-Partagas and Estoque (1970) showed that the majority of tropical disturbances in the eastern Caribbean Sea and BOMEX area were induced by the upper tropospheric cells.

ACKNOWLEDGMENTS

Appreciation is expressed to Mr. Louis Oda for plotting and drafting the figures and to Mrs. S. Arita for typing the manuscript. Thanks are given to the personnel of the 1st Weather Wing, Air Weather Service, for making the DMSP photographs available and to the Fleet Weather Central at Pearl Harbor for a listing of the pilot reports.

REFERENCES

Brand, S., 1968: Interaction of binary tropical cyclone of the western North Pacific Ocean. NAVWEARSCHFAC Tech. Paper No. 26-68, 25 pp.

Conover, J.H., and J.C. Sadler, 1960: Cloud patterns as seen from altitudes of 250-850 miles -- preliminary results. Bull. Amer. Meteor. Soc., 41, No. 6, pp. 291-297.

Dvorak, V.F., 1973: A technique for the analysis and forecasting of tropical cyclone intensities from satellite pictures. NOAA Tech. Memo. NESS 45. National Environmental Satellite Service, Washington, D.C., 19 pp.

Fernandez-Partagas, J.J., 1969: A synoptic meteorological study for the eastern Caribbean area, July 10-25, 1967. University of Miami Tech. Report under Grant No. E-22-29-69-G, 42 pp.

Fernandez-Partagas, J.J., and M. Estoque, 1970: A preliminary report on meteorological conditions during BOMEX, fourth phase (July 11-28, 1969). University of Miami report under Grant NSF GA-10201, 95 pp.

Frank N.L., 1970: The energetics of cold lows. Proc. Symp. on Trop. Meteor., Honolulu, Hawaii. Boston, Amer. Meteor. Soc., EIV-1-EIV-5.

Joint Typhoon Warning Center, 1970 and 1973: Annual Typhoon Reports.

Miyakoda, K., J.C. Sadler, G.D. Hembree, 1974: An experimental prediction of the tropical atmosphere for the case of March 1965. Mon. Wea. Rev., 102, No. 8, pp. 571-591.

Murakami, T., and J.C. Sadler, 1974: On the fluctuation of the mid-Pacific trough during the early summer of 1971. Paper presented at Annual Meeting of Amer. Meteor. Soc., Honolulu, Hawaii. To be published.

Ramage, C.S., 1971: Monsoon Meteorology. New York: Academic Press.

Ricks, E.L., 1969: On the structure and maintenance of high-tropospheric cold-core cyclones of the tropics. M.S. Dissertation, University of Chicago.

Sadler, J.C., 1962: Utilization of meteorological satellite data in tropical meteorology. Proc. First Inter. Symp. on Rocket and Satellite Meteor. Amsterdam: North Holland Publishing Co., pp. 333-356.

Sadler, J.C., 1967: The tropical upper tropospheric trough as a secondary source of typhoons and a primary source of trade wind disturbances. University of Hawaii, HIG 67-12 and AFCRL-67-0203, 44 pp.

Sadler, J.C., 1972: The mean winds of the upper troposphere over the central and eastern Pacific. University of Hawaii, UHMET 72-04 and EPRF Tech. Paper No. 8-72, 29 pp.

Sadler, J.C., 1974: A role of the tropical upper tropospheric trough in early season typhoon development. University of Hawaii, UHMET 73-04 and EPRF Tech. Paper No. 9-74, 54 pp.

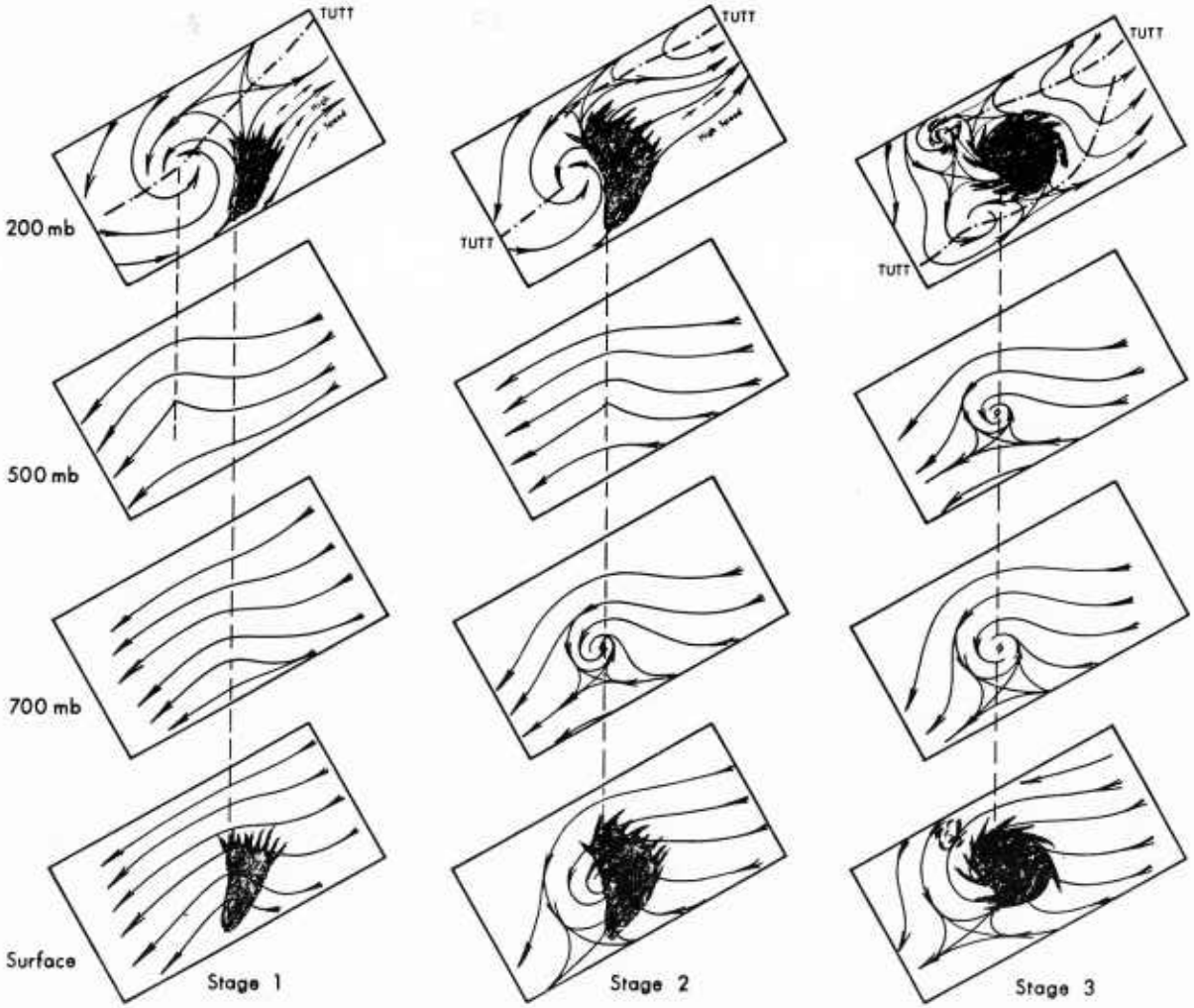

Figure 1. Schematic model of a tropical cyclone initiated by a circulation in the upper troposphere. See text for description.

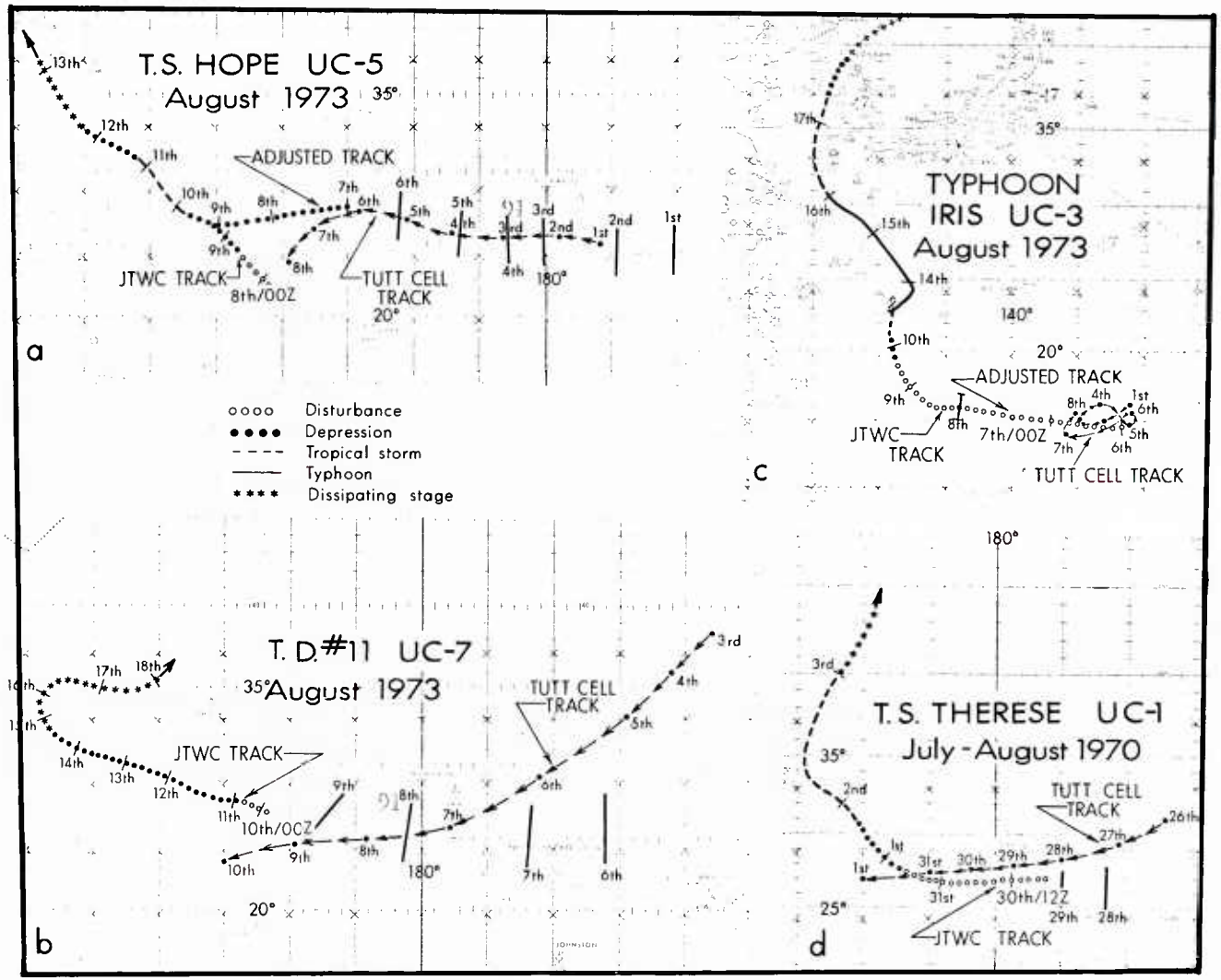

Figure 2. The tracks of Typhoon Iris, Tropical Storms Therese and Hope, and T.D. No. 11 (from JTWC, 1970 and 1973) plus adjustments and extensions. The tracks of parent TUTT cells are shown by lines of short arrows.

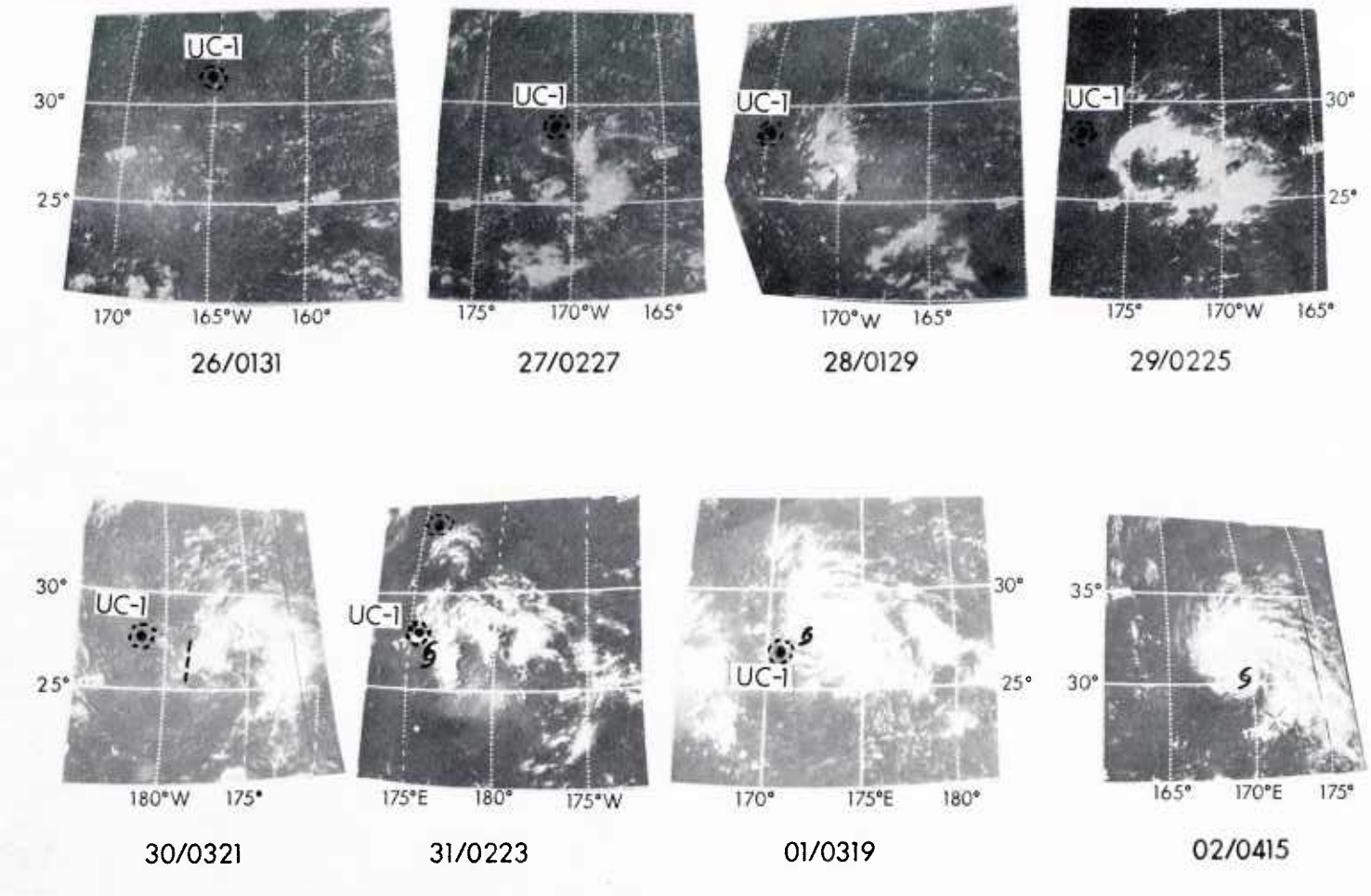

Figure 3. Daily IOTS-1 satellite observations for 26 July - 2 August 1970 during the development period of Tropical Storm Therese. The picture times are GMT. The position of the TUTT cell is noted by a circle and the surface cell by the standard symbol.

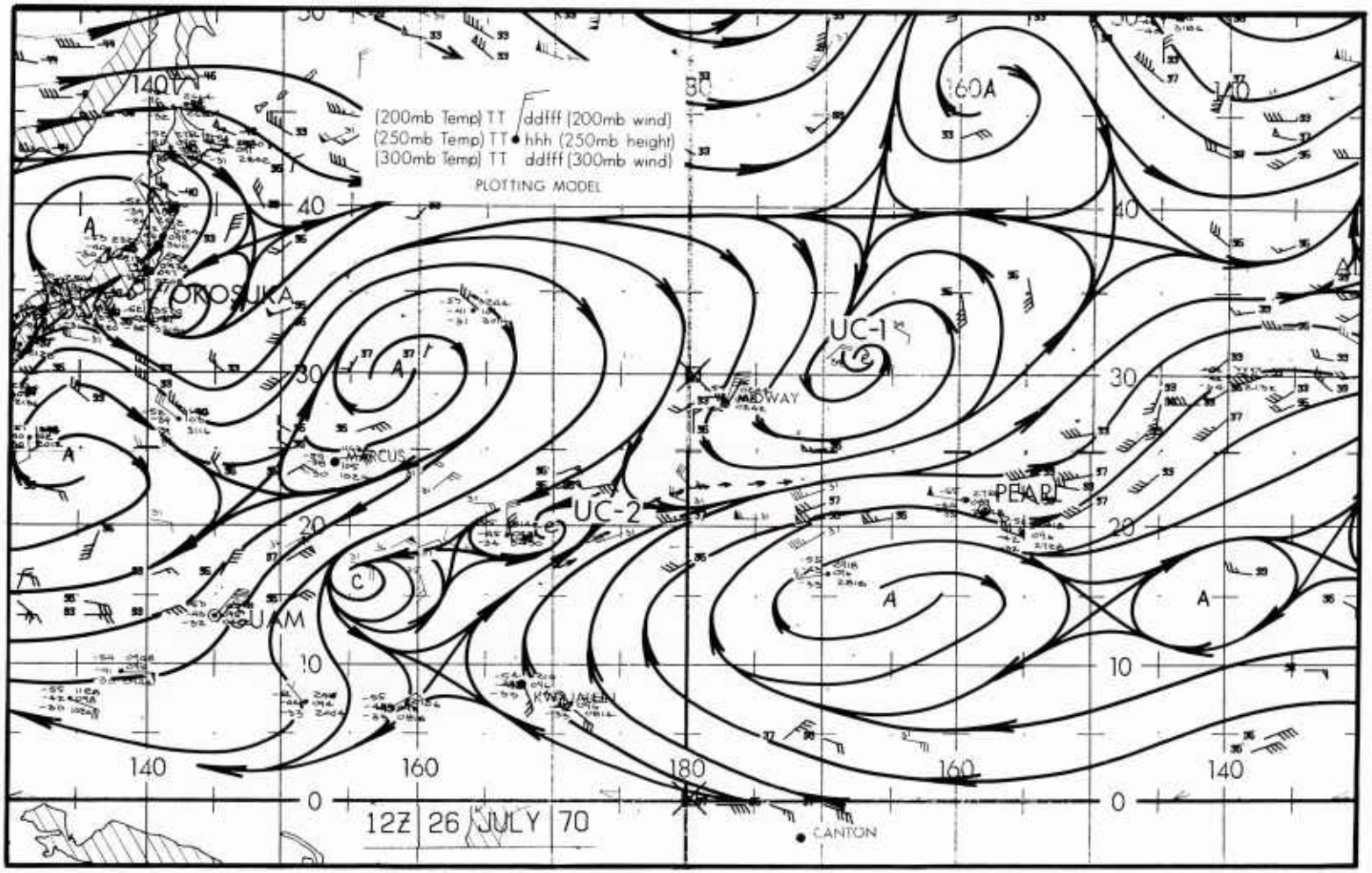

Figure 4. 250 mb streamline analysis for 1200 GMT 26 July 1970.

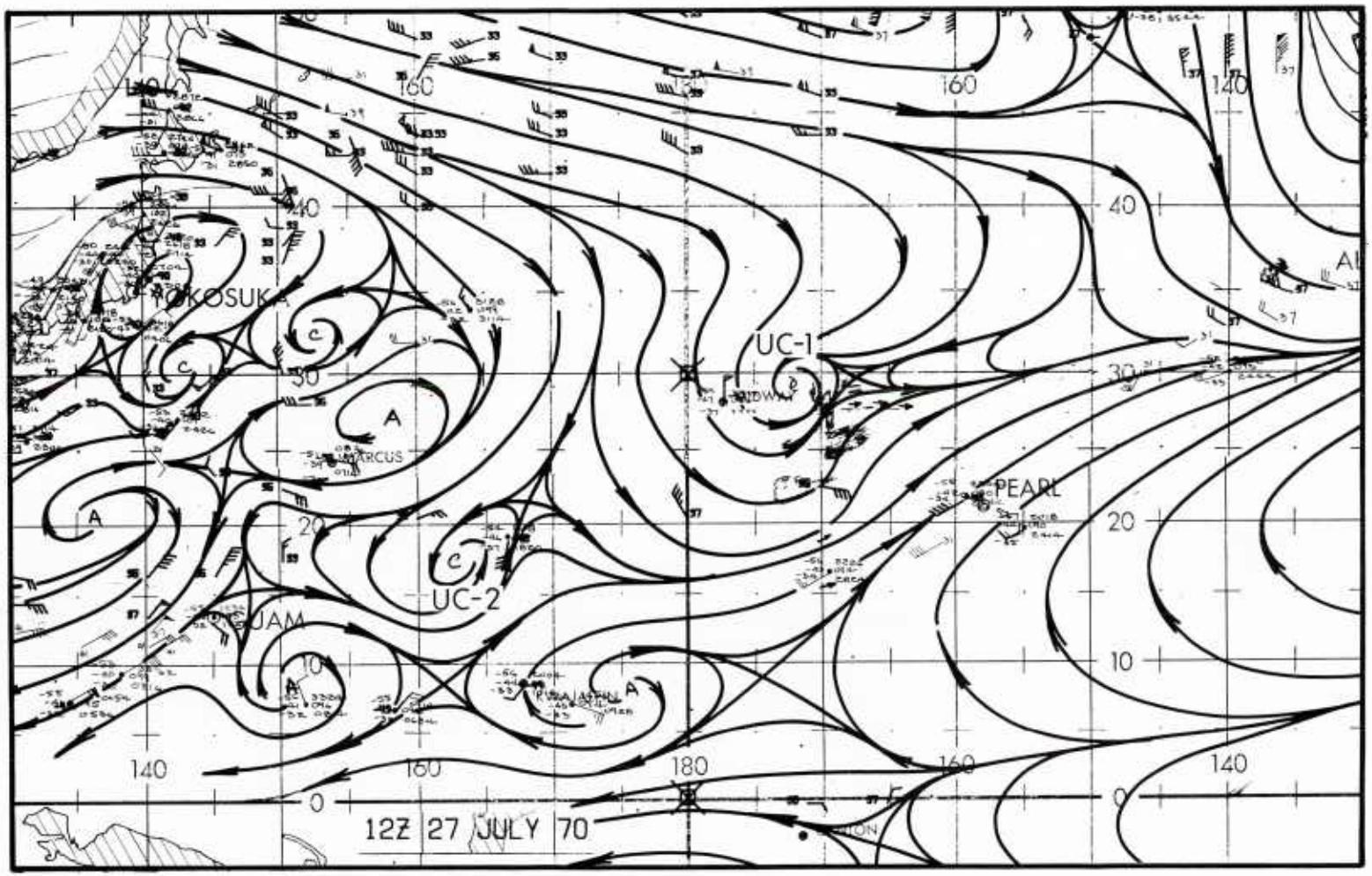

Figure 5. 250 mb streamline analysis for 1200 GMT 27 July 1970.

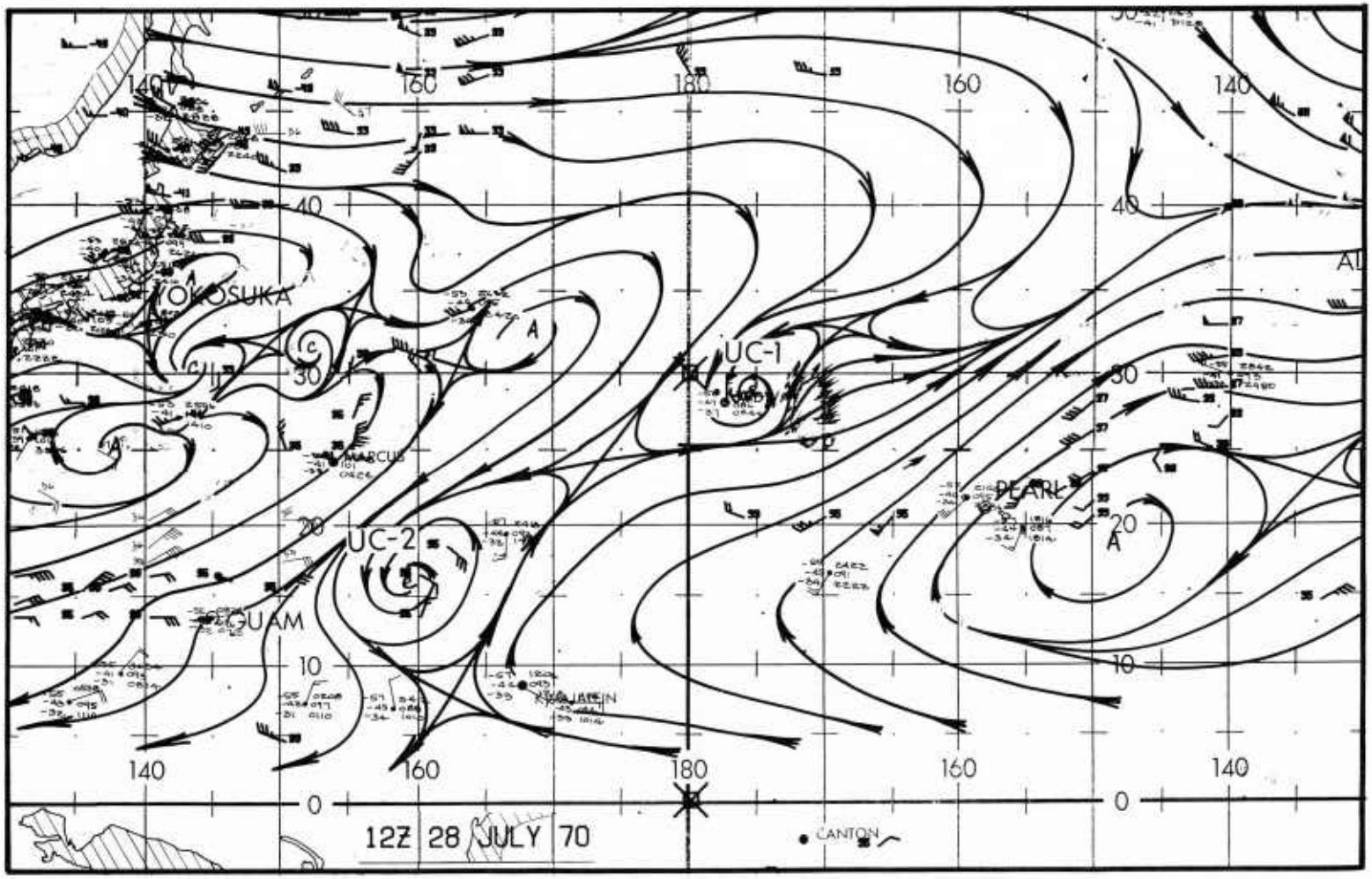

Figure 6. 250 mb streamline analysis for 1200 GMT 28 July 1970.

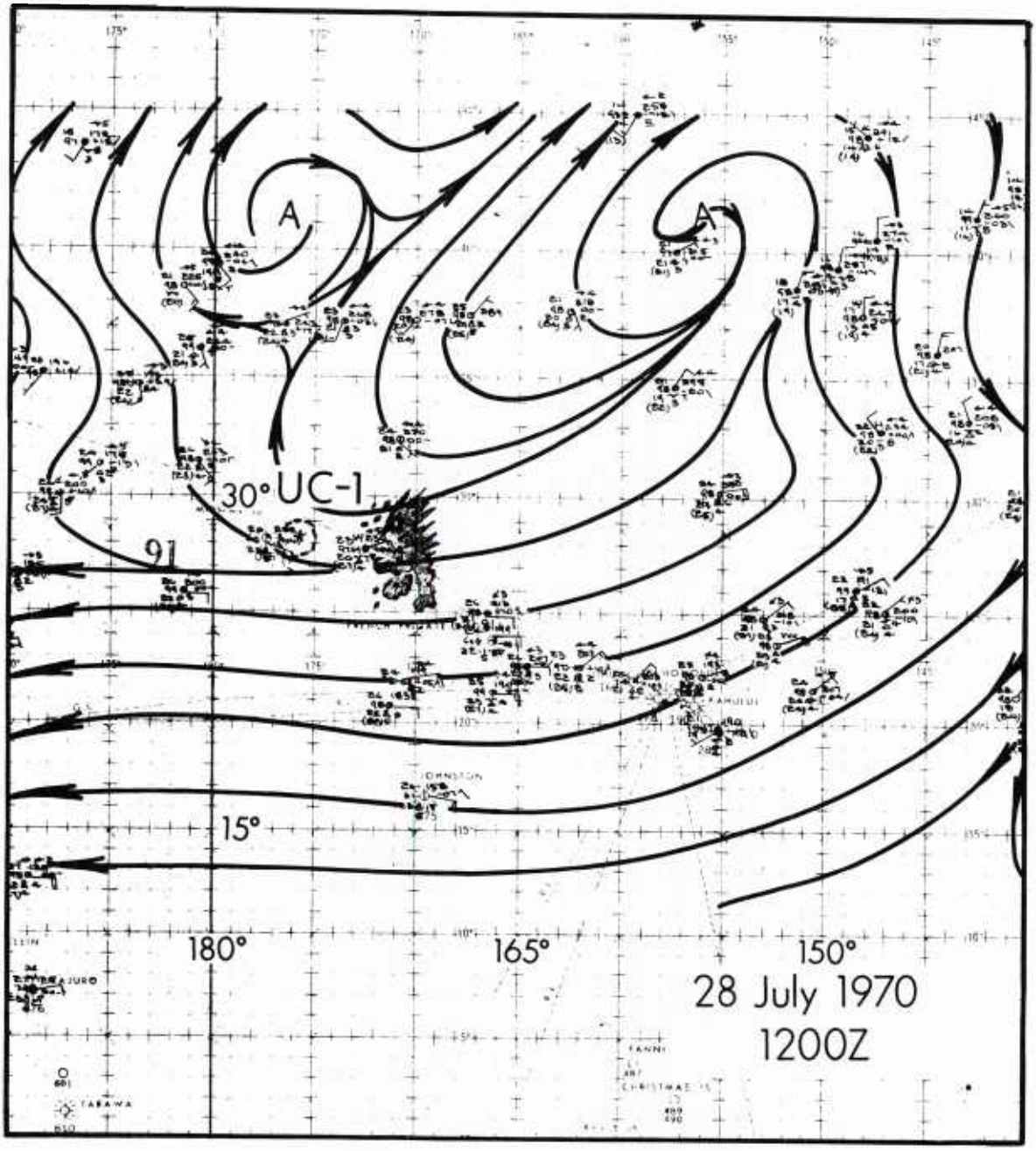

Figure 7. Surface streamline analysis for 1200 GMT 28 July 1970.

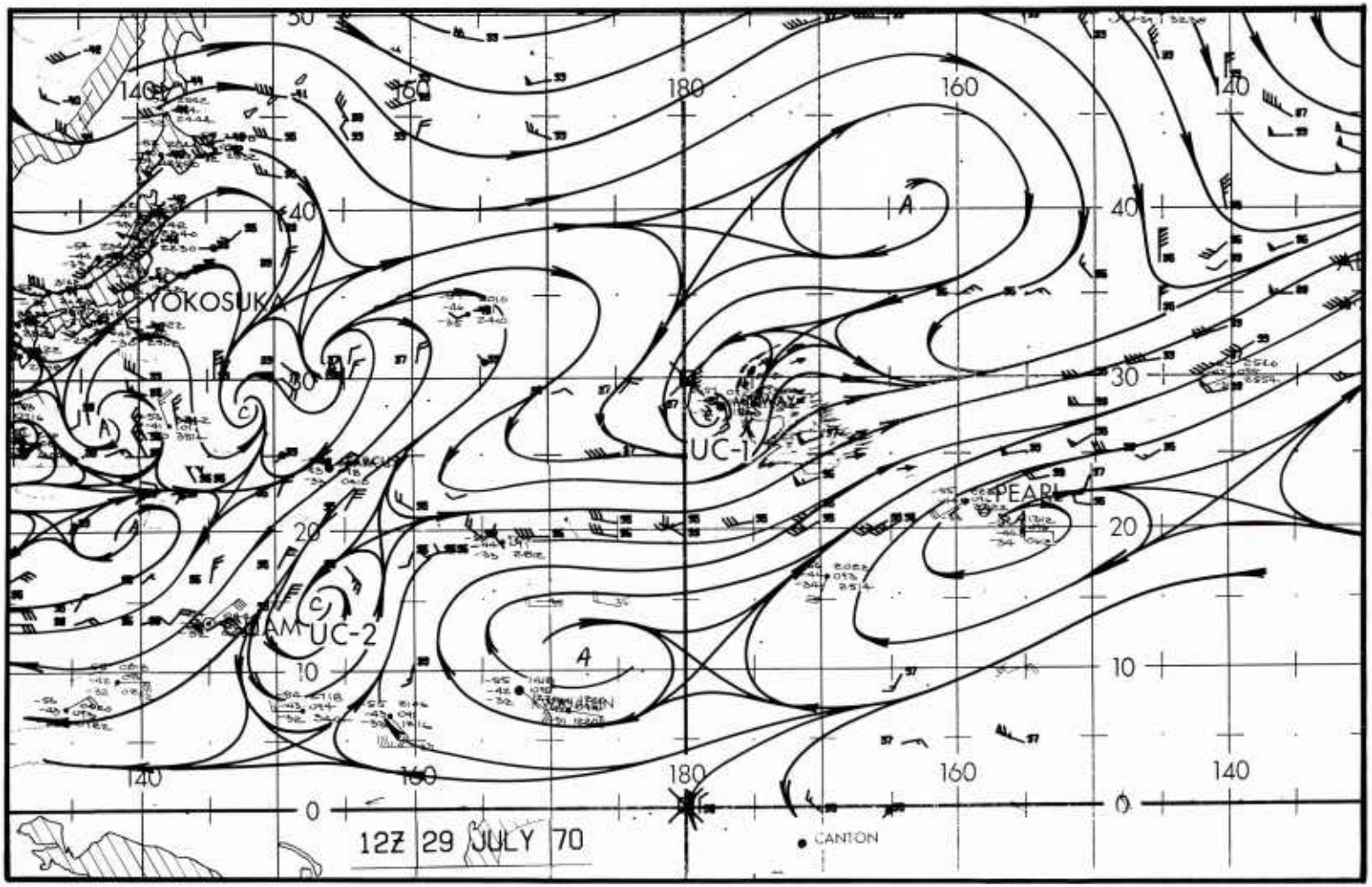

Figure 8. 250 mb streamline analysis for 1200 GMT 29 July 1970.

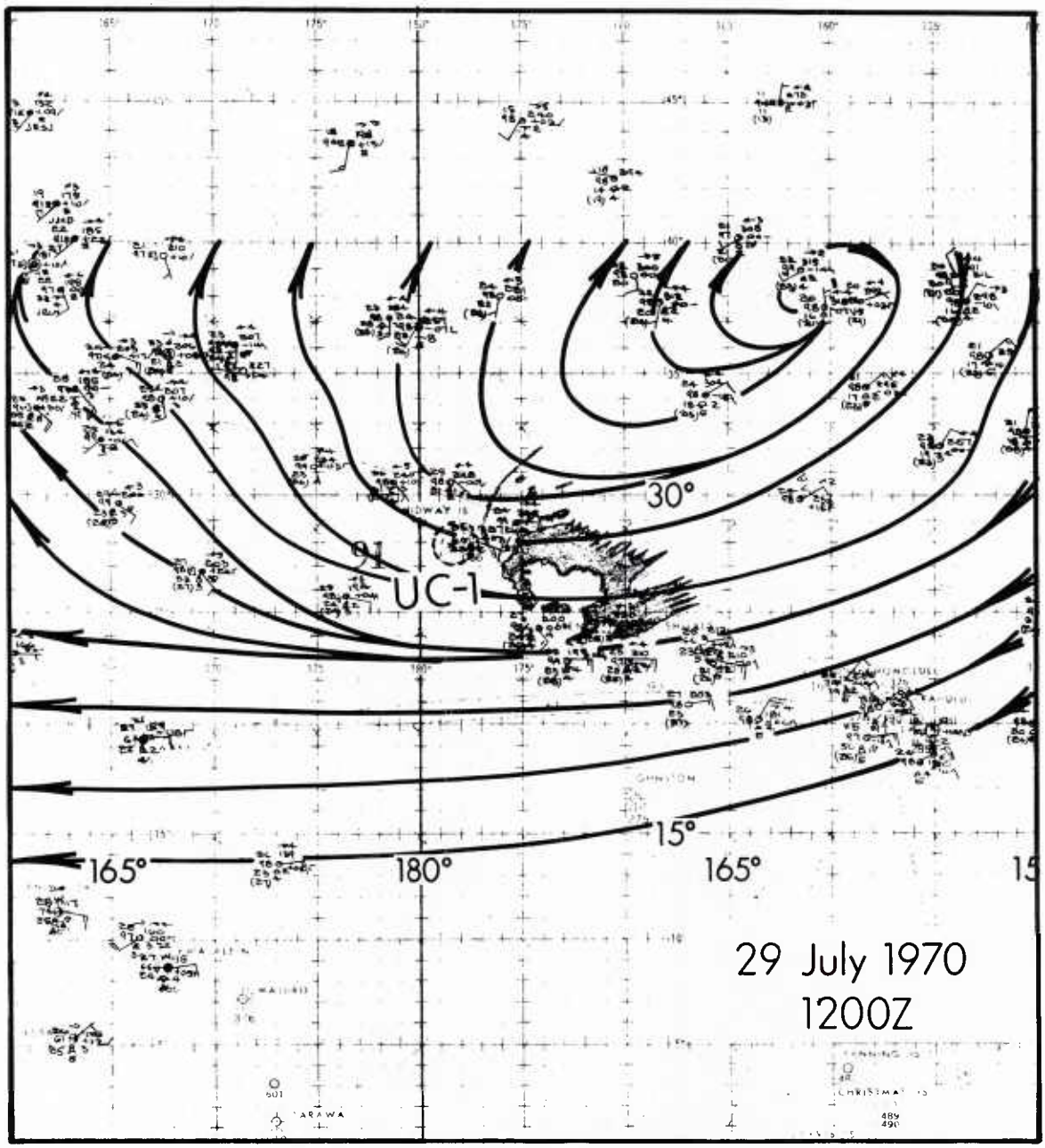

Figure 9. Surface streamline analysis for 1200 GMT 29 July 1970.

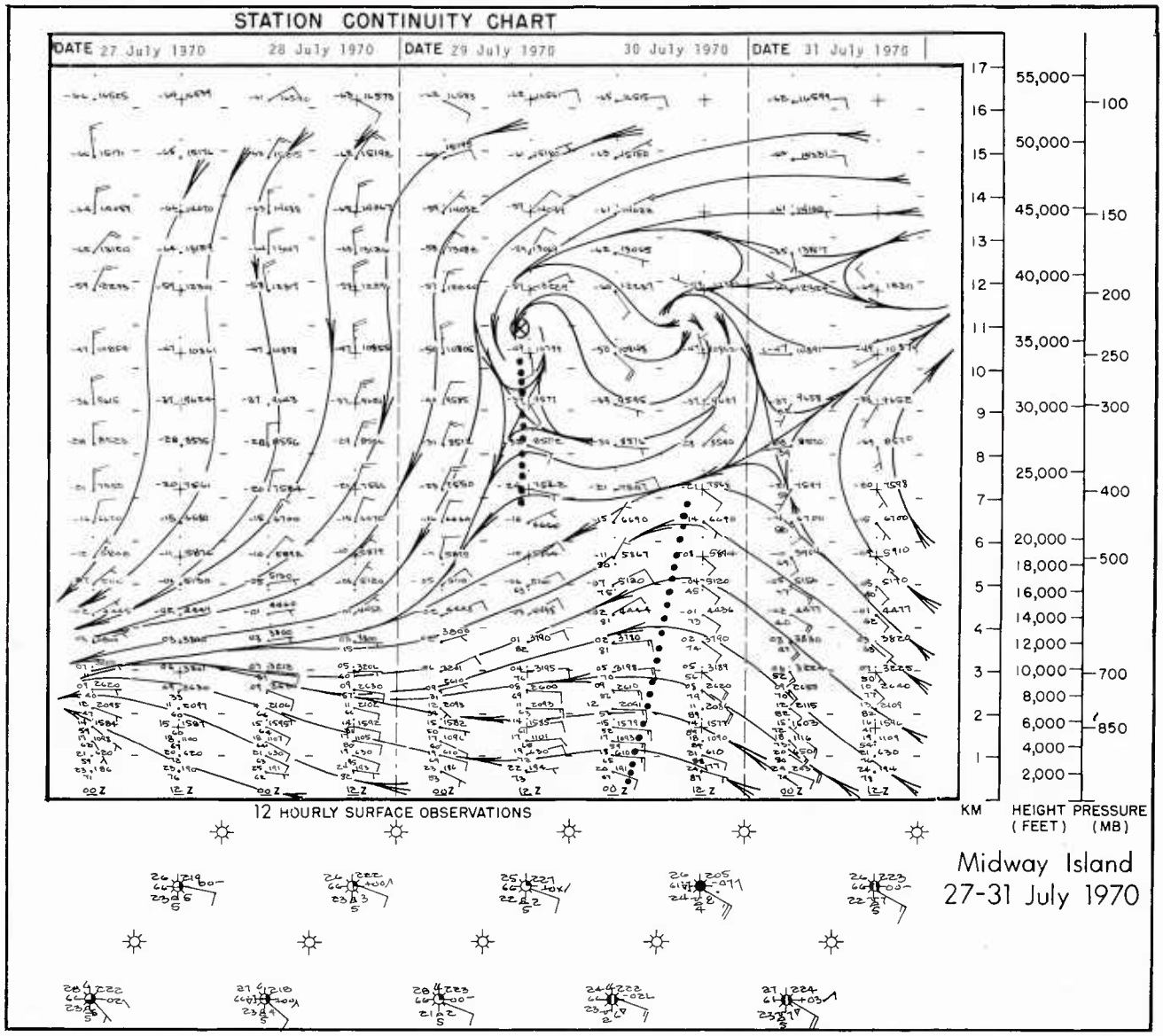

Figure 10. Time-altitude section and 12-hourly surface observations for Midway Island. Upper wind speed in m sec^{-1}. Surface wind speed in kt. UC-1 shown by crossed circle and a dotted line and lower trough by a dotted line.

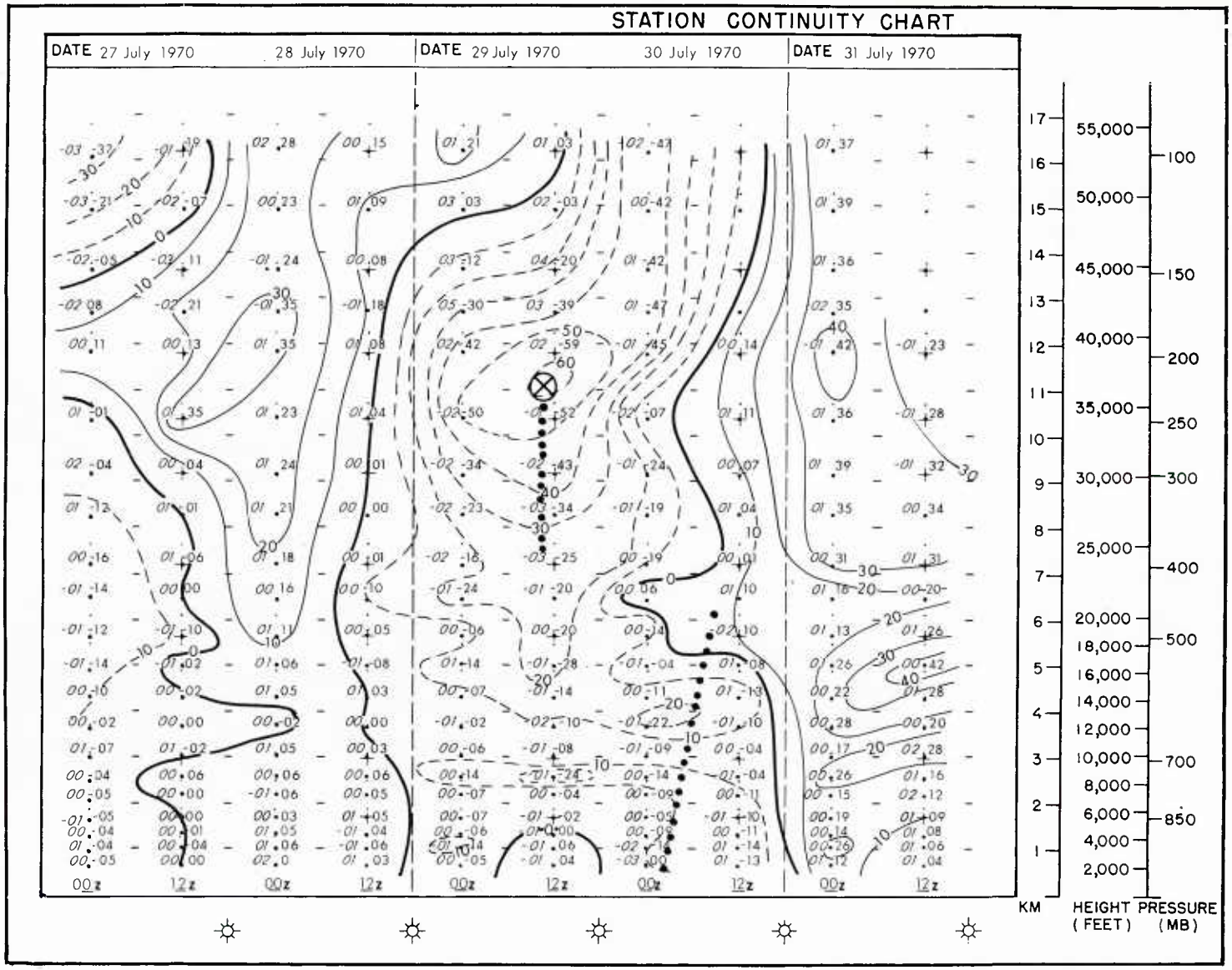

Figure 11. Height anomaly from the 5-day average of 27-31 July 1970. Isolines in meters. Negative anomalies are dashed. UC-1 and lower trough shown from Fig. 10 wind analysis.

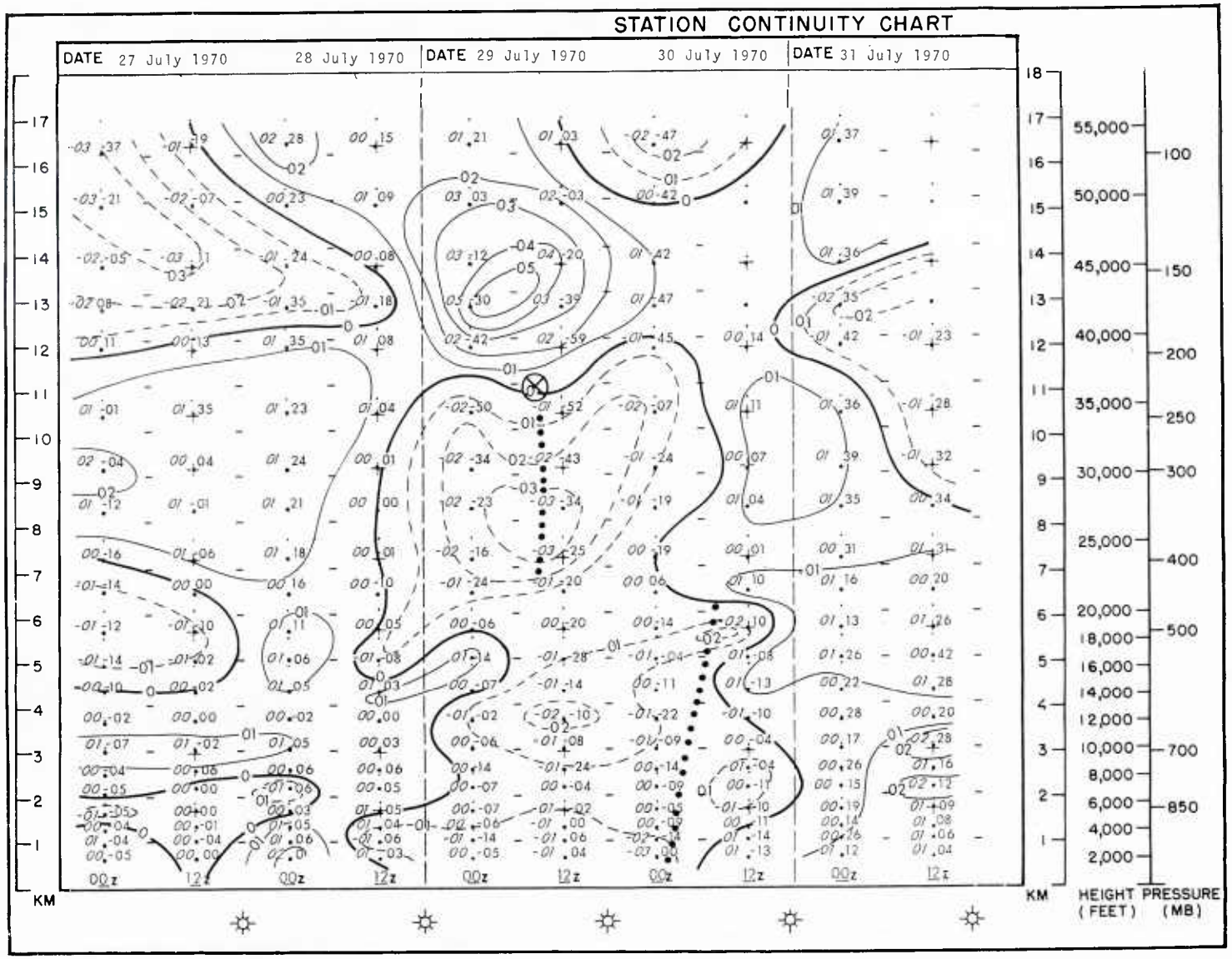

Figure 12. Temperature anomaly from the 5-day average of 27-31 July 1970. Negative anomalies are dashed. UC-1 and lower trough shown from Fig. 10.

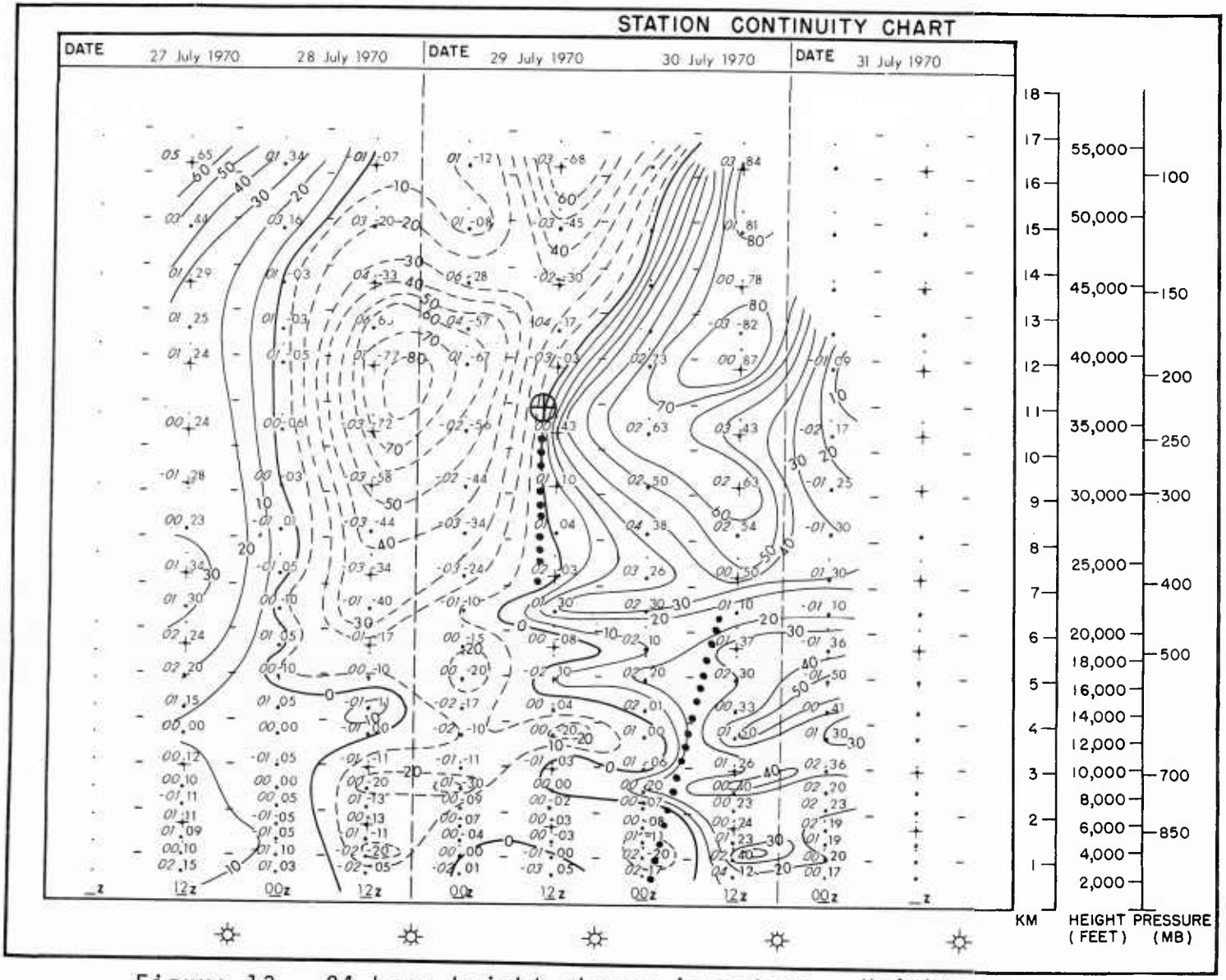

Figure 13. 24-hour height change in meters. Height falls are dashed. UC-1 and lower trough shown from Fig. 10.

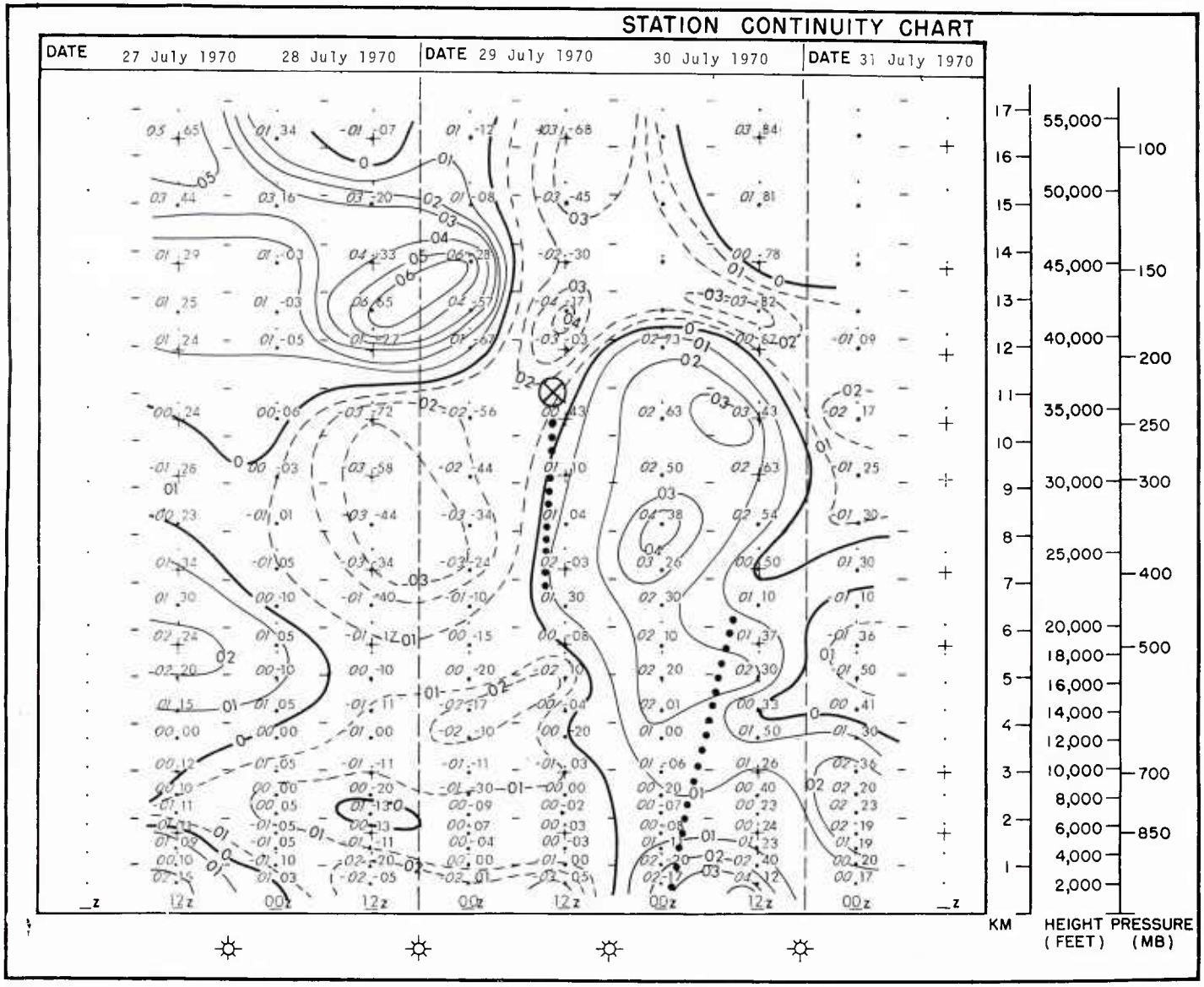

Figure 14. 24-hour temperature change in degrees Celsius. Temperature decreases are dashed. UC-1 and lower trough shown from Fig. 10.

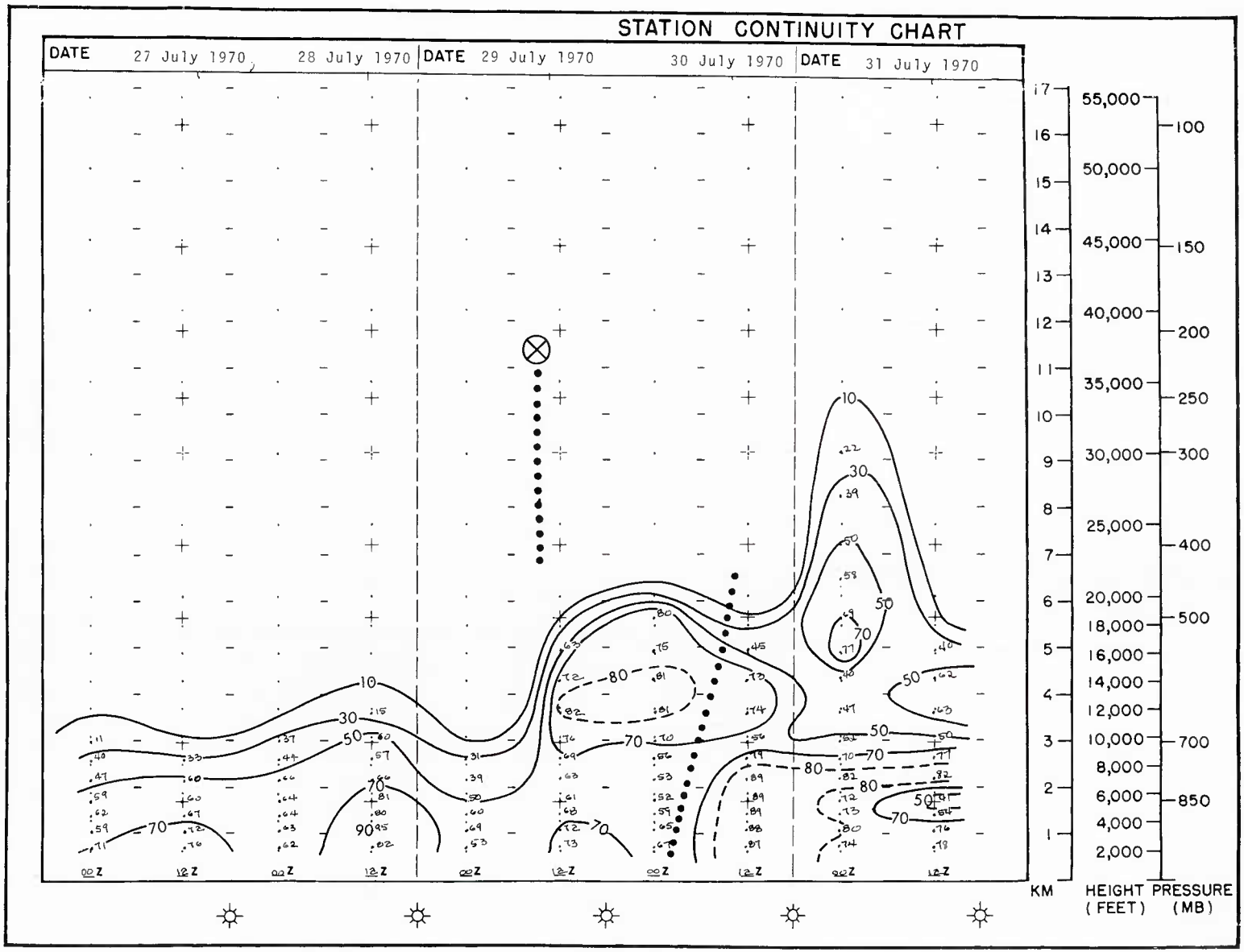

Figure 15. Relative humidity in percent. UC-1 and lower trough shown from Fig. 10.

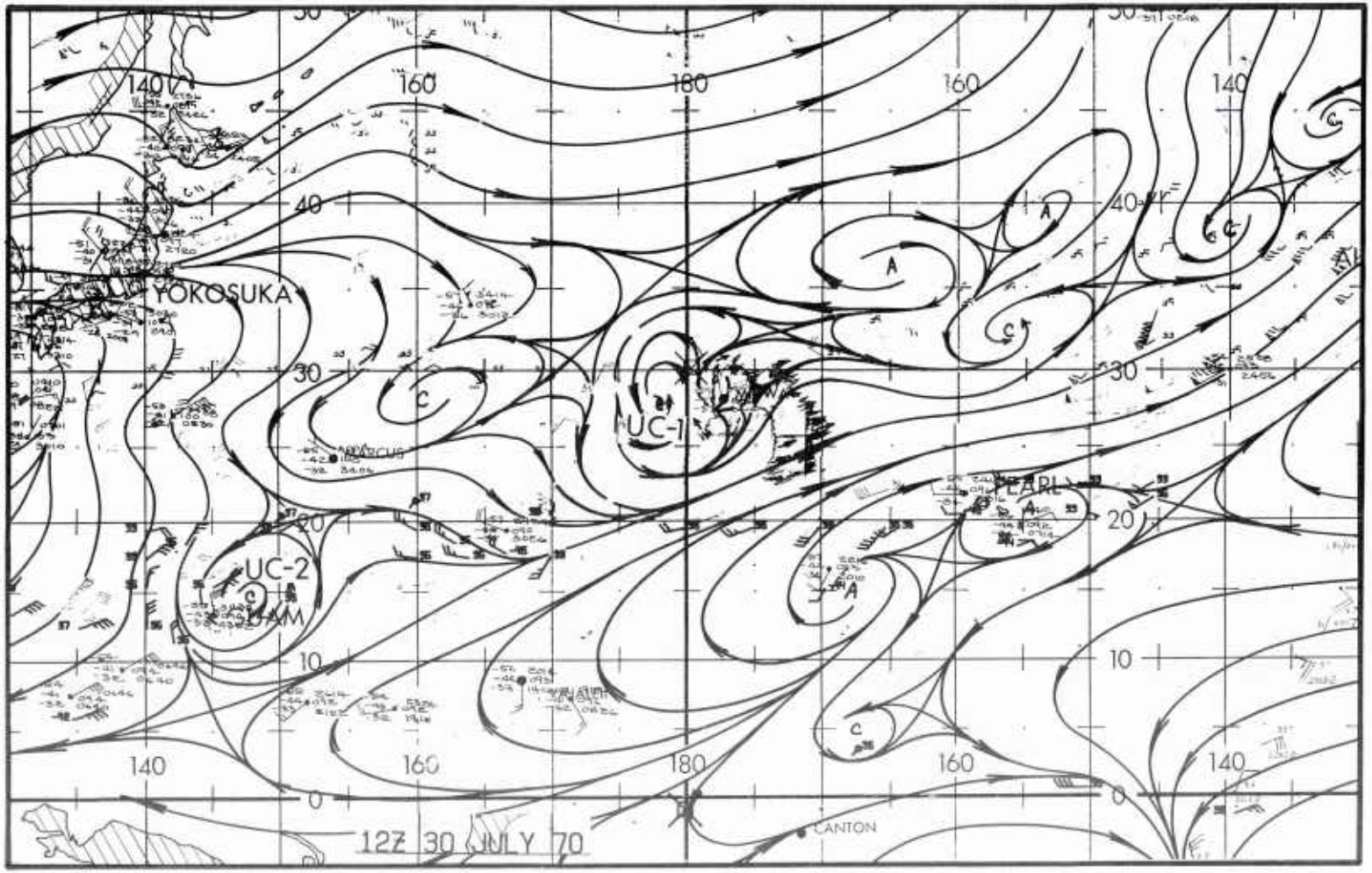

Figure 16. 250 mb streamline analysis for 1200 GMT 30 July 1970.

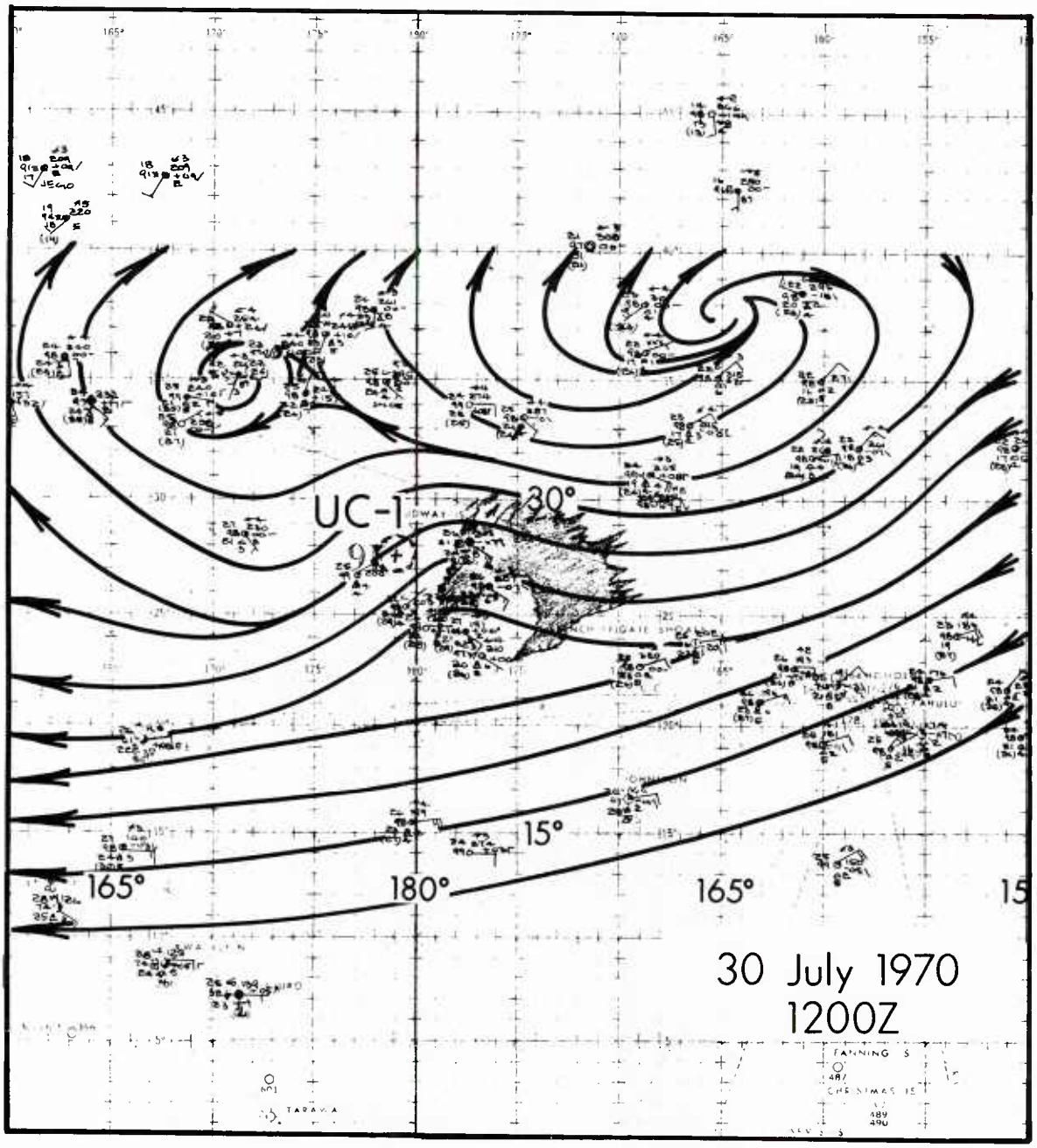

Figure 17. Surface streamline analysis for 1200 GMT 30 July 1970.

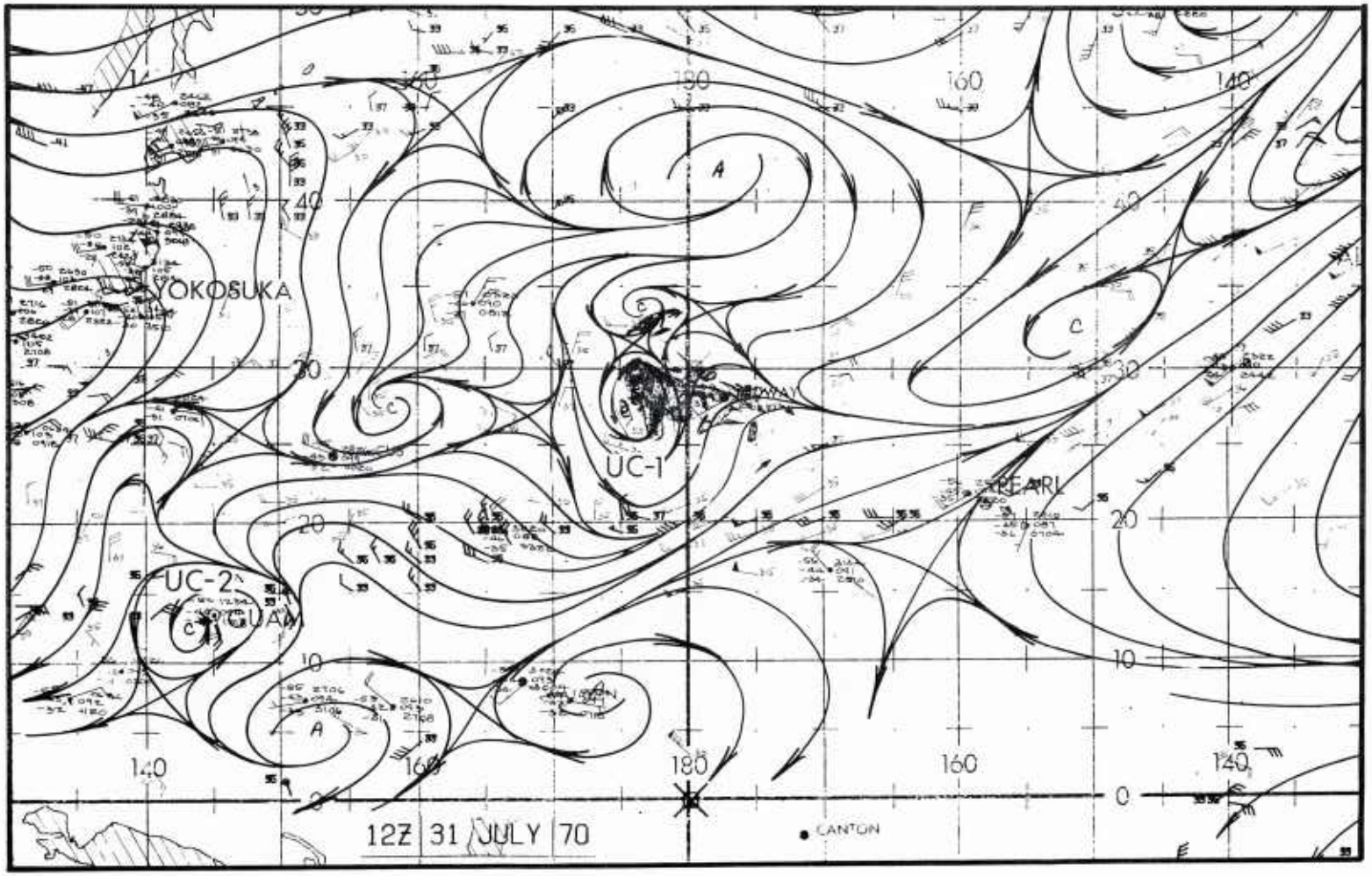

Figure 18. 250 mb streamline analysis for 1200 GMT 31 July 1970.

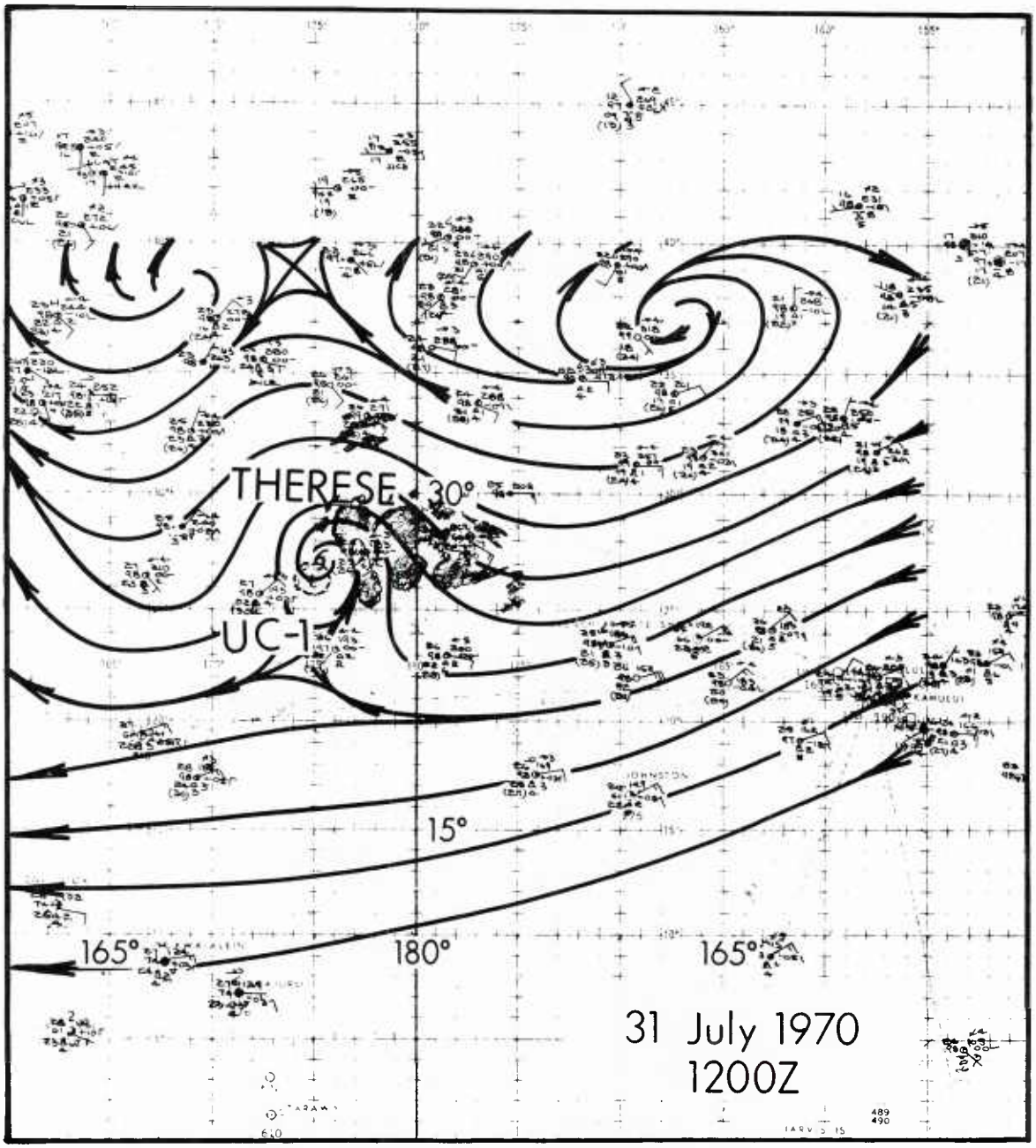

Figure 19. Surface streamline analysis for 1200 GMT 31 July 1970.

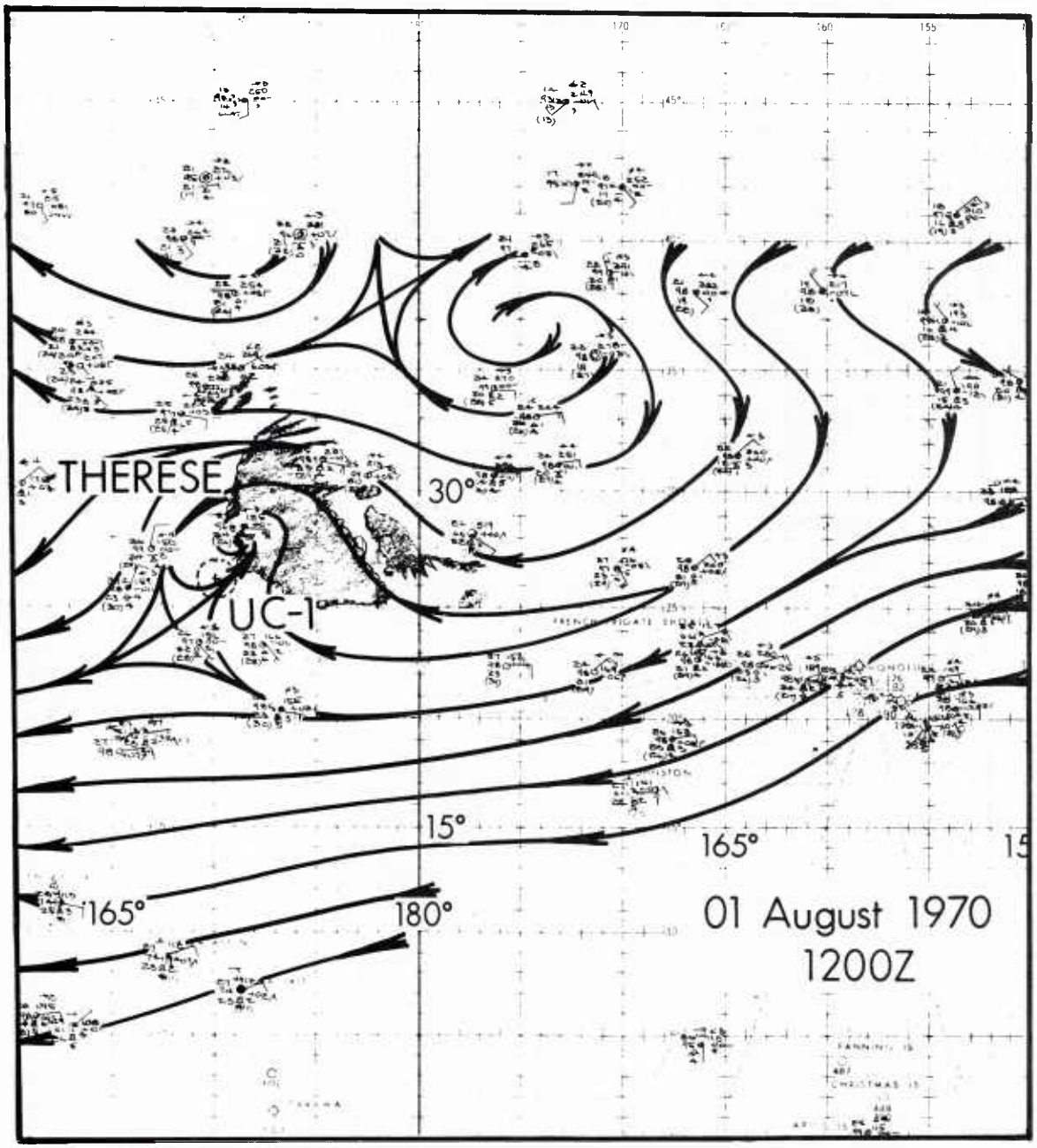

Figure 20. Surface streamline analysis for 1200 GMT 1 August 1970.

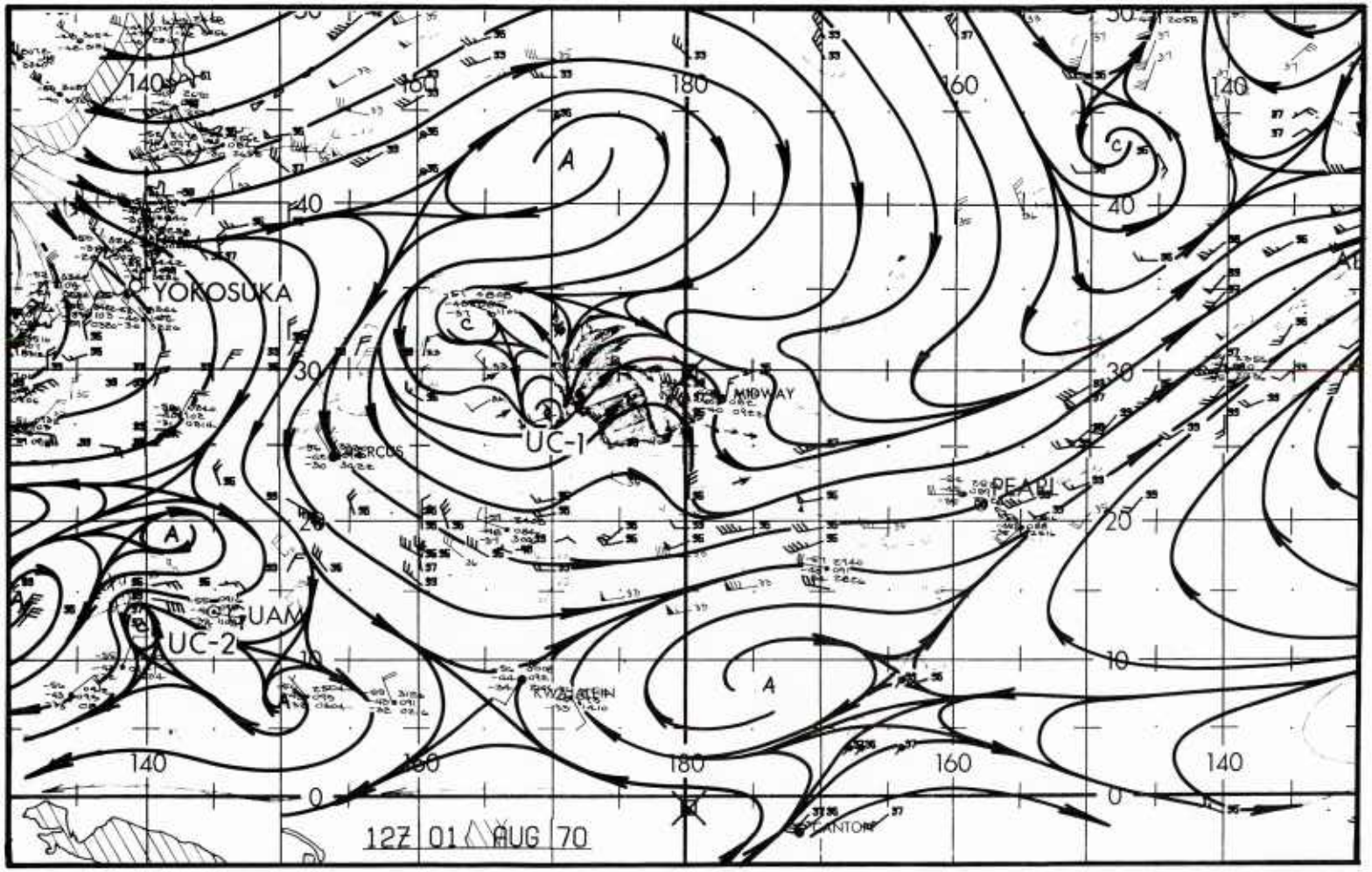

Figure 21. 250 mb streamline analysis for 1200 GMT 1 August 1970.

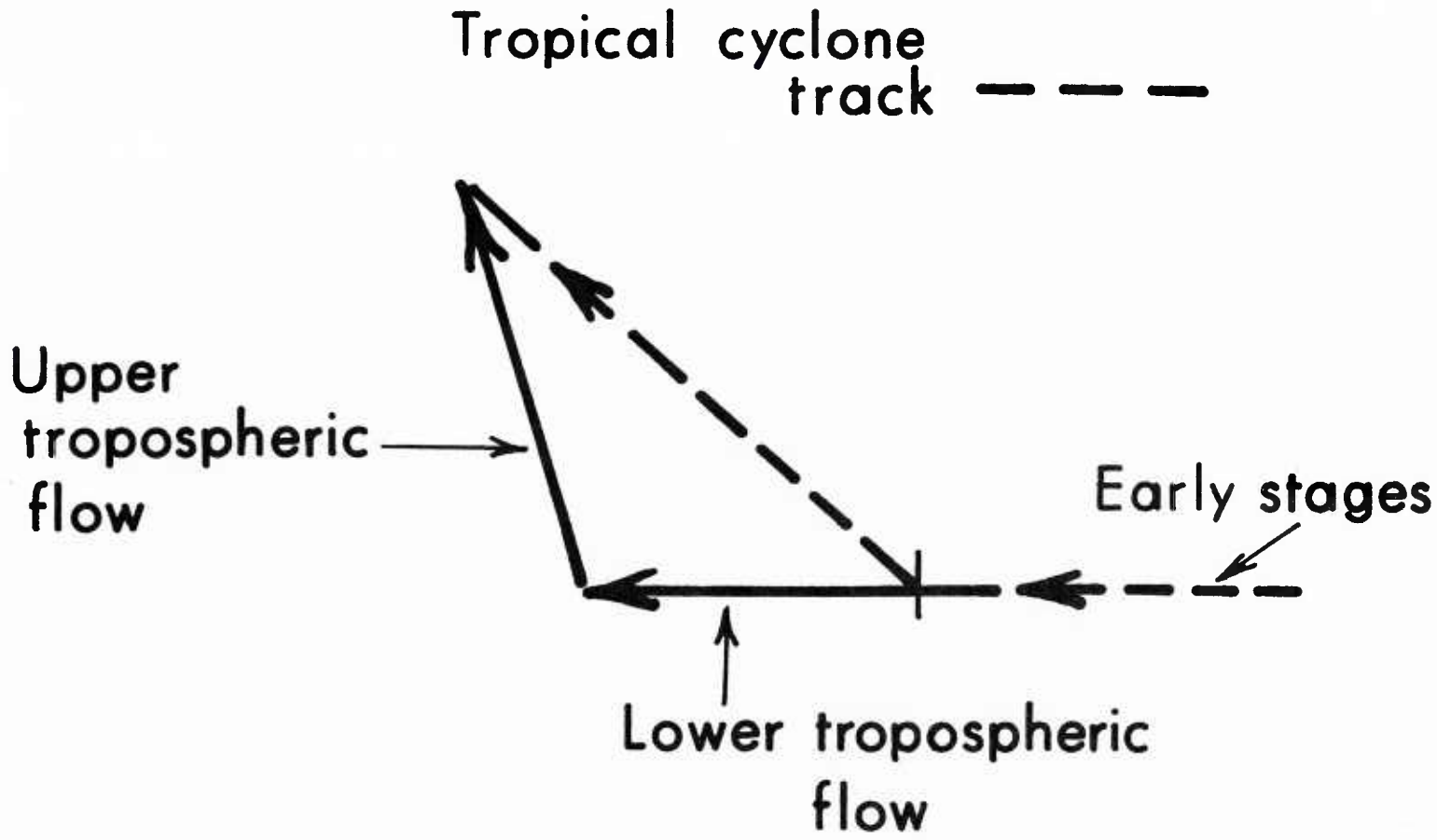

Figure 22. Common track of tropical cyclones initiated by upper tropospheric flow.

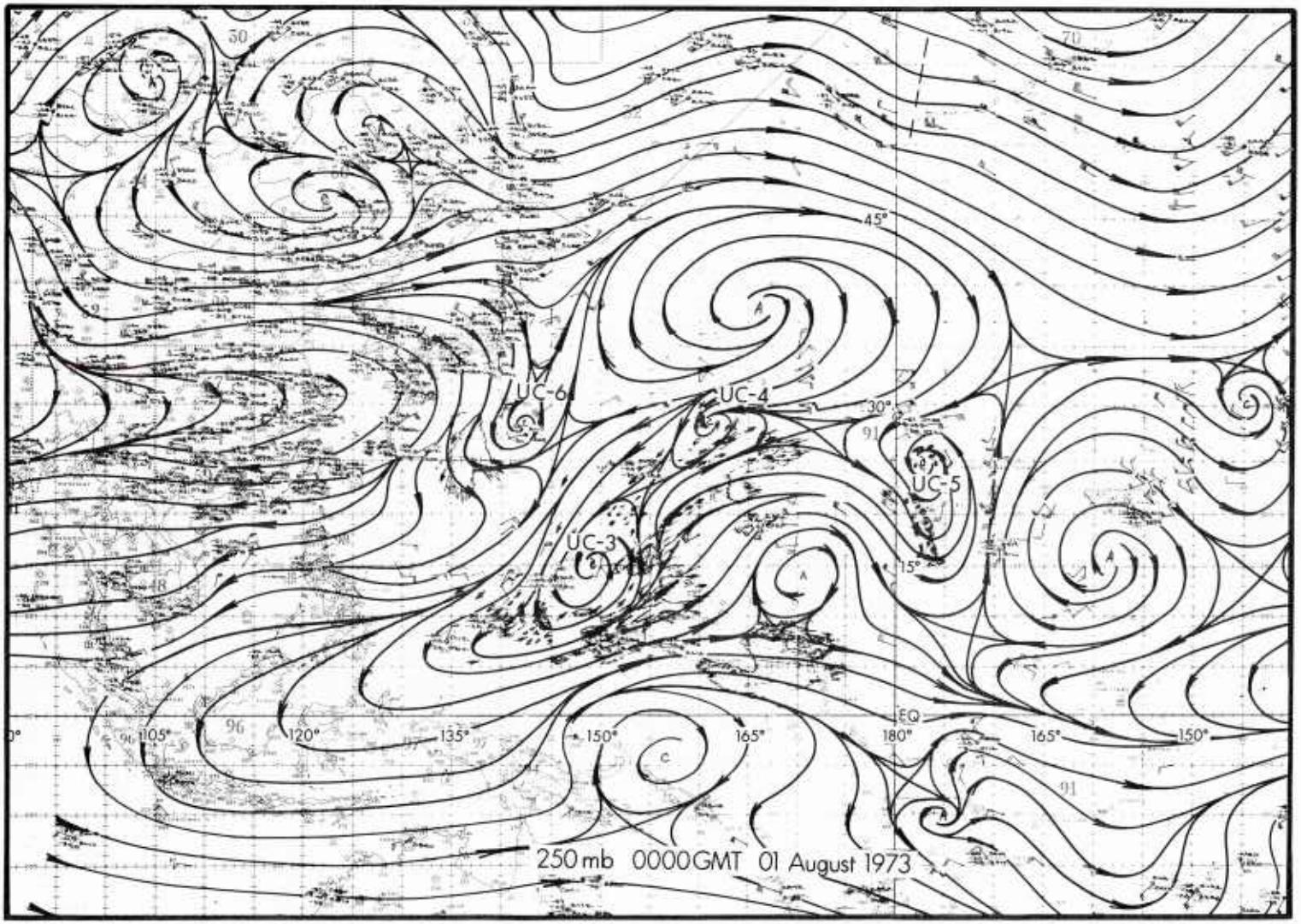

Figure 23. 250 mb streamline analysis for 1 August 1973.

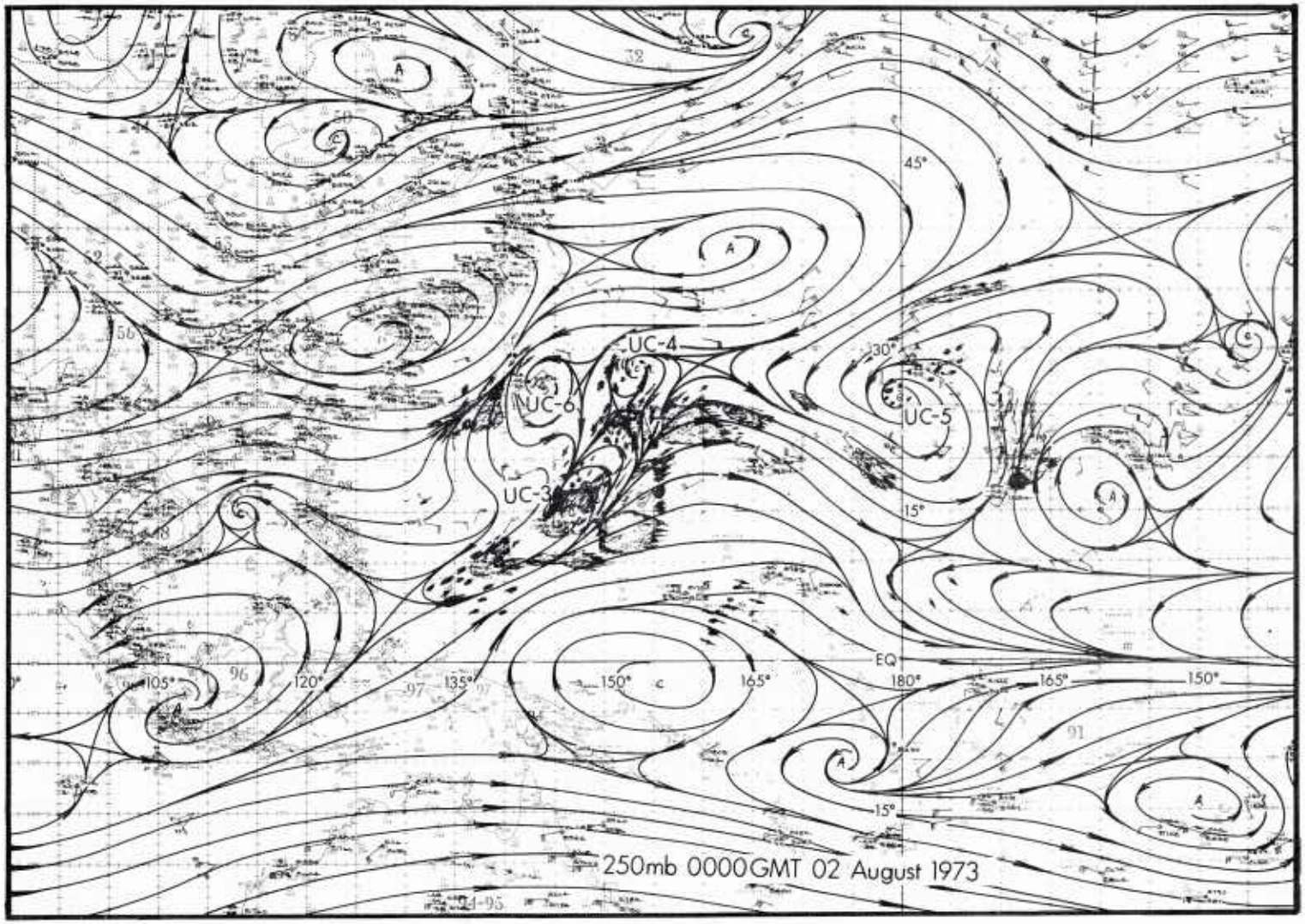

Figure 24. 250 mb streamline analysis for 2 August 1973.

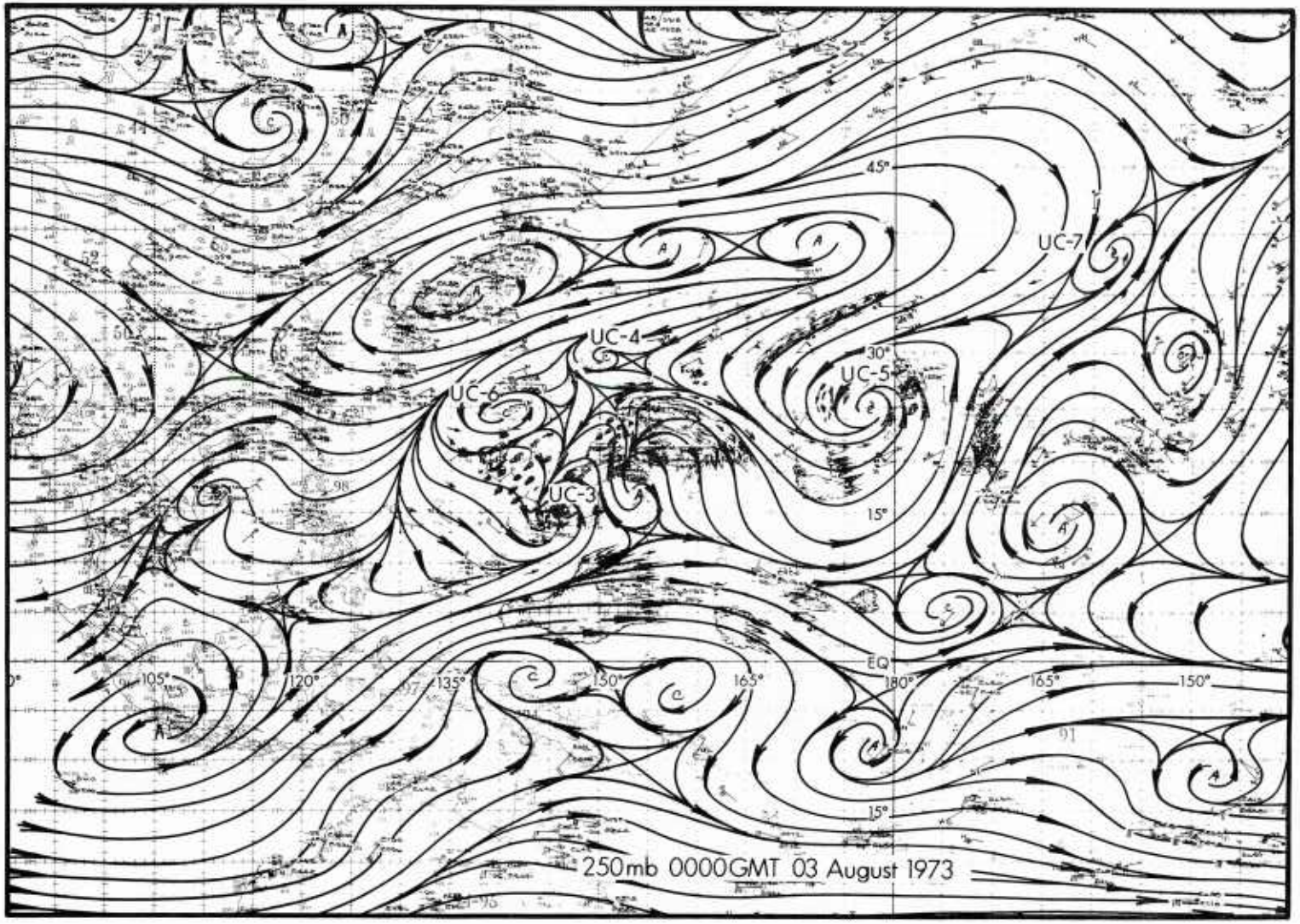

Figure 25. 250 mb streamline analysis for 3 August 1973.

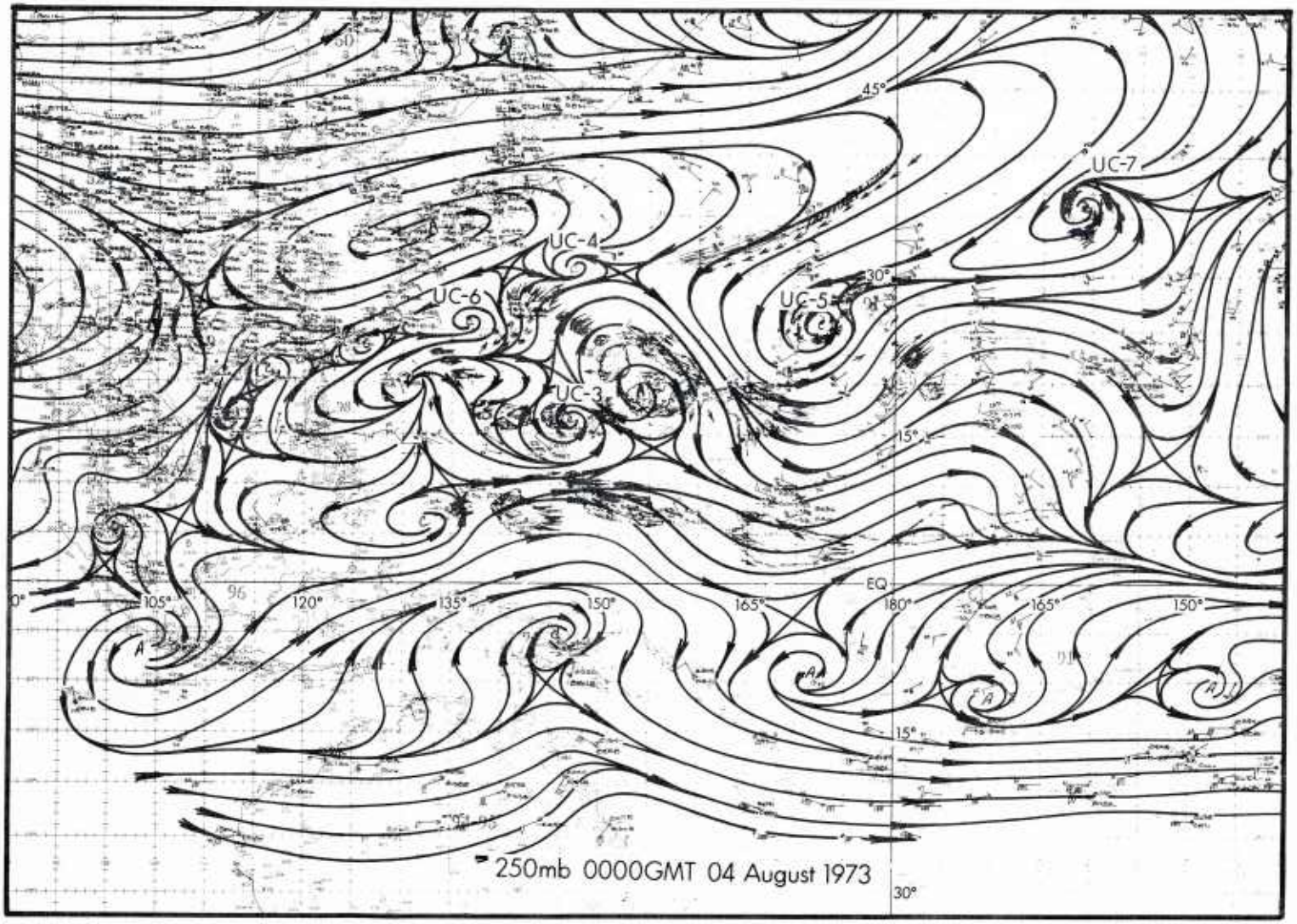

Figure 26. 250 mb streamline analysis for 4 August 1973.

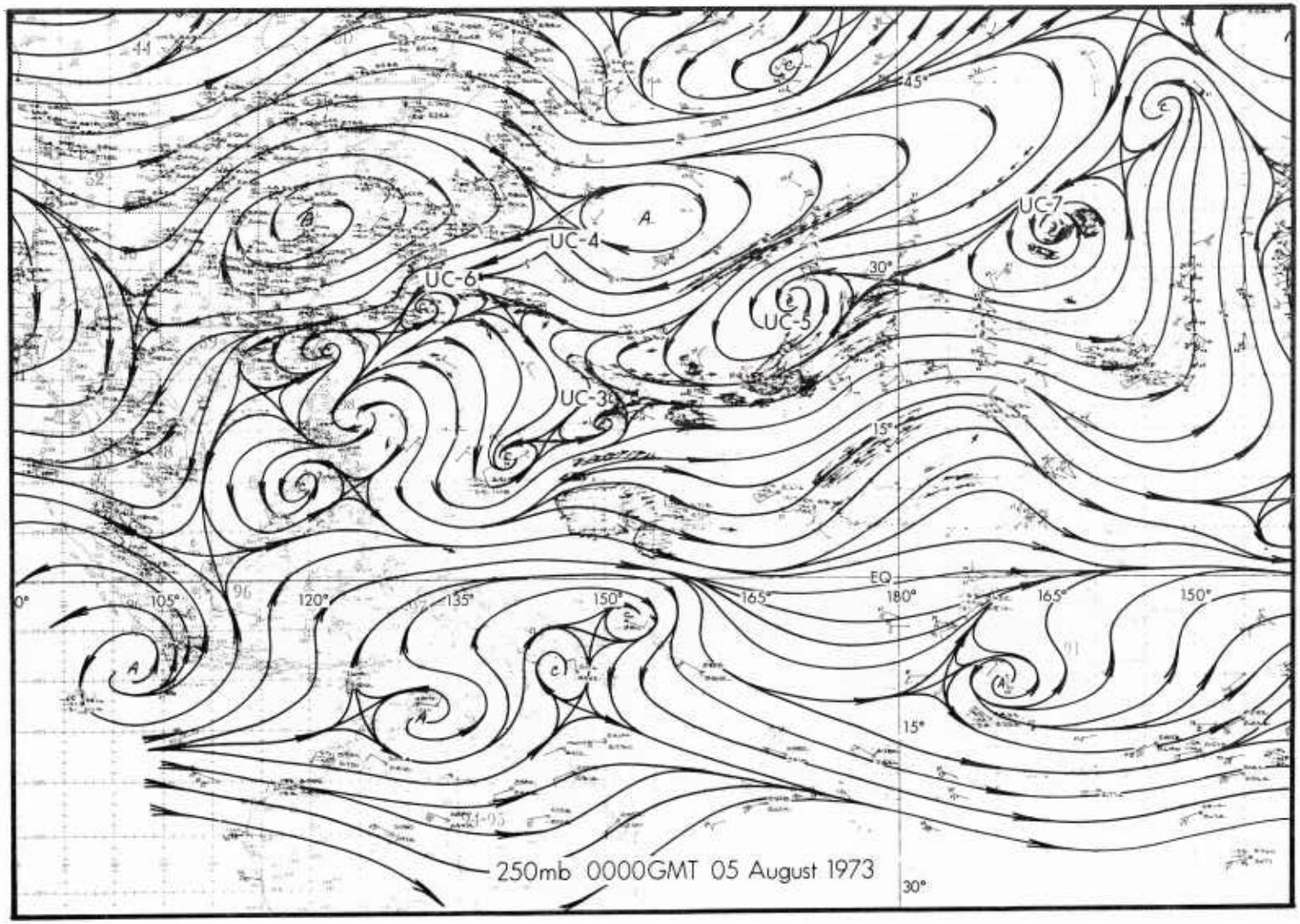

Figure 27. 250 mb streamline analysis for 5 August 1973.

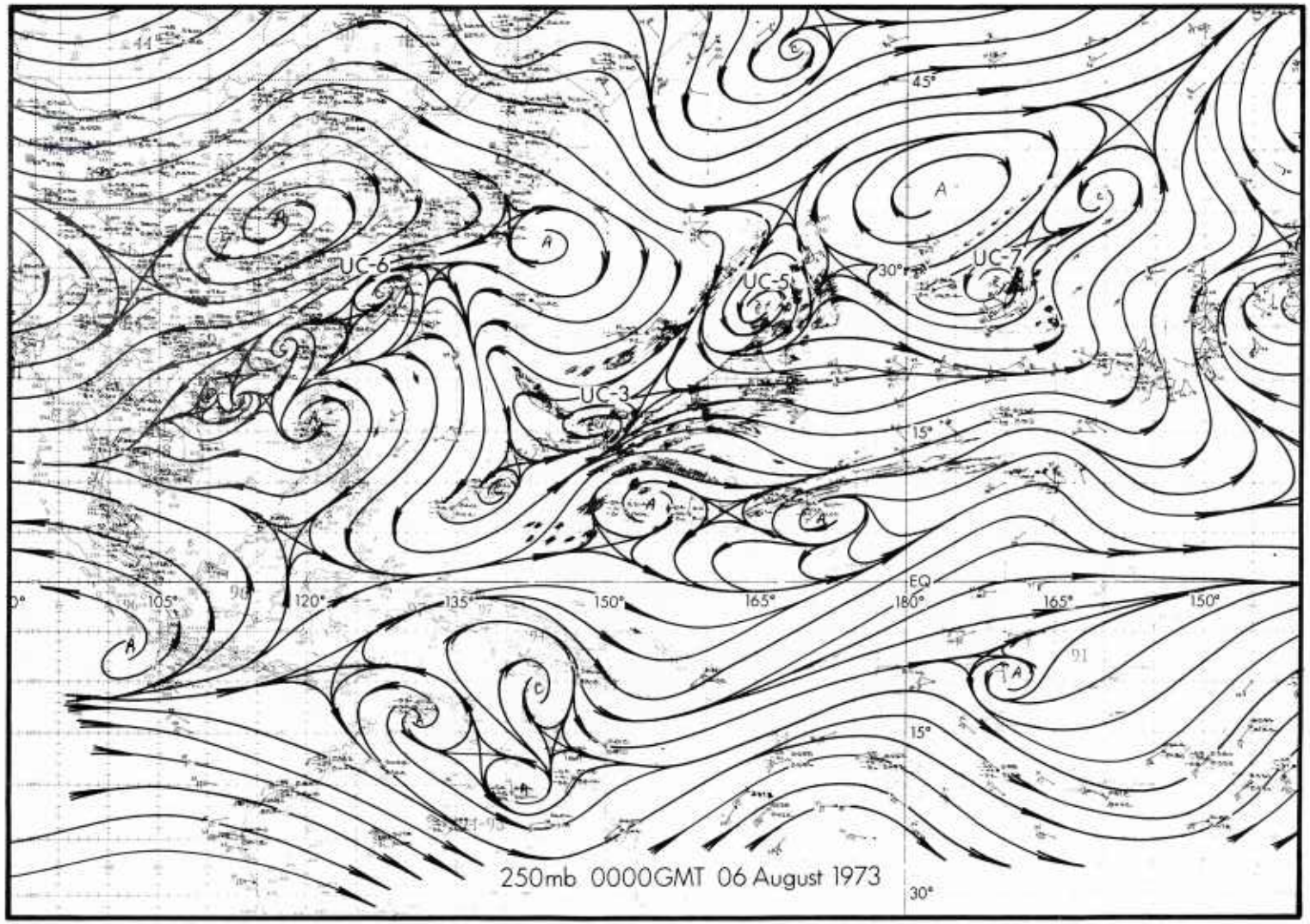

Figure 28. 250 mb streamline analysis for 6 August 1973.

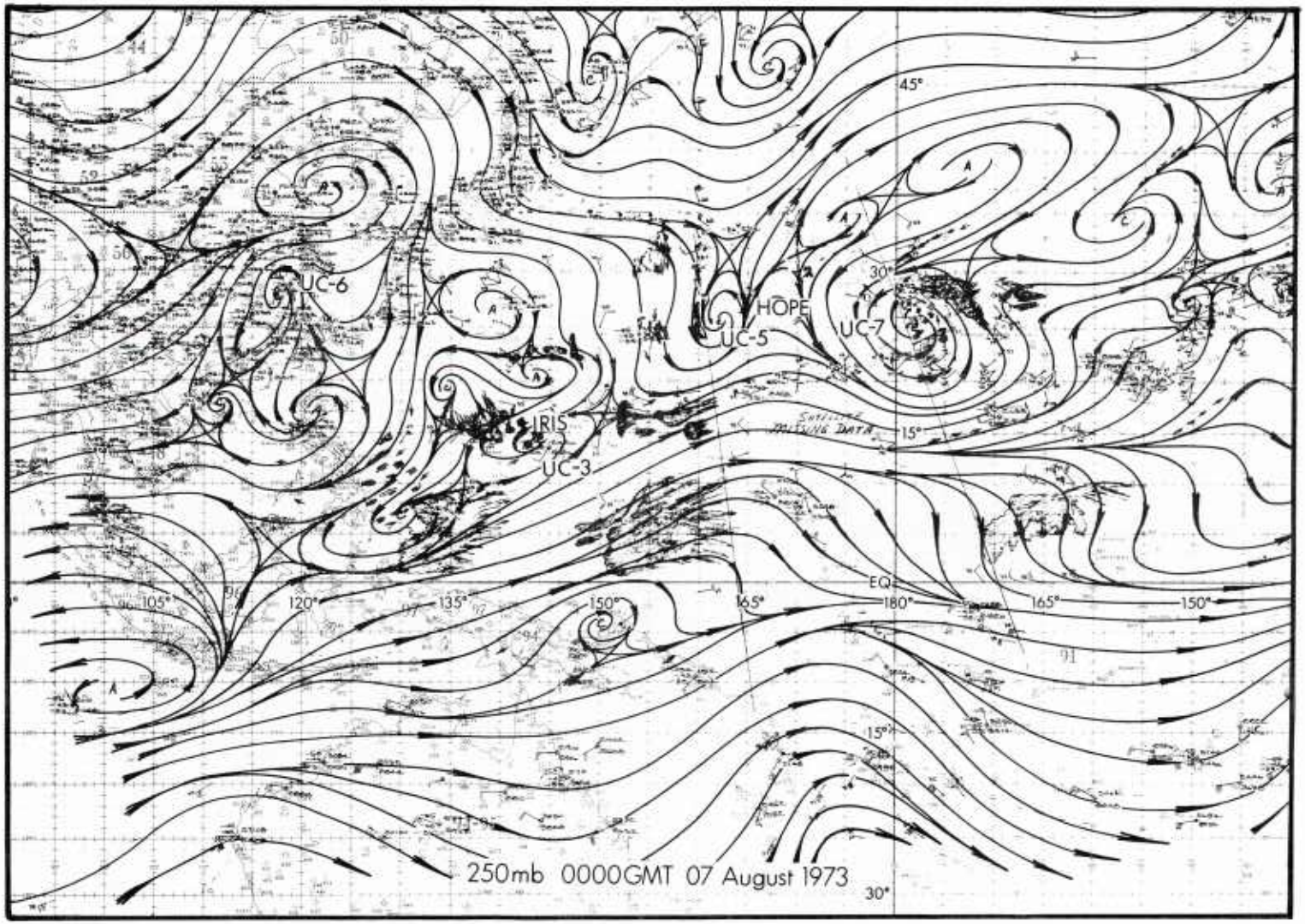

Figure 29. 250 mb streamline analysis for 7 August 1973.

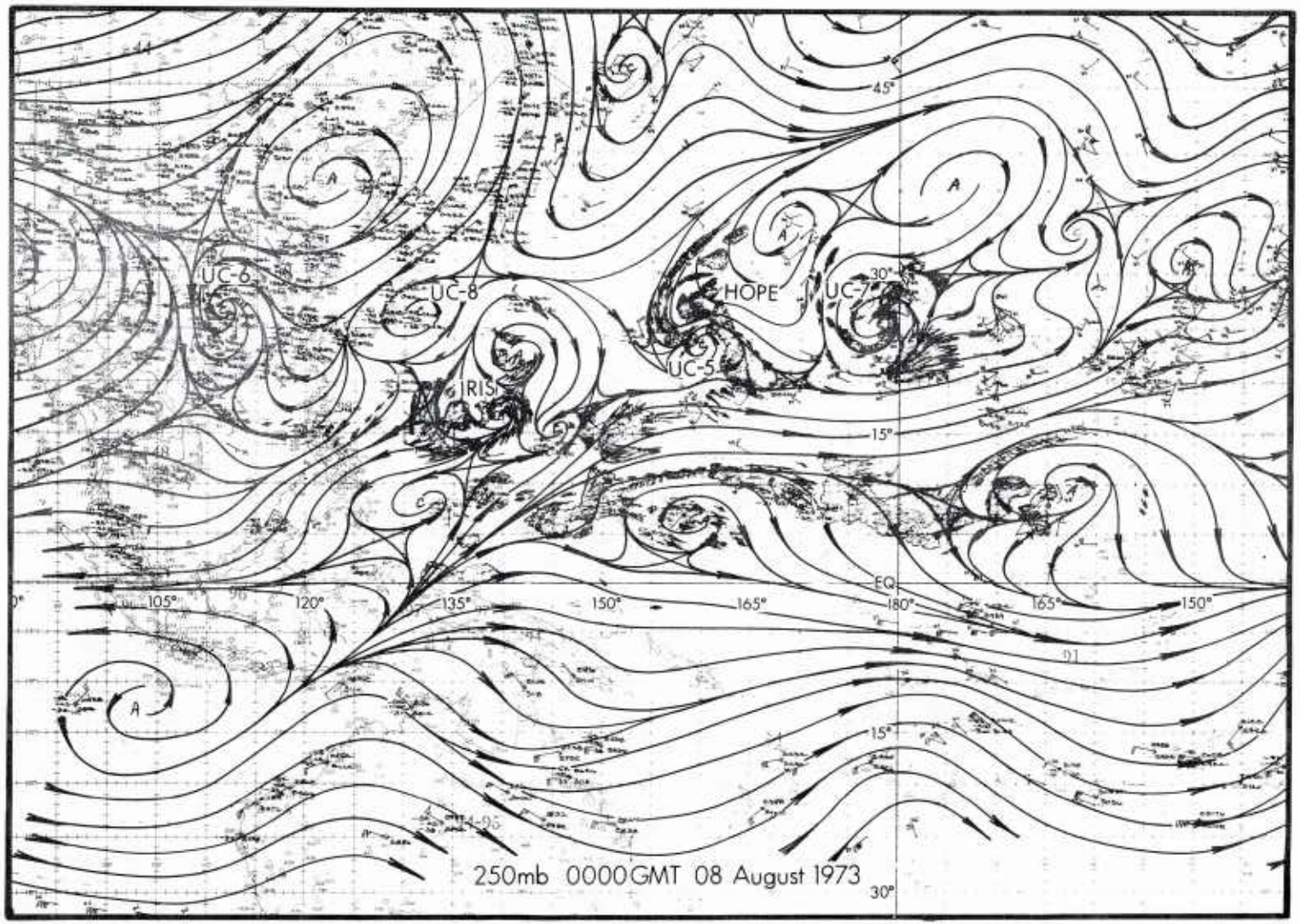

Figure 30. 250 mb streamline analysis for 8 August 1973.

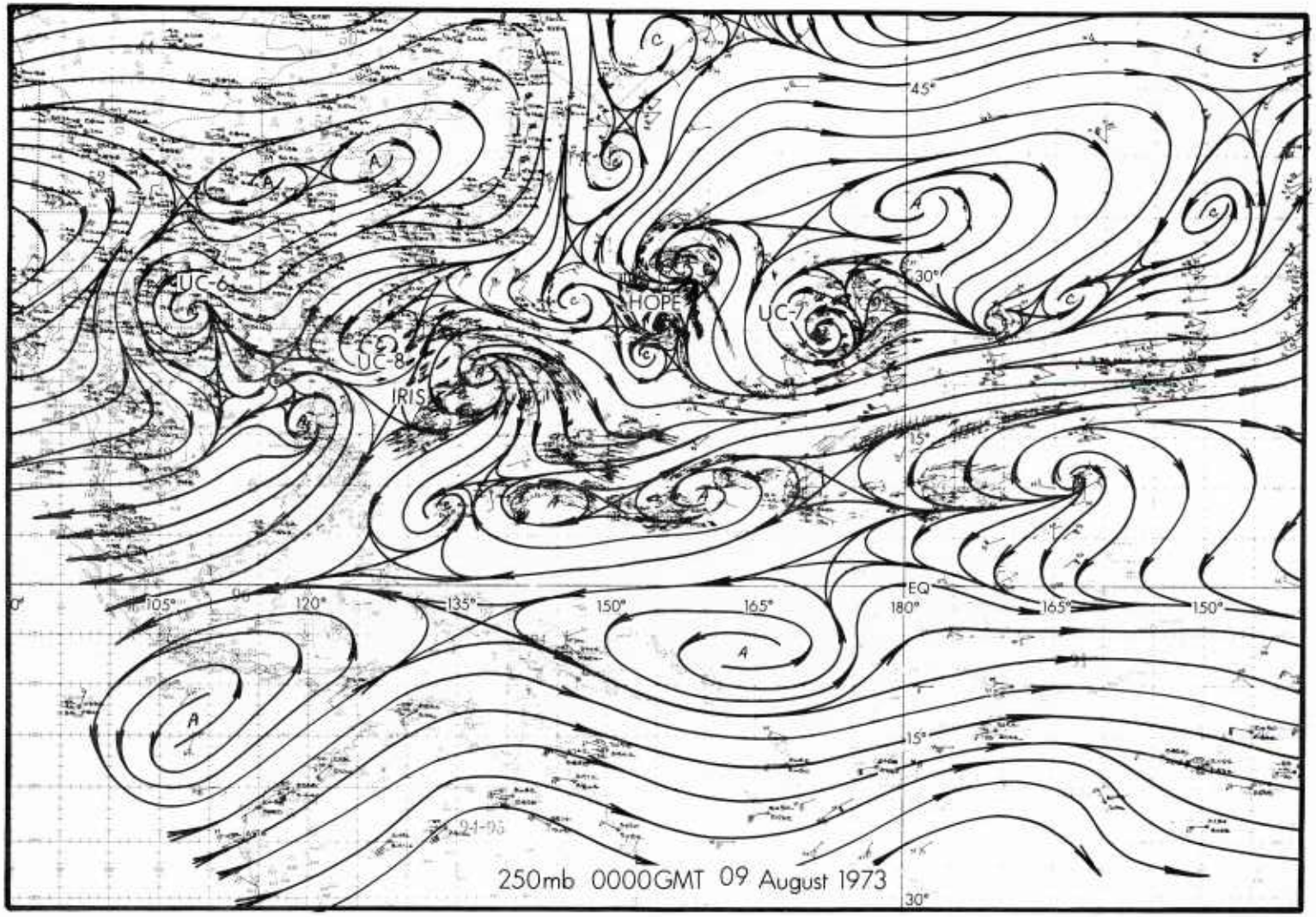

Figure 31. 250 mb streamline analysis for 9 August 1973.

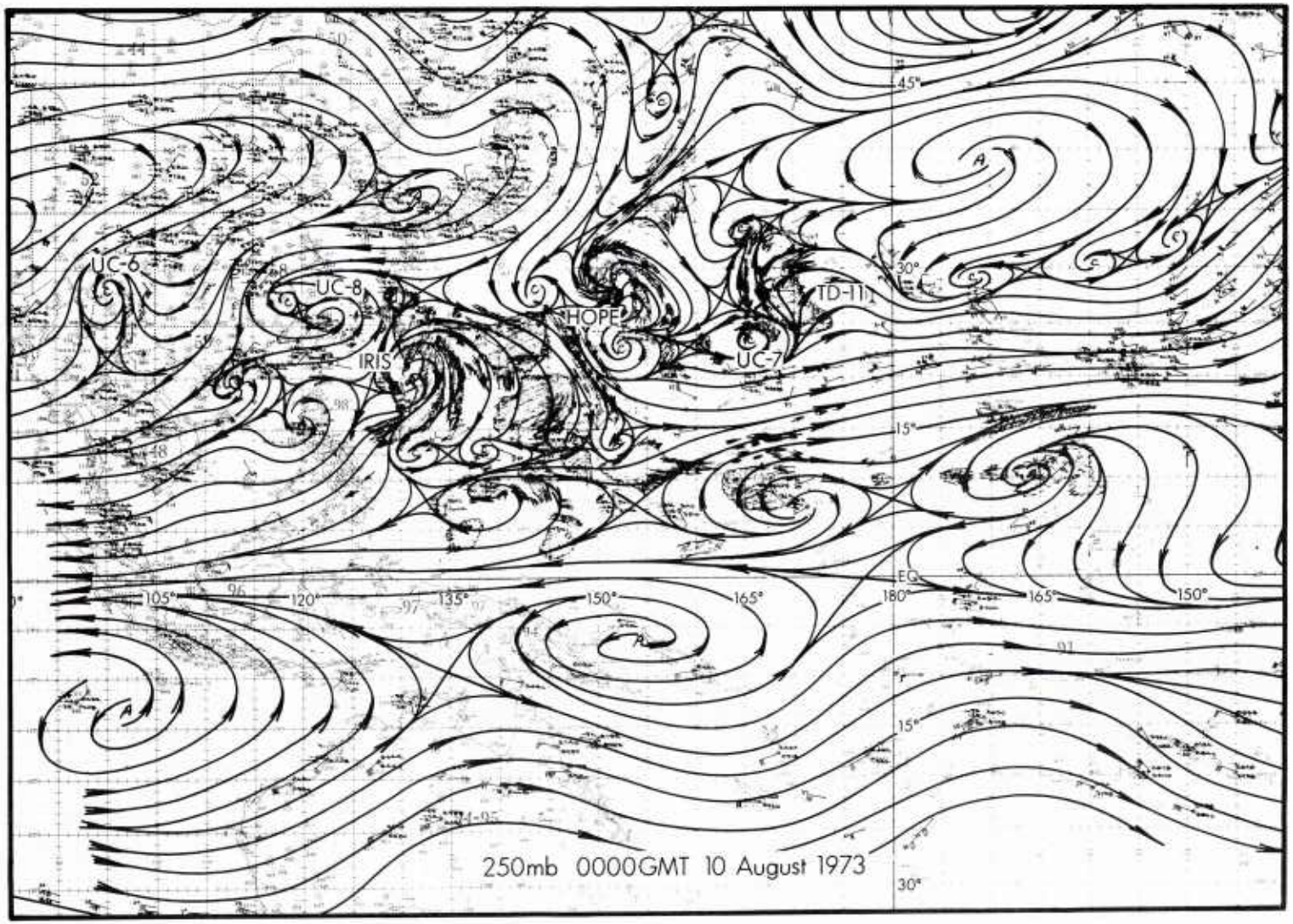

Figure 32. 250 mb streamline analysis for 10 August 1973.

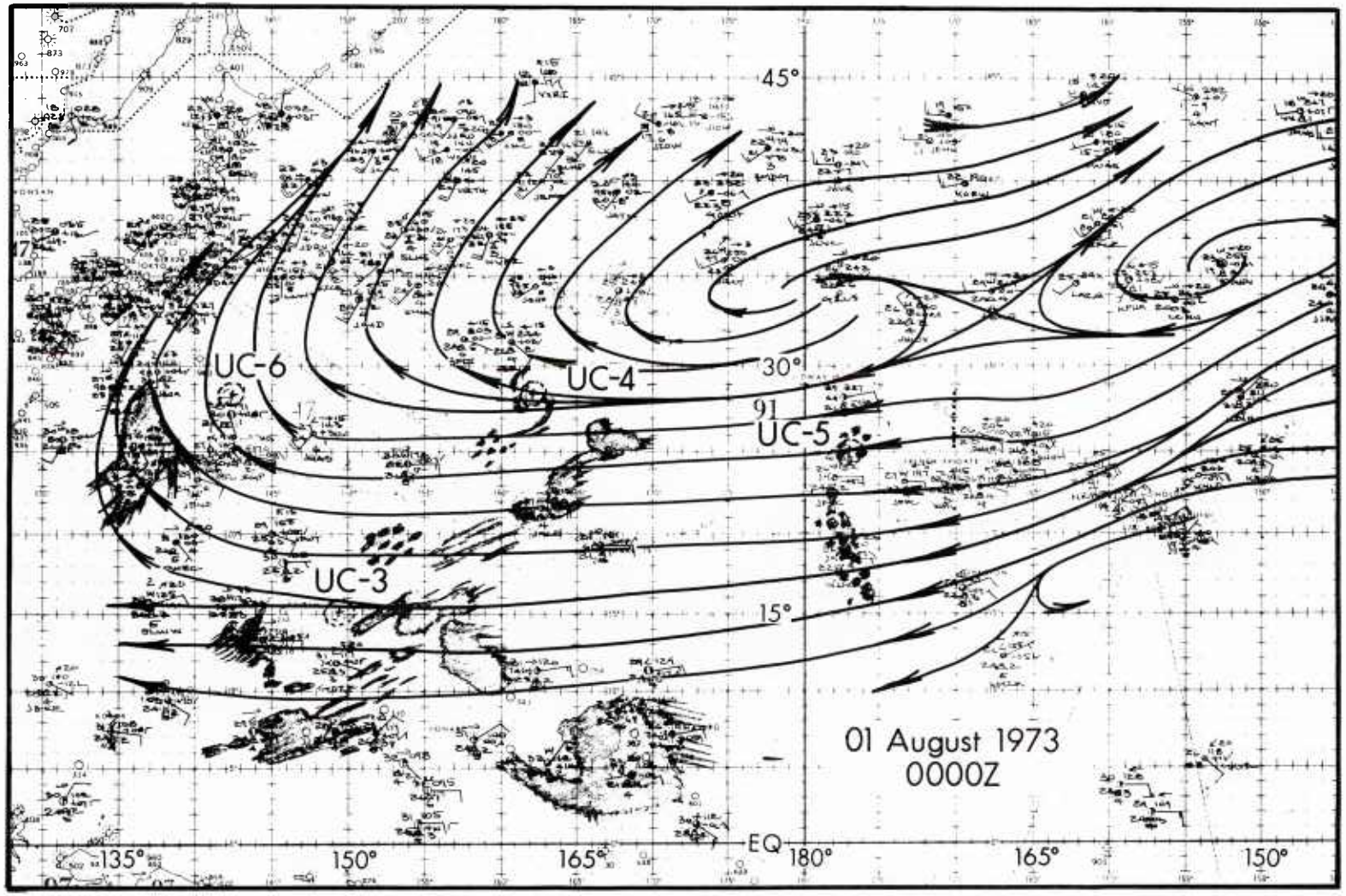

Figure 33. Surface streamline analysis for 1 August 1973.

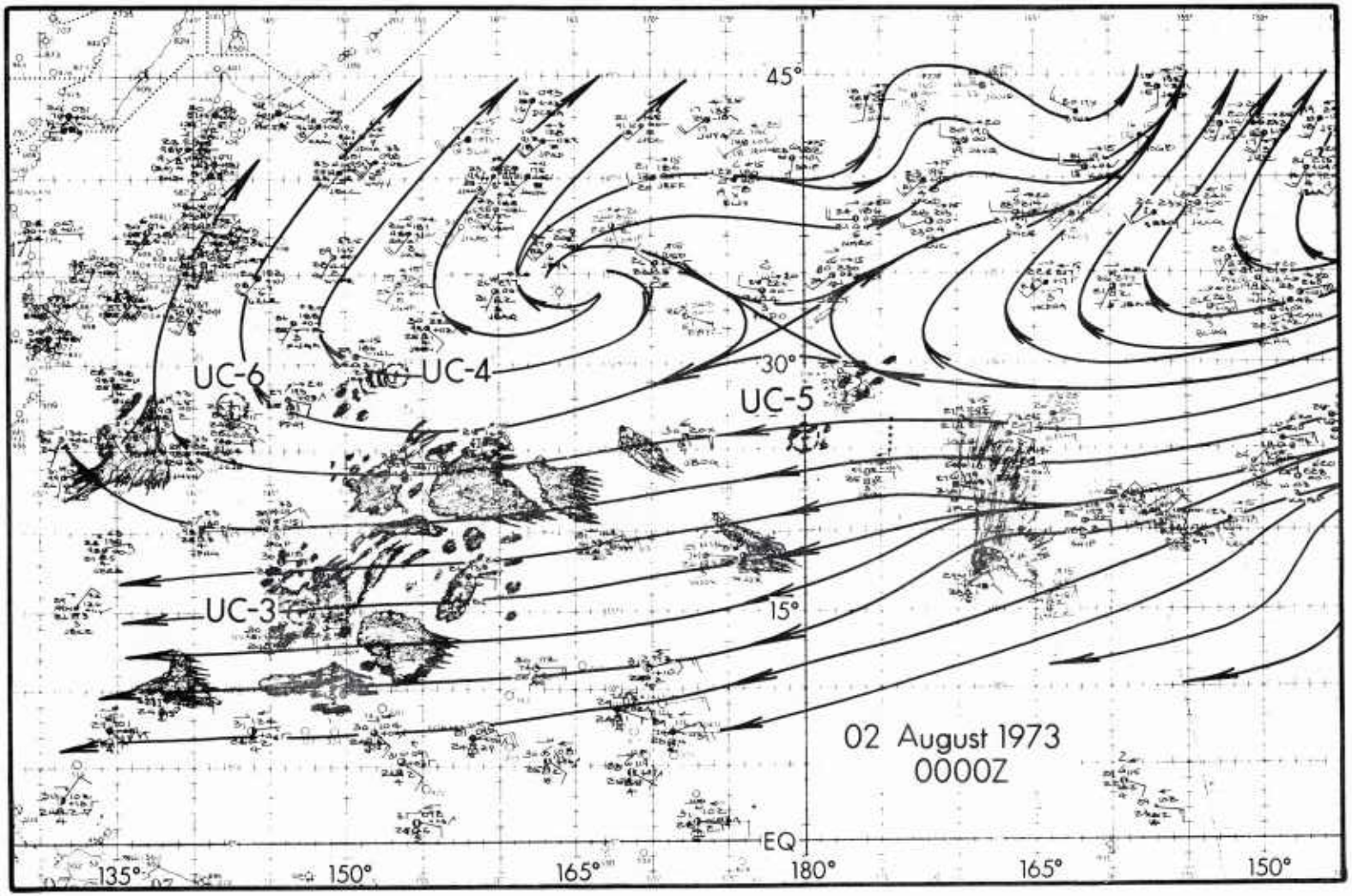

Figure 34. Surface streamline analysis for 2 August 1973.

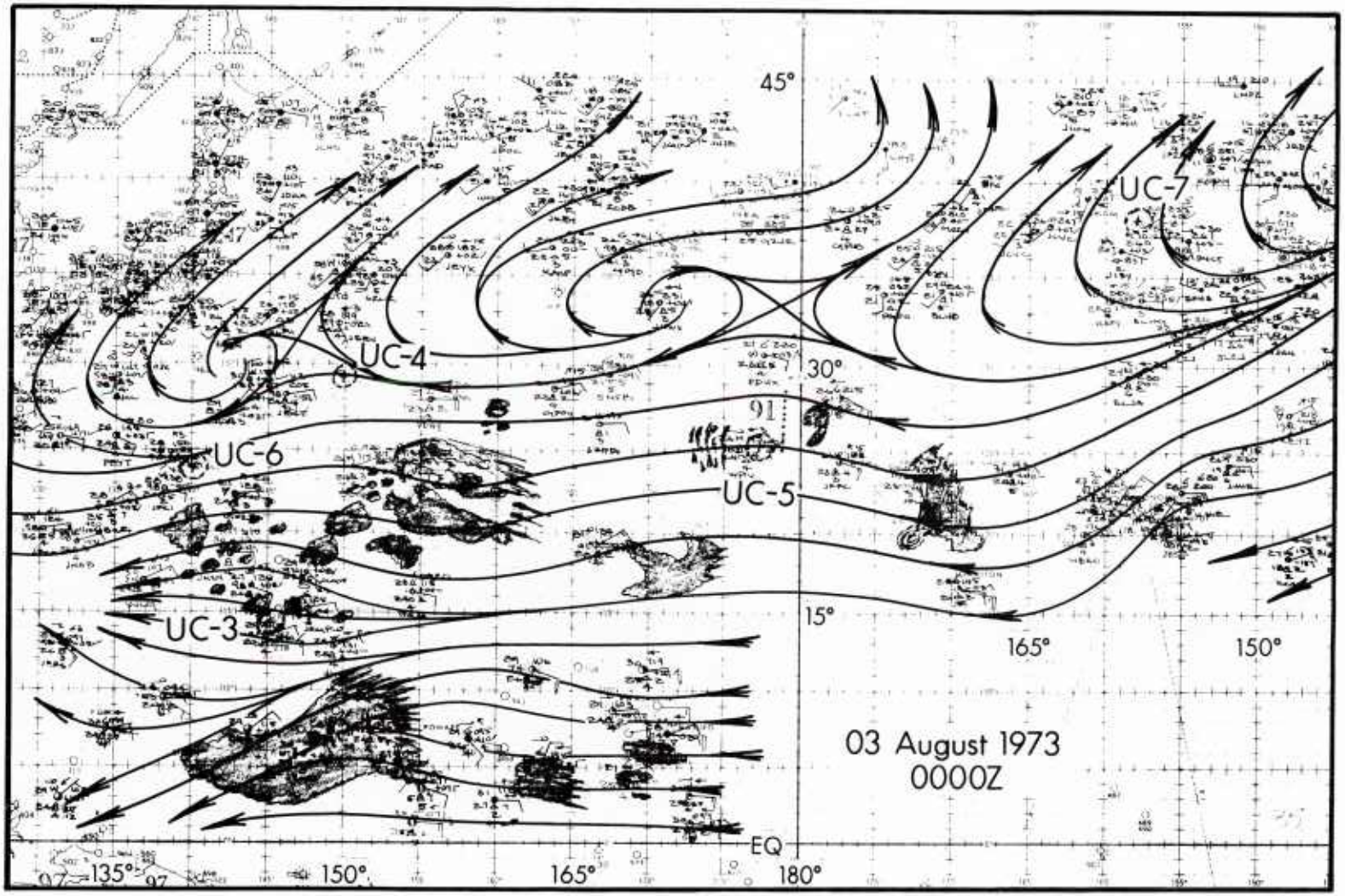

Figure 35. Surface streamline analysis for 3 August 1973.

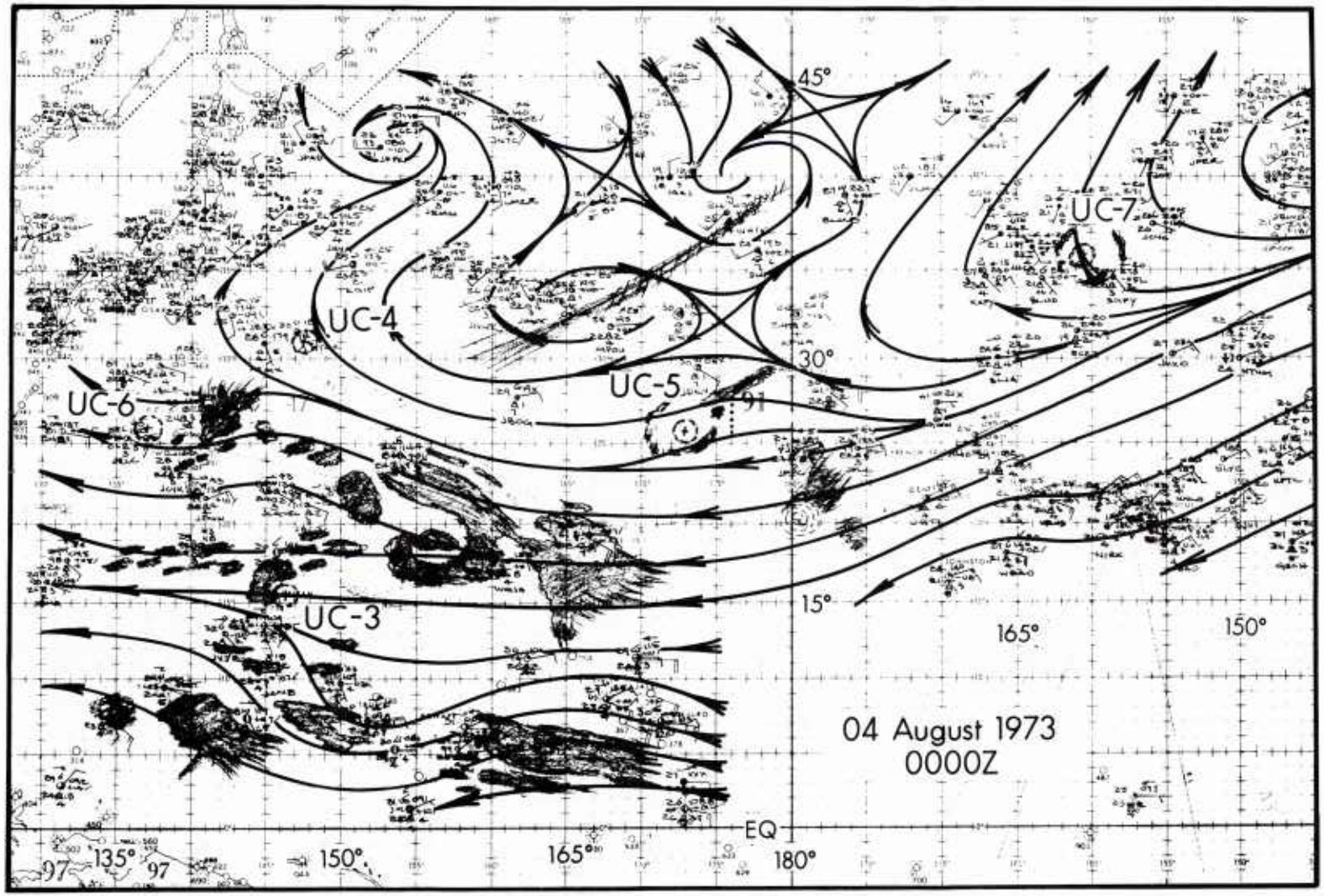

Figure 36. Surface streamline analysis for 4 August 1973.

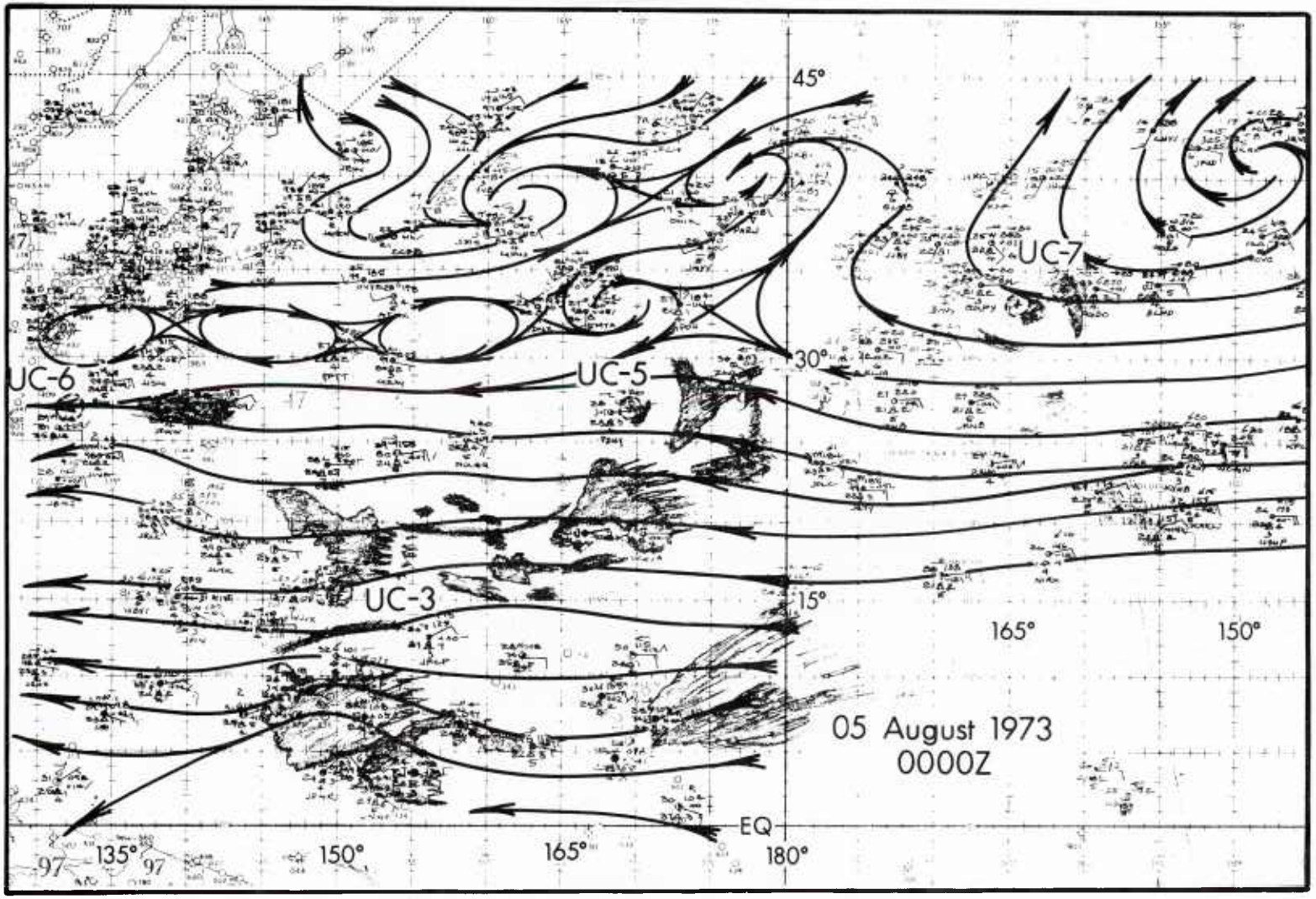

Figure 37. Surface streamline analysis for 5 August 1973.

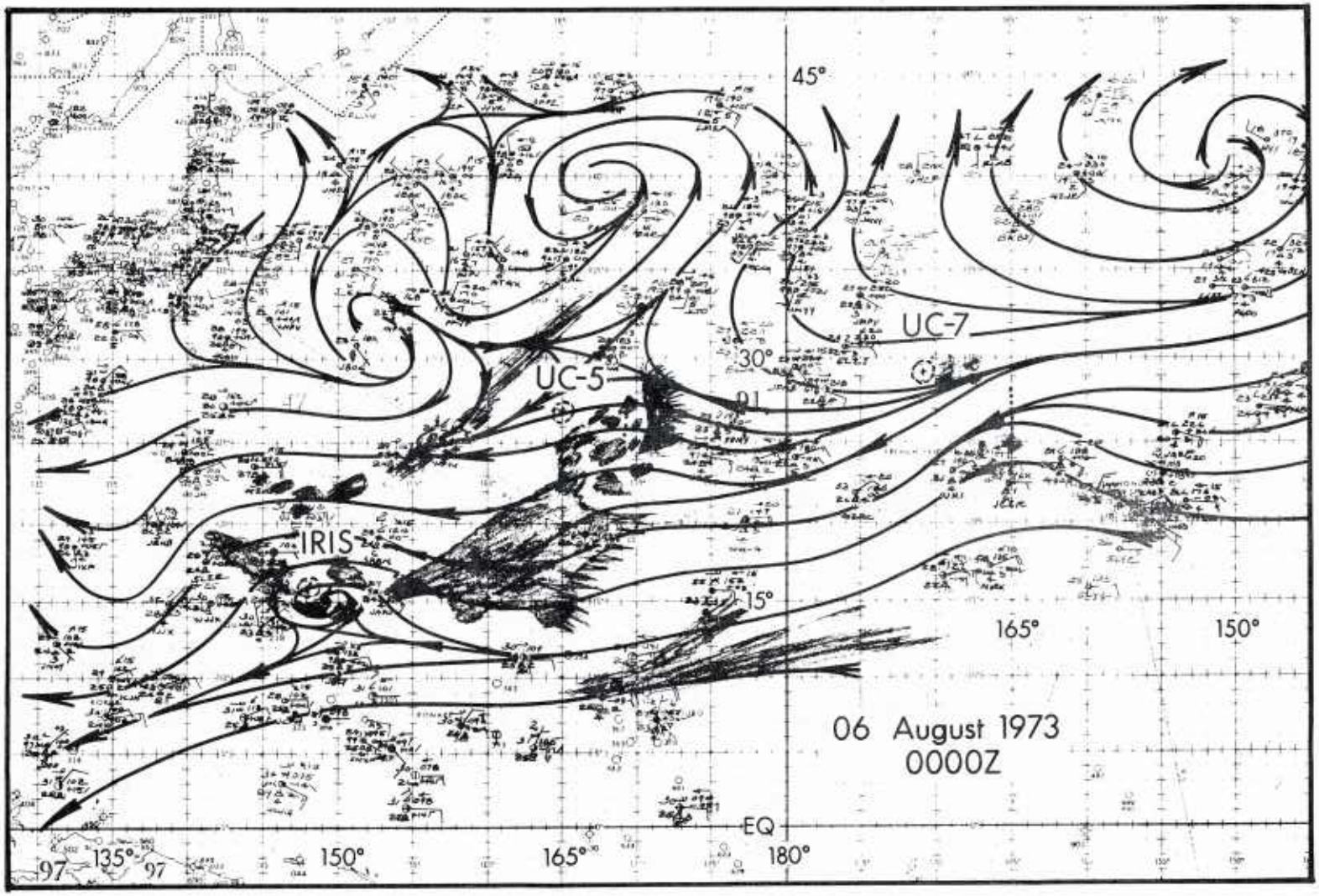

Figure 38. Surface streamline analysis for 6 August 1973.

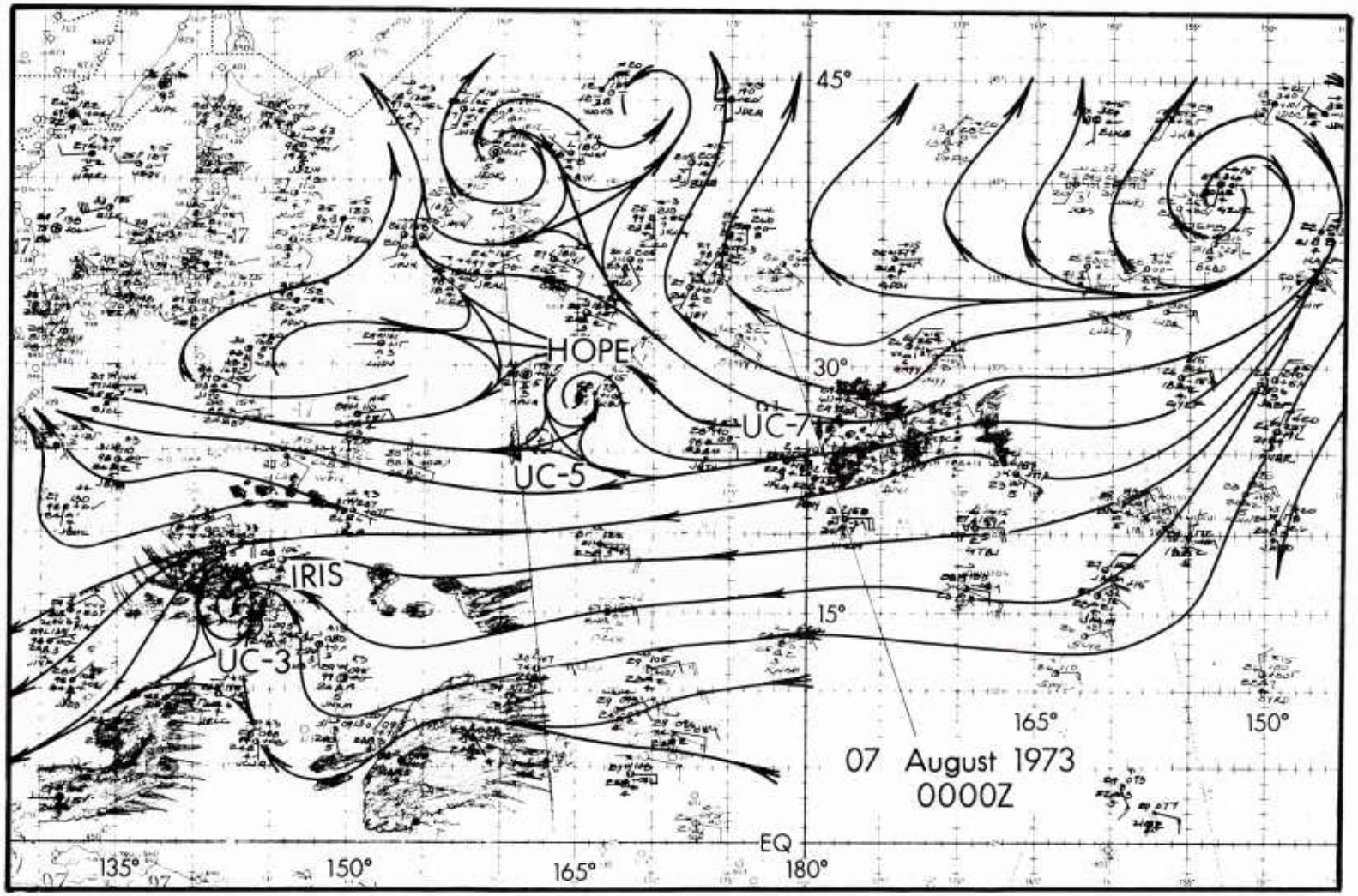

Figure 39. Surface streamline analysis for 7 August 1973.

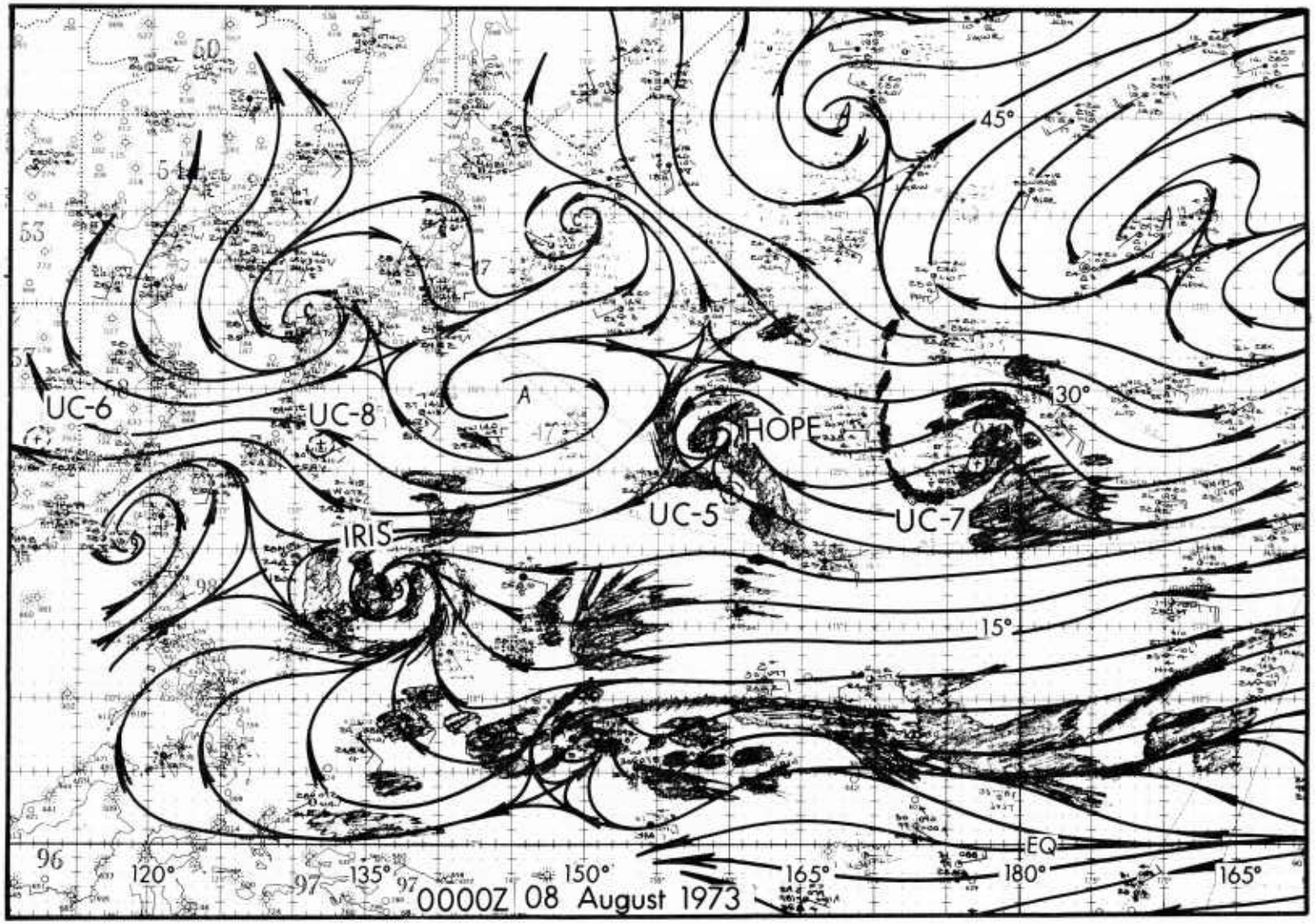

Figure 40. Surface streamline analysis for 8 August 1973.

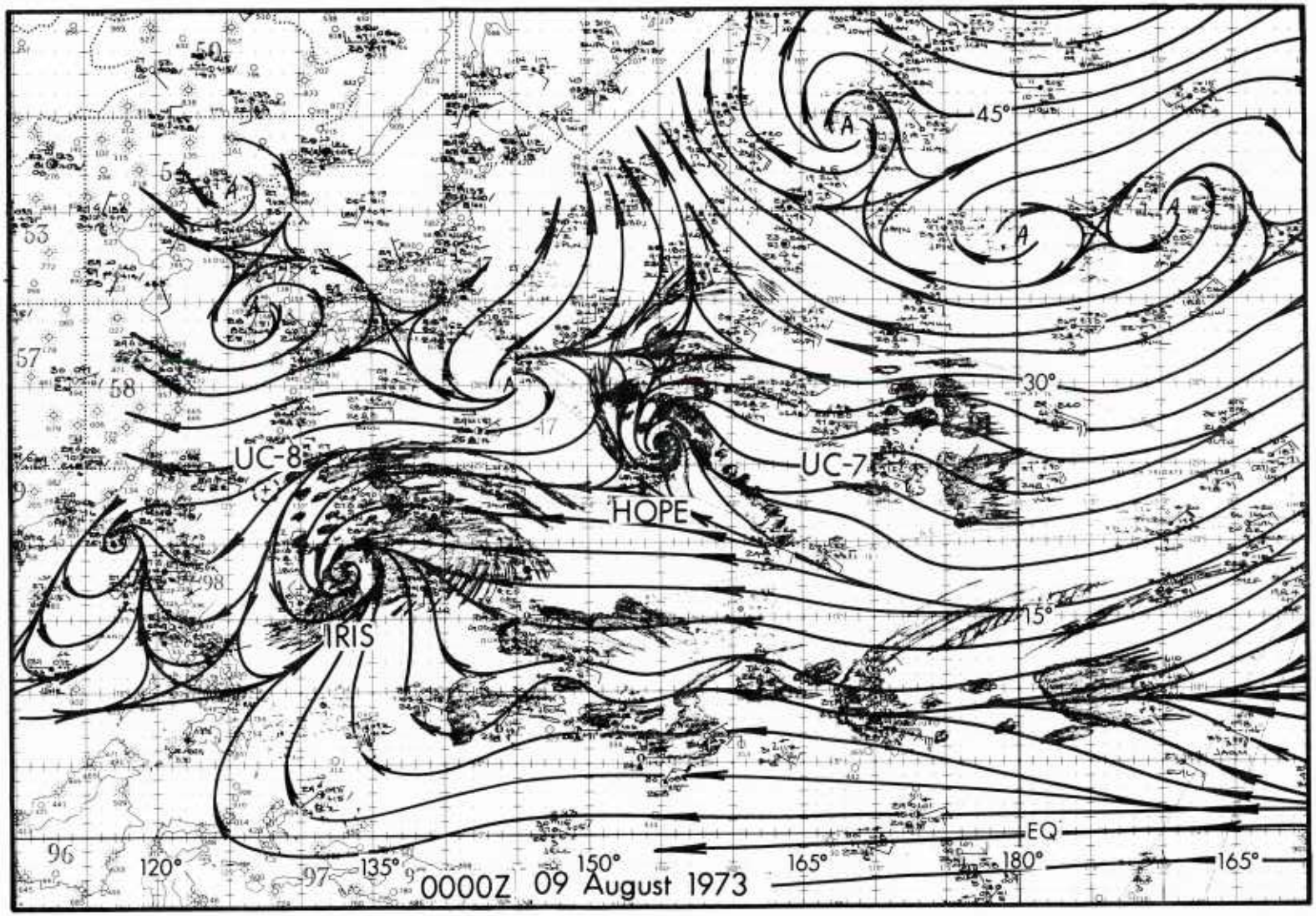

Figure 41. Surface streamline analysis for 9 August 1973.

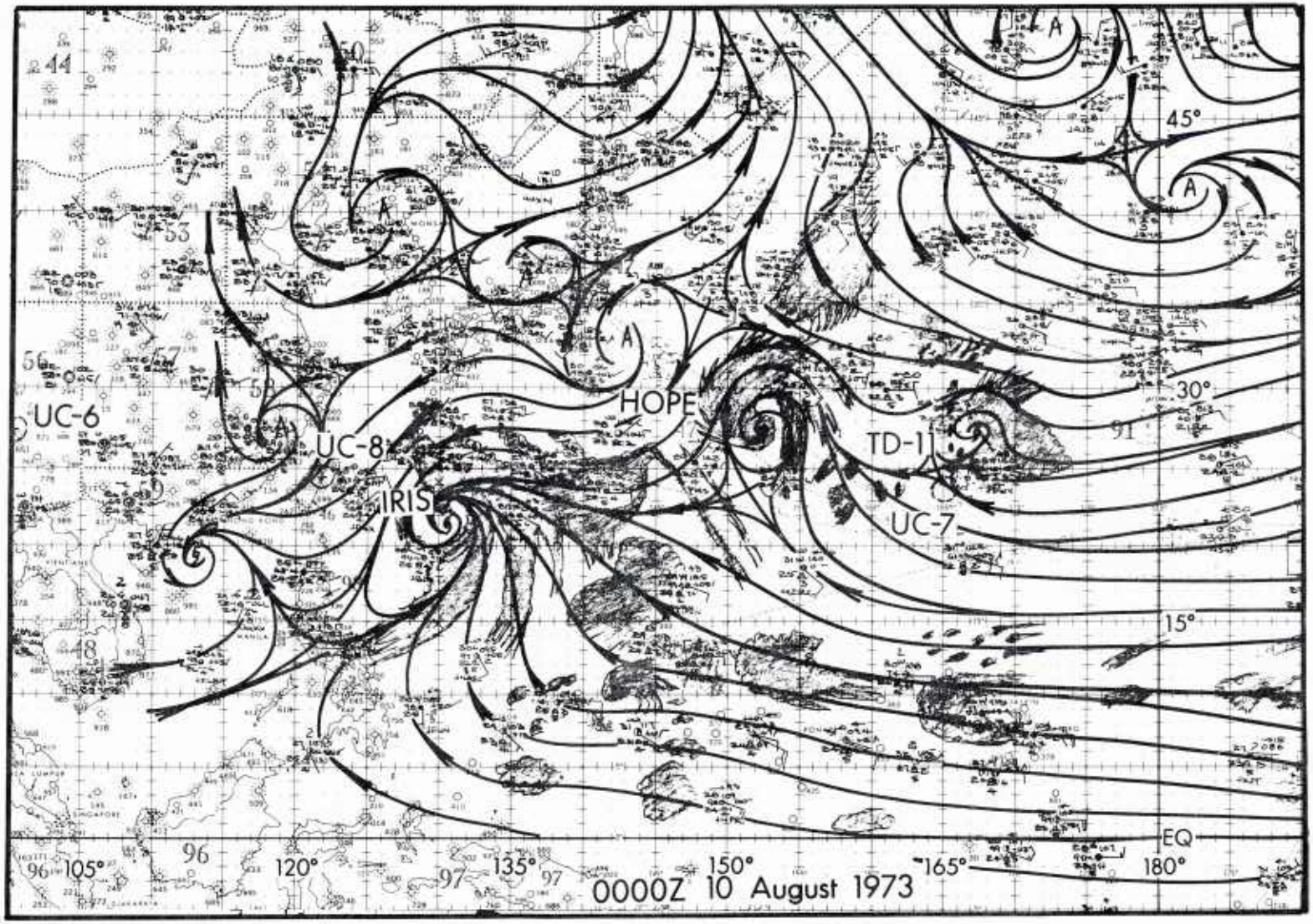

Figure 42. Surface streamline analysis for 10 August 1973.

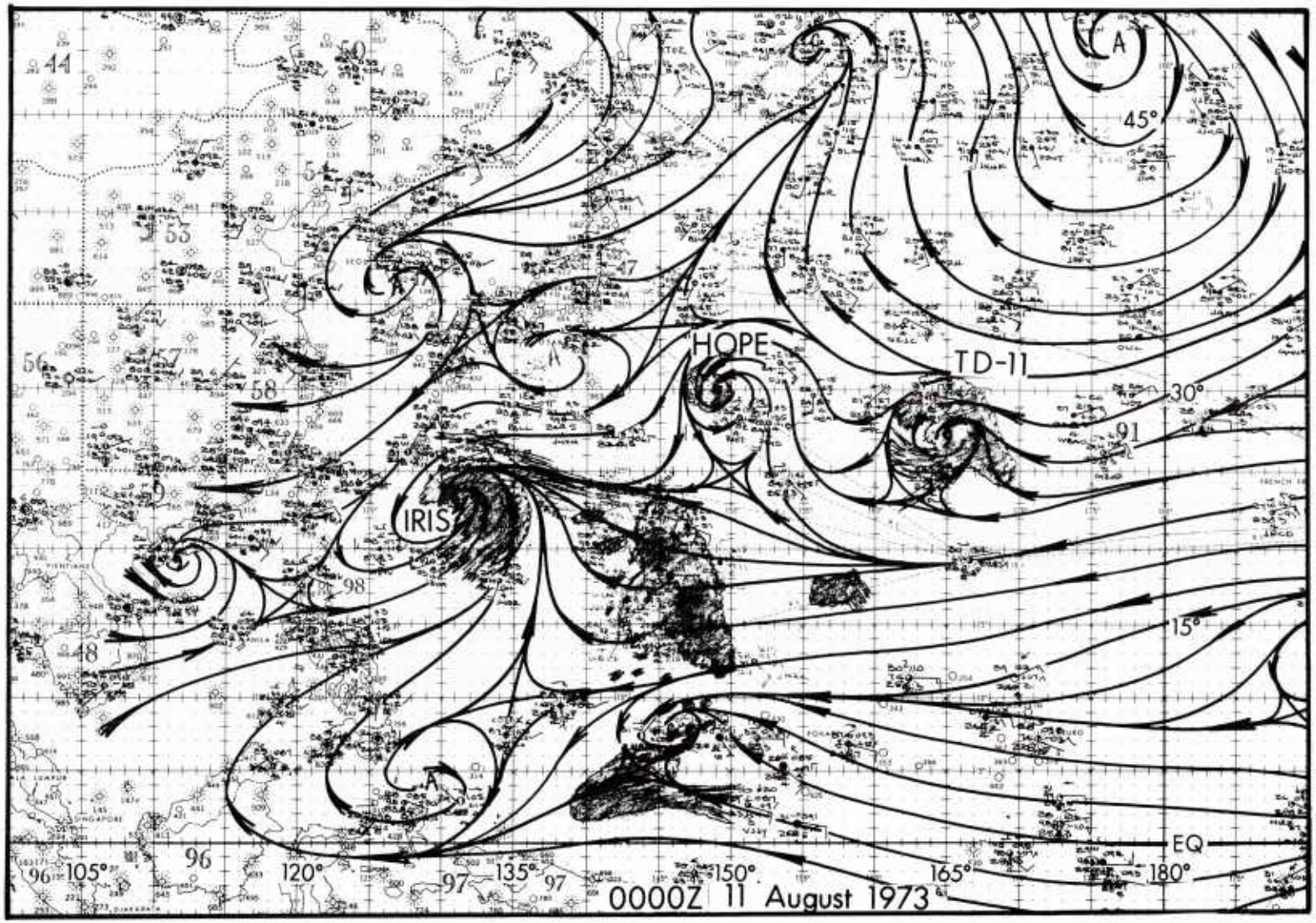

Figure 43. Surface streamline analysis for 11 August 1973.

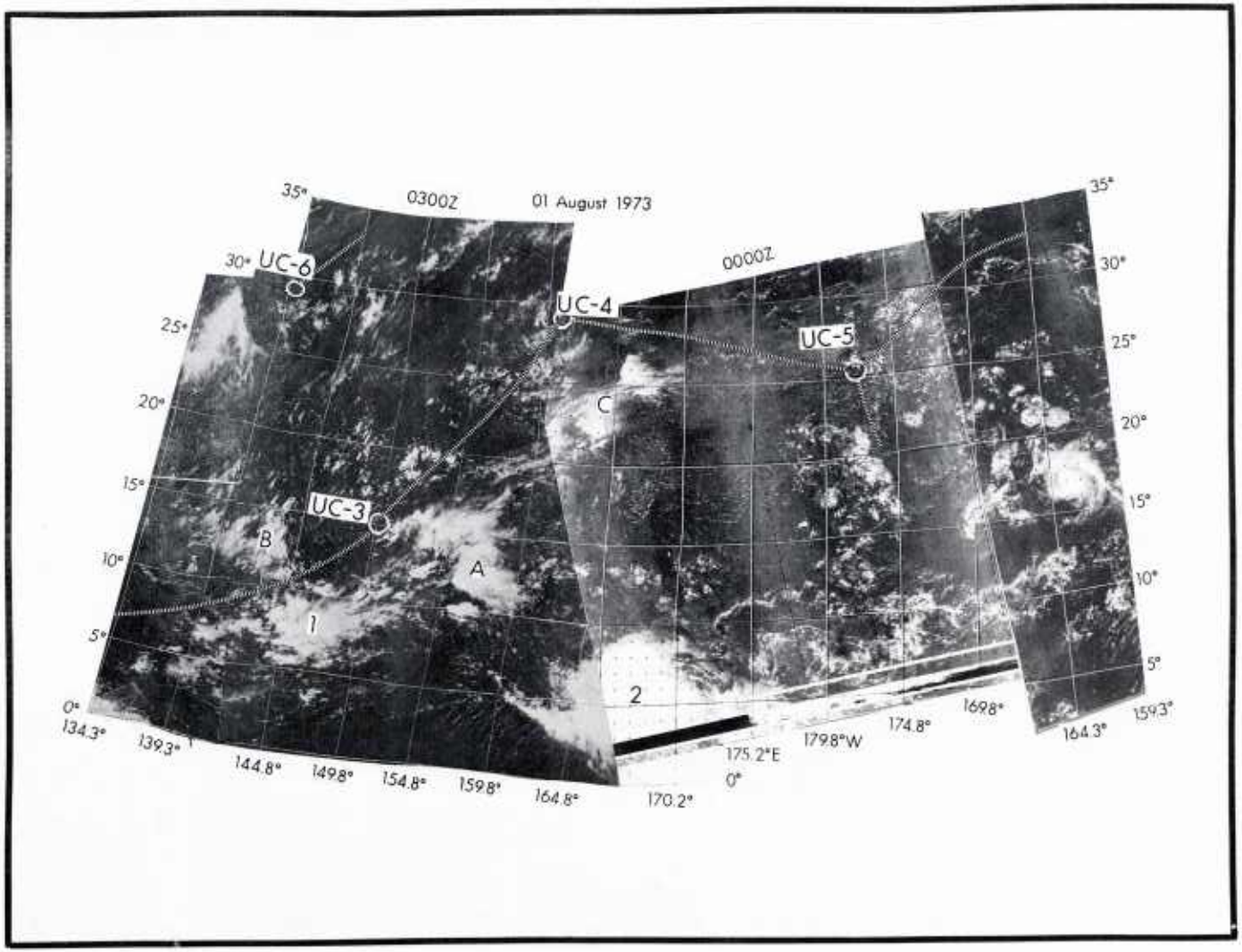

Figure 44. DMSP satellite mosaic for 1 August 1973.

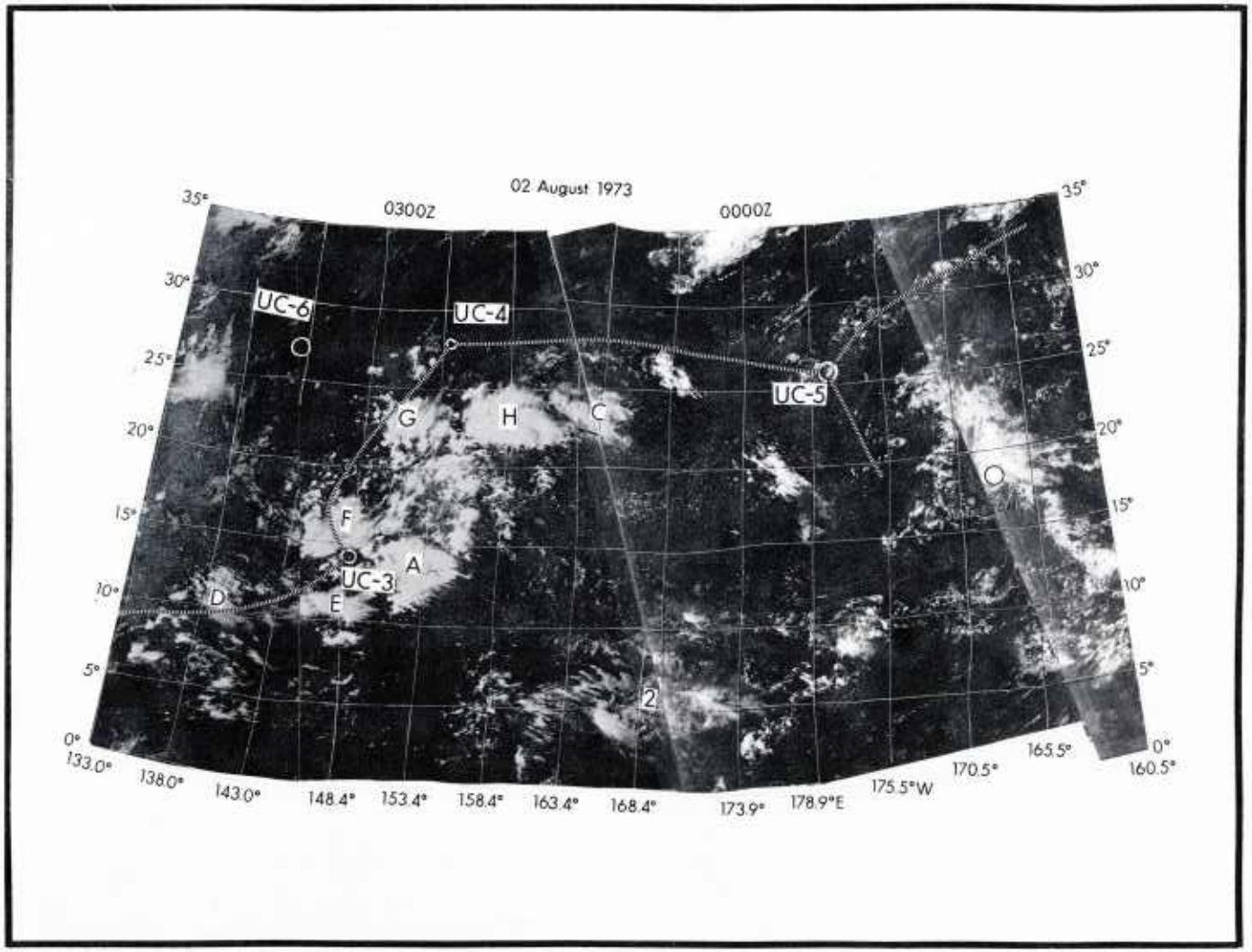

Figure 45. DMSP satellite mosaic for 2 August 1973.

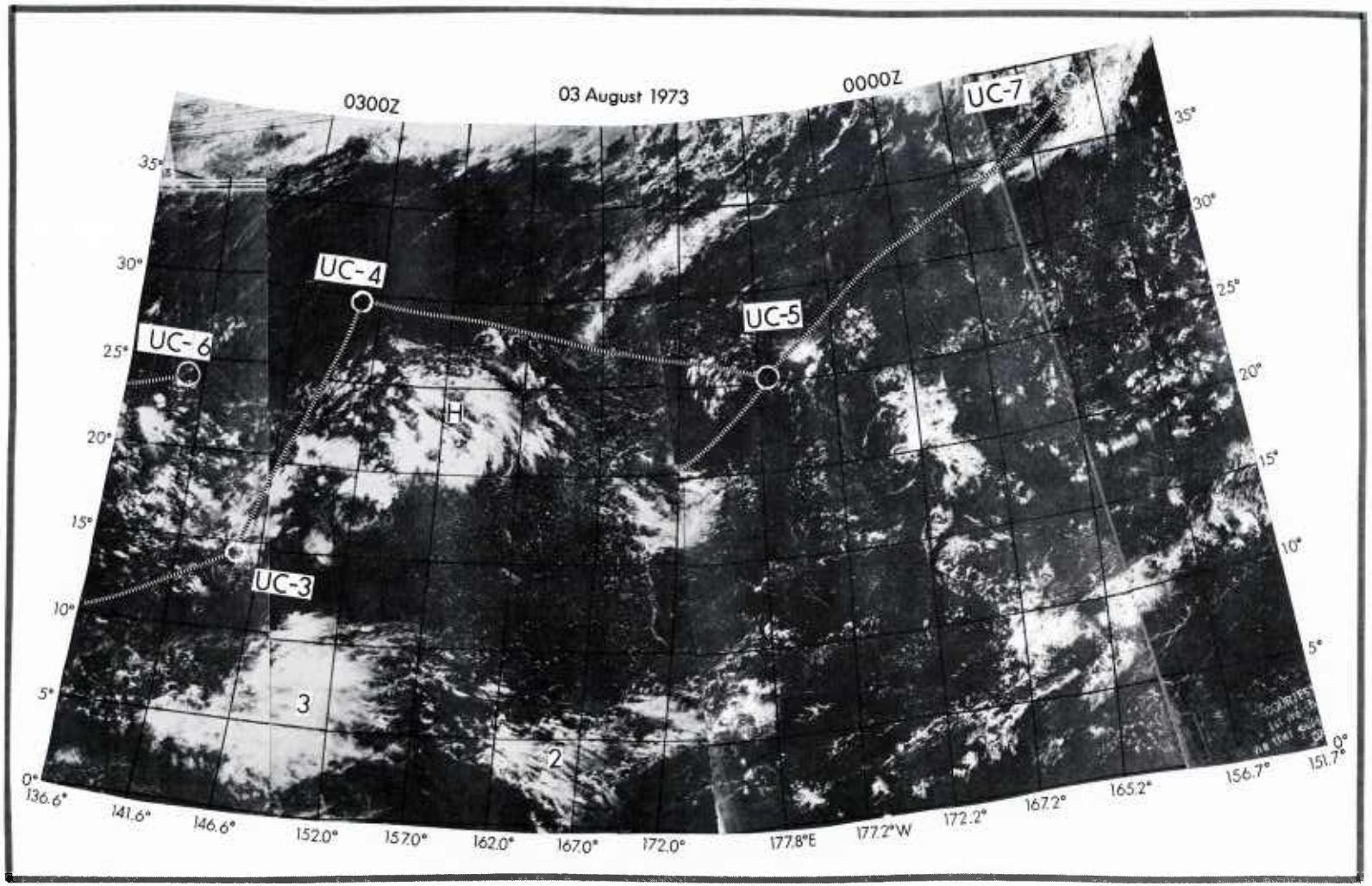

Figure 46. DMSP satellite mosaic for 3 August 1973.

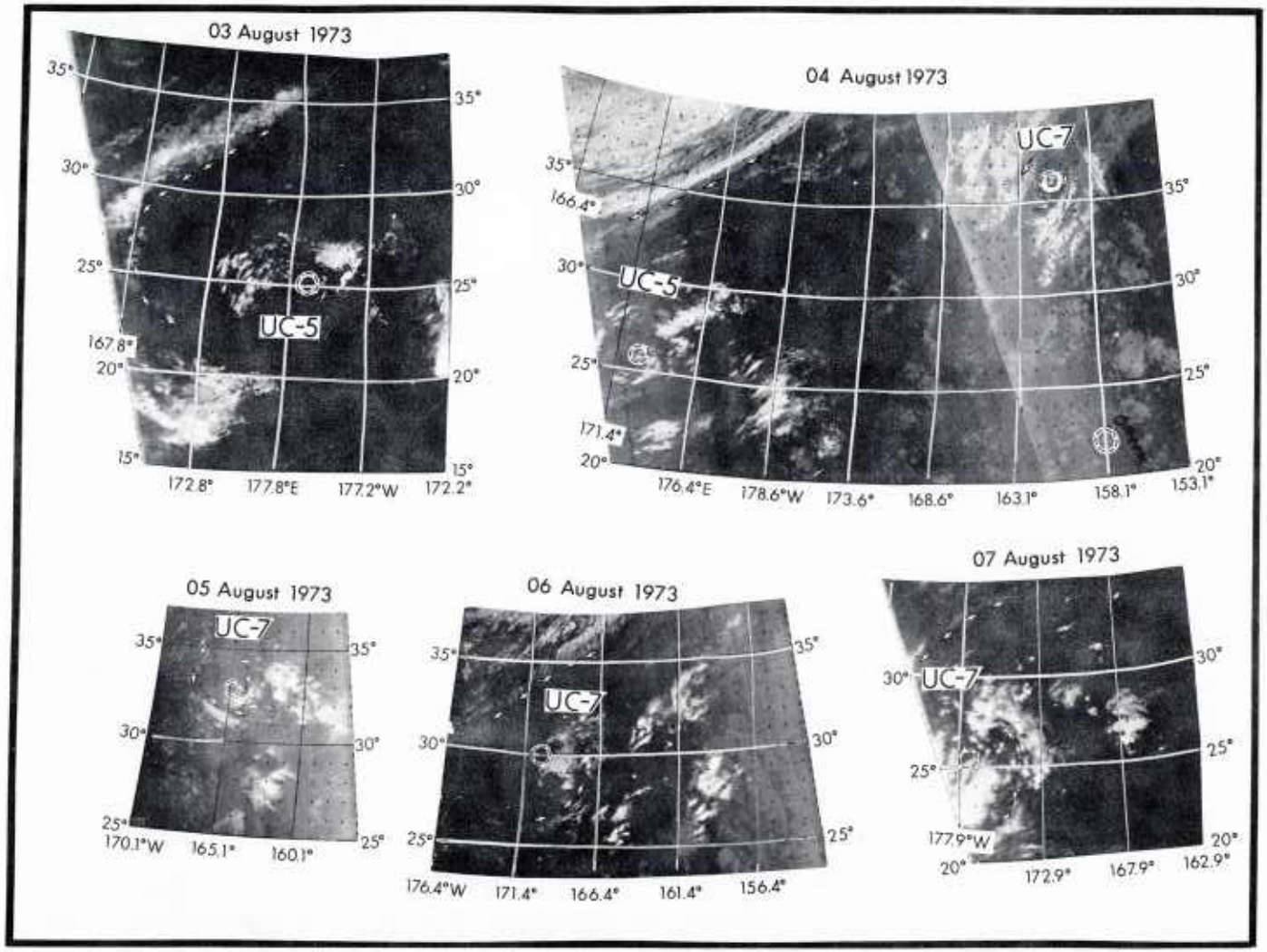

Figure 47. Selected days of DMSP satellite infrared photographs.

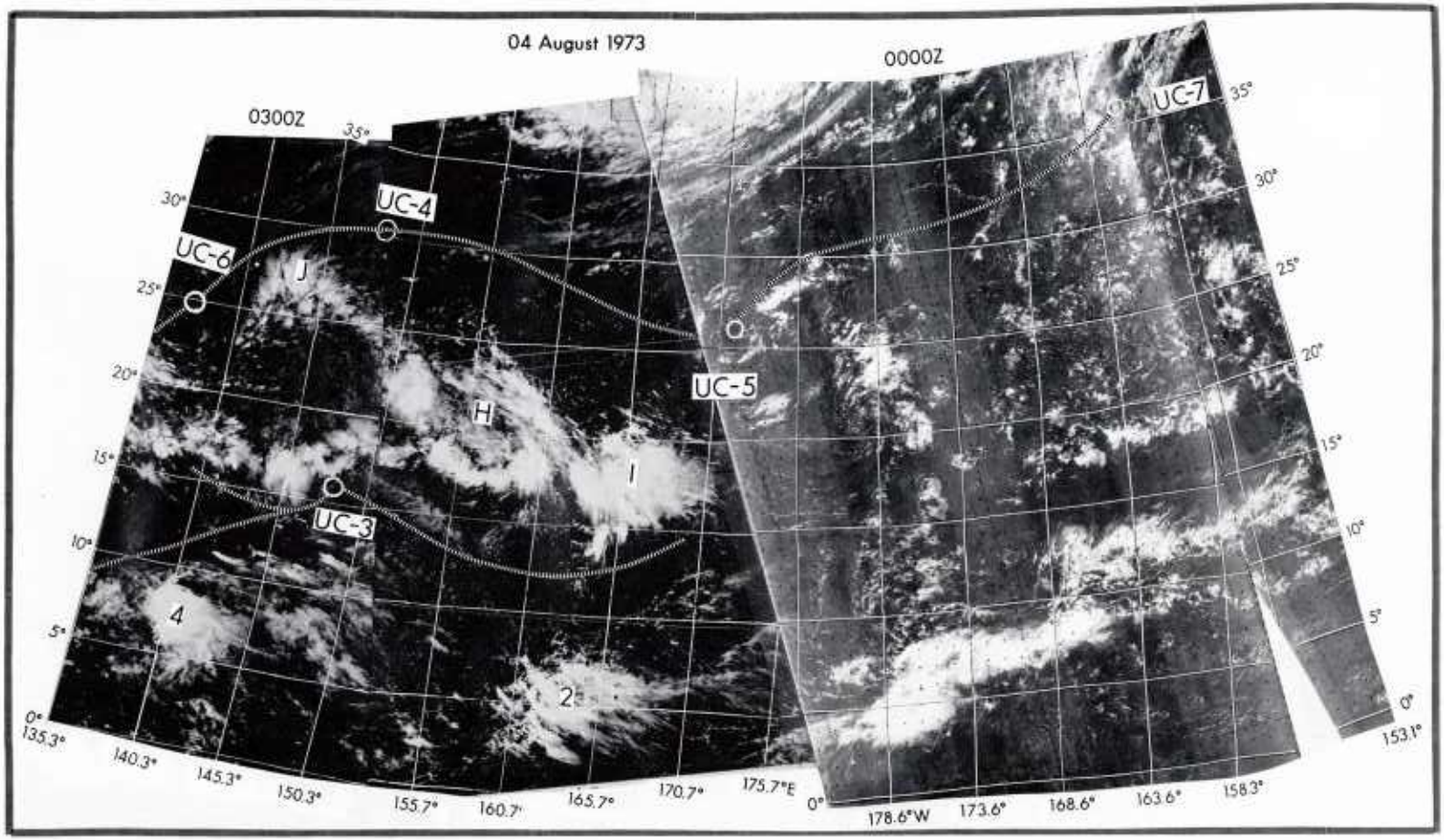

Figure 48. DMSP satellite mosaic for 4 August 1973.

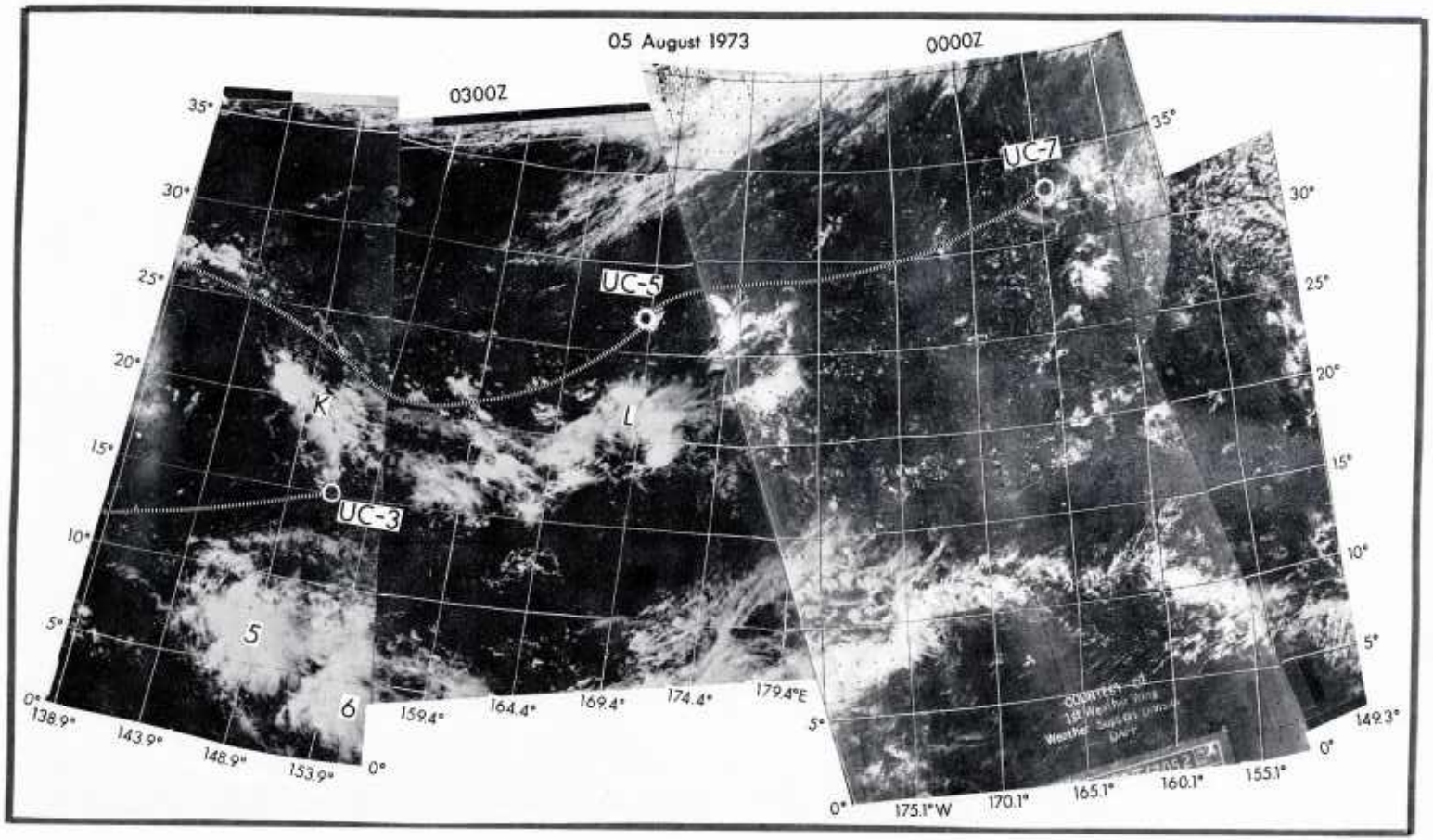

Figure 49. DMSP satellite mosaic for 5 August 1973.

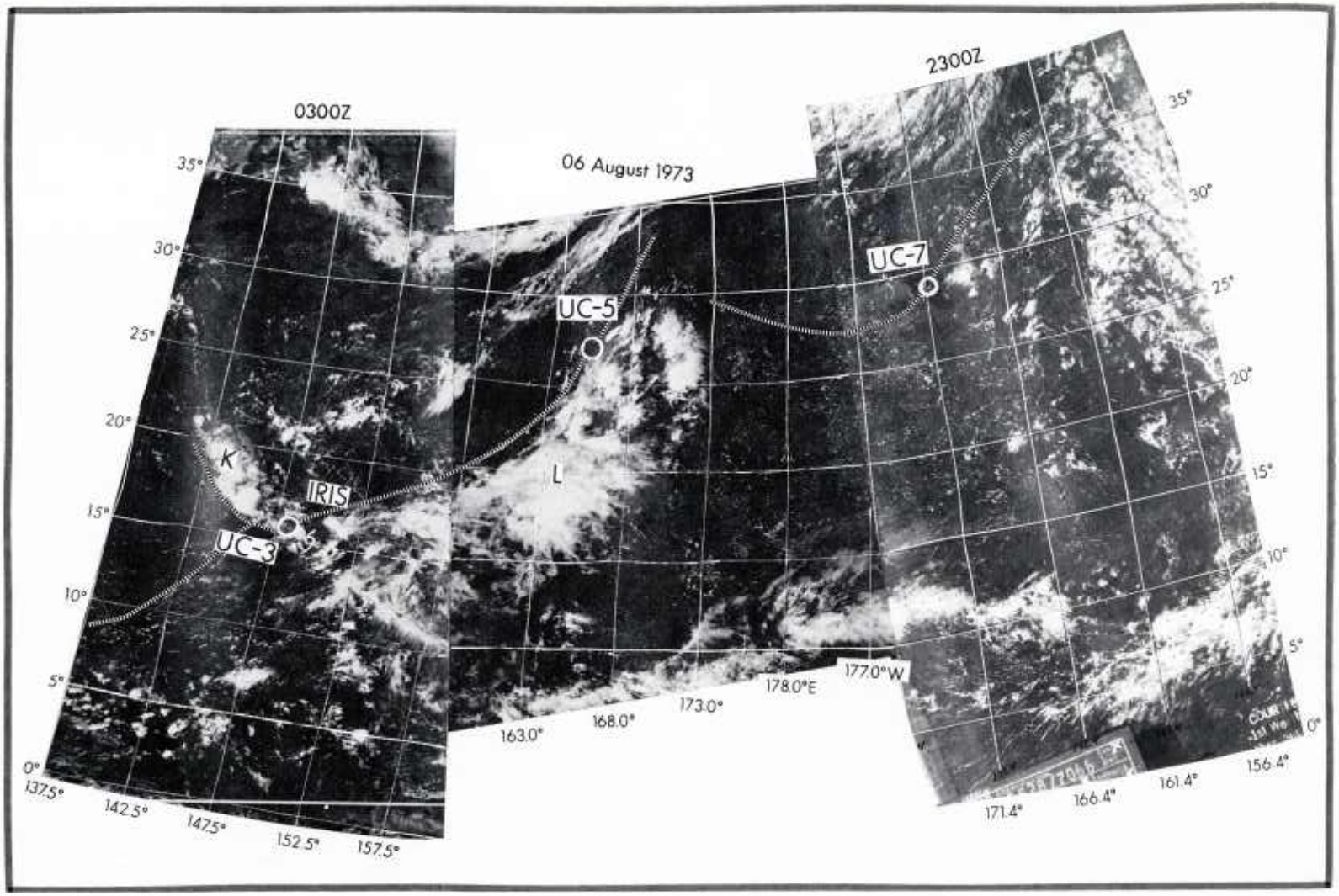

Figure 50. DMSP satellite mosaic for 6 August 1973.

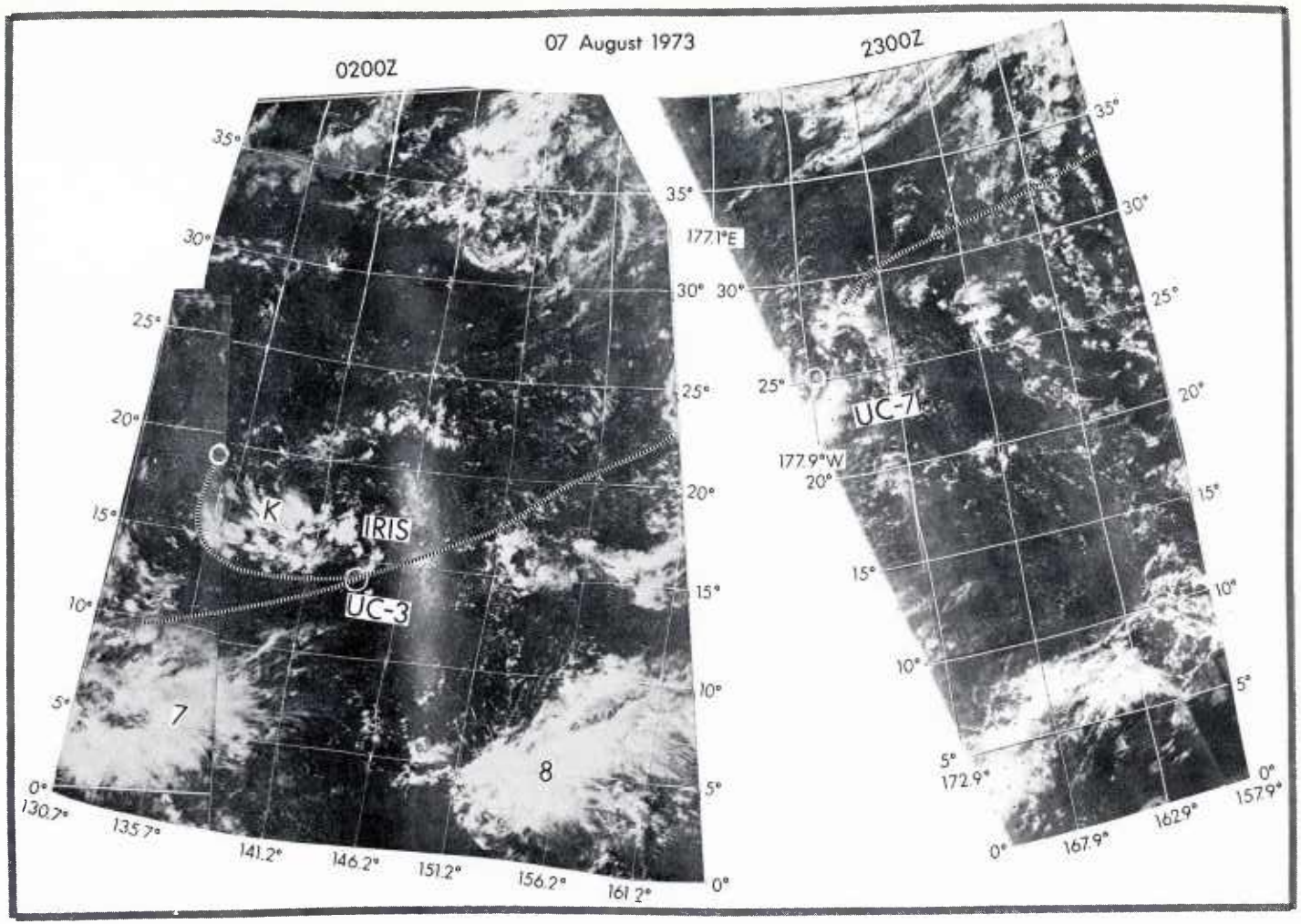

Figure 51. DMSP satellite mosaic for 7 August 1973.

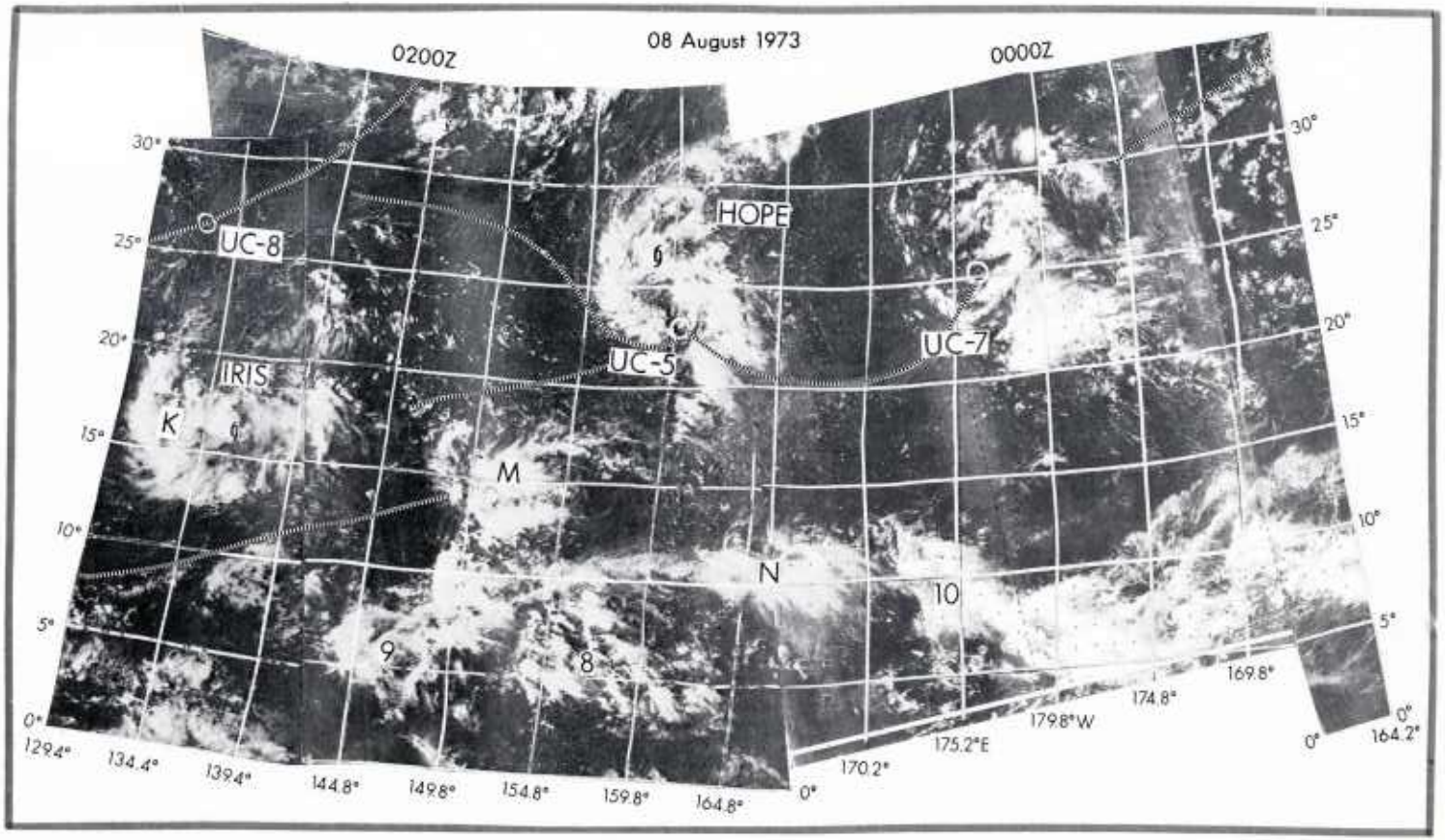

Figure 52. DMSP satellite mosaic for 8 August 1973.

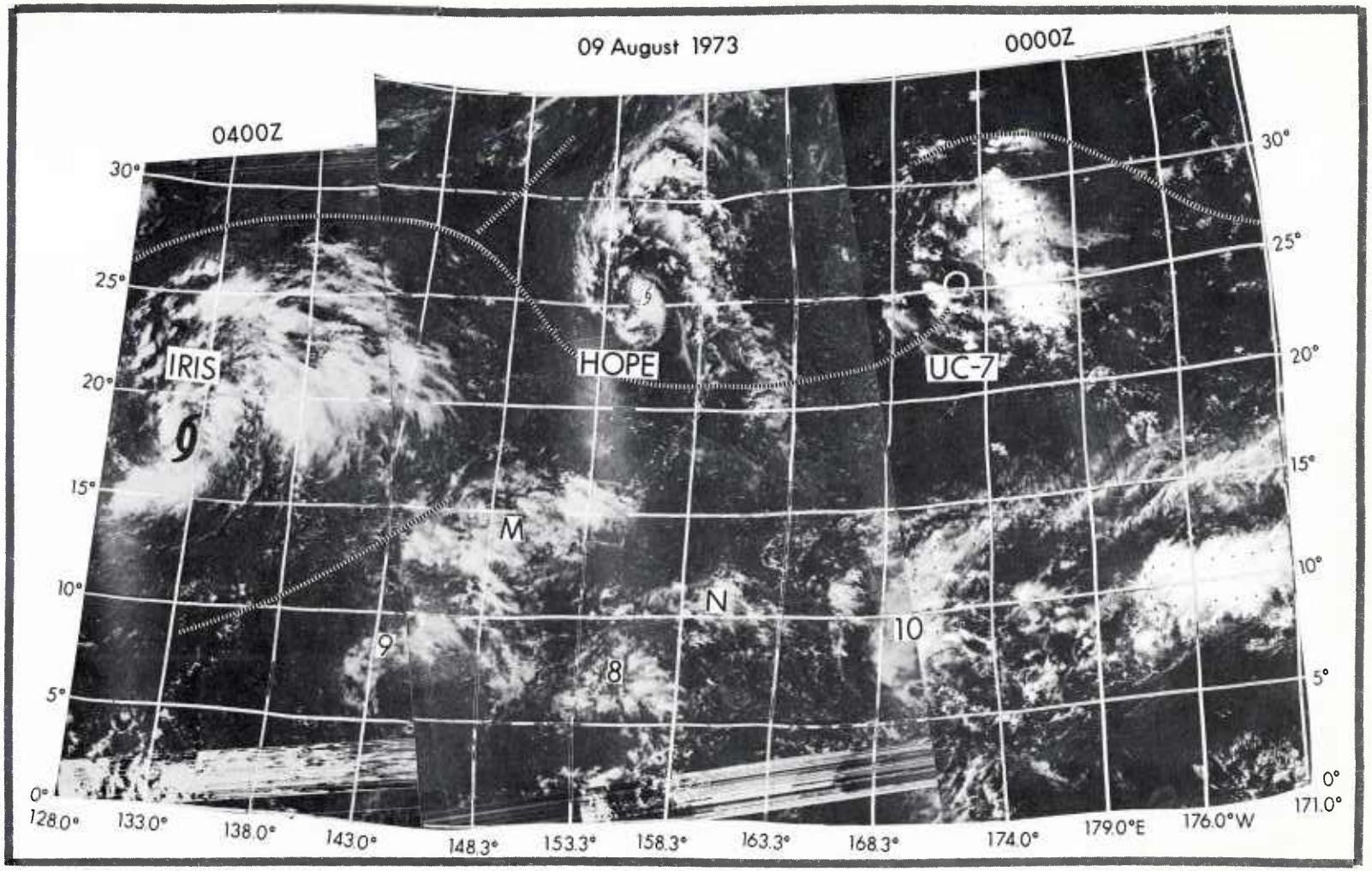

Figure 53. DMSP satellite mosaic for 9 August 1973.

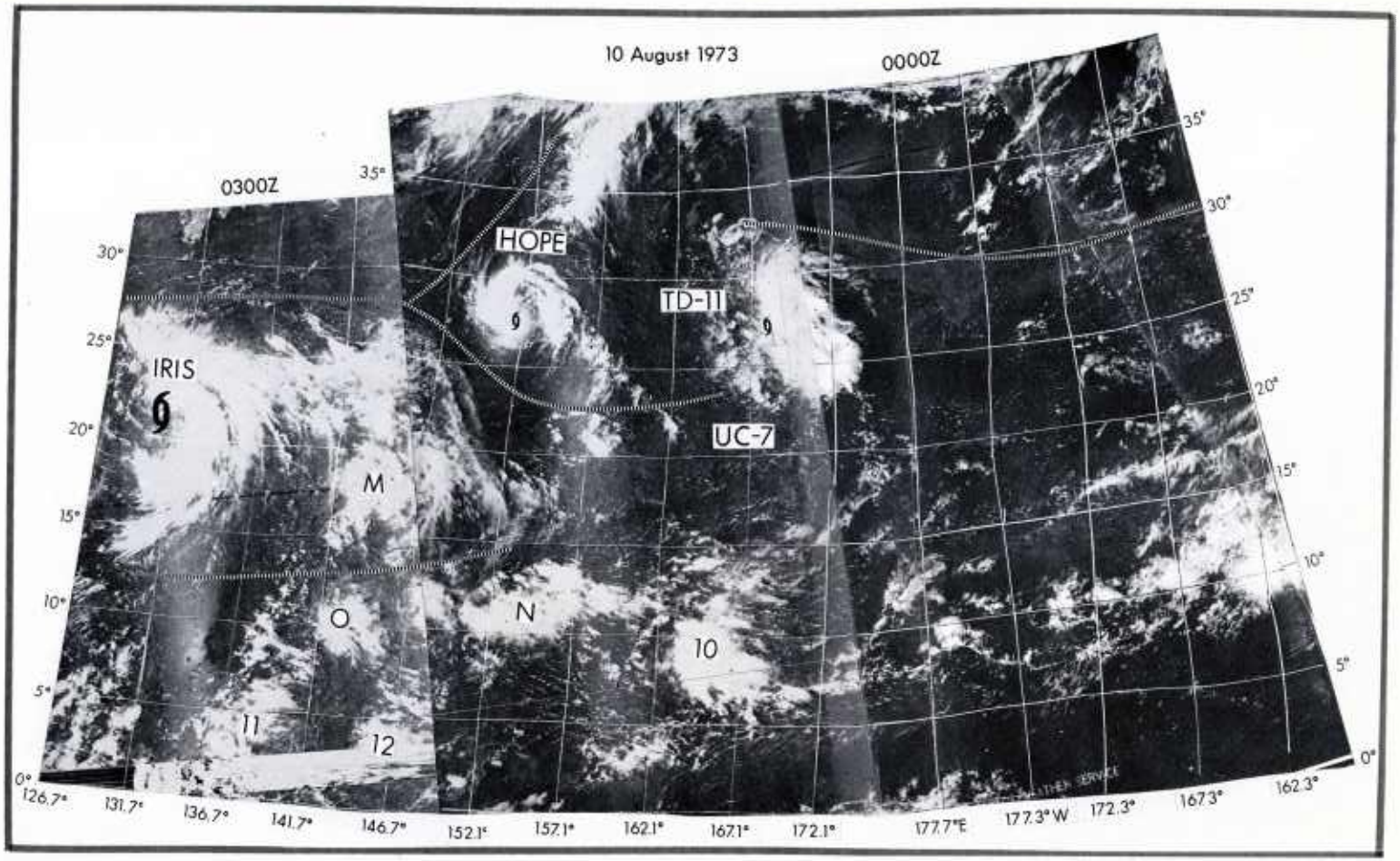

Figure 54. DMSP satellite mosaic for 10 August 1973.

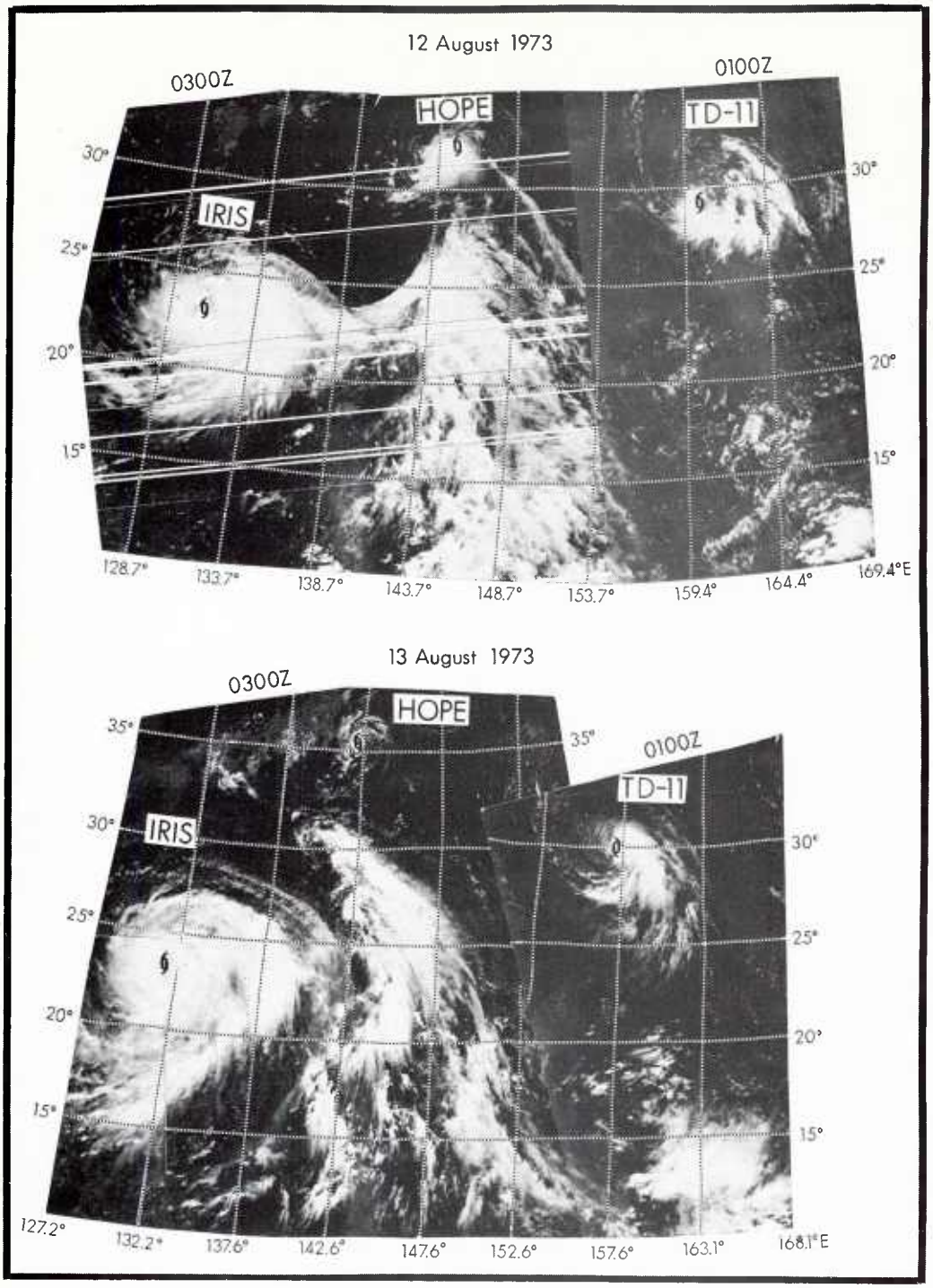

Figure 56. DMSP satellite mosaics for 12 and 13 August 1973.

☆GPO 691-044-1976